

SEPARATION PROCESS PRINCIPLES

J. D. Seader

*Department of Chemical and Fuels Engineering
University of Utah*

Ernest J. Henley

*Department of Chemical Engineering
University of Houston*



John Wiley & Sons, Inc.

*New York/Chichester/Weinheim
Brisbane/Singapore/Toronto*

Chapter 14

Membrane Separations

In a membrane separation process, a feed consisting of a mixture of two or more components is partially separated by means of a semipermeable barrier (the membrane) through which one or more species move faster than another or other species. The most general membrane process is shown in Figure 14.1 where the feed mixture is separated into a *retentate* (that part of the feed that does not pass through the membrane, i.e., is retained) and a *permeate* (that part of the feed that does pass through the membrane). Although the feed, retentate, and permeate are usually liquid or gas, they may also be solid. The barrier is most often a thin, nonporous polymeric film, but may also be porous polymer, ceramic, or metal materials, or even a liquid or gas. The barrier must not dissolve, disintegrate, or break. The optional sweep, shown in Fig. 14.1, is a liquid or gas, used to help remove the permeate. Many of the industrially important membrane separation operations are listed in Tables 1.2 and 14.1.

In membrane separations: (1) the two products are usually miscible, (2) the separating agent is a semipermeable barrier, and (3) a sharp separation is often difficult to achieve. Thus, membrane separations differ in two or three of these respects from the more common separation operations of absorption, stripping, distillation, and liquid-liquid extraction.

Although membranes as separating agents have been known for more than 100 years [1], large-scale applications have only appeared in the past 50 years. In the 1940s, porous fluorocarbons were used to separate $^{235}\text{UF}_6$ from $^{238}\text{UF}_6$ [2]. In the mid-1960s, reverse osmosis with cellulose acetate was first used to desalinate seawater to produce potable water (drinkable water with less than 500 ppm by weight of dissolved solids) [3]. In 1979, Monsanto Chemical Company introduced a hollow-fiber membrane of polysulfone to separate certain gas mixtures—for example, to enrich hydrogen- and carbon dioxide-containing streams [4]. Commercialization of alcohol dehydration by pervaporation began in the late 1980s, as did the large-scale application of emulsion liquid membranes for removal of metals and organics from wastewater.

The replacement of the more common separation operations with membrane separations has the potential to save large amounts of energy. This replacement requires the production of high mass-transfer flux, defect-free, long-life membranes on a large scale and the fabrication of the membrane into compact, economical modules of high surface area per unit volume.

A common application of membranes is to the separation of hydrogen from methane. Following World War II, during which large amounts of toluene were required to produce TNT (trinitrotoluene) explosives, petroleum refiners sought other markets for tolu-

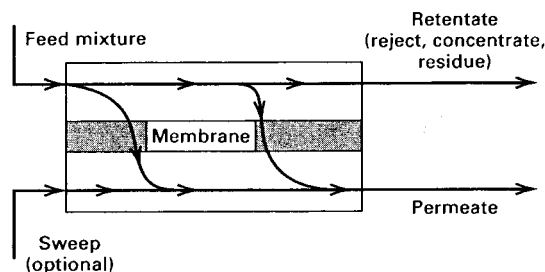
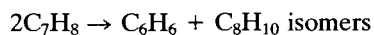
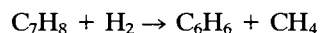


Figure 14.1 General membrane process.

ene. One potential market was the use of toluene as a feedstock for the manufacture of benzene, a precursor for nylon, and xylenes, precursors for a number of other chemicals, including polyesters. Toluene can be catalytically disproportionated to benzene and mixed xylenes in an adiabatic reactor with the feed entering at 950°F and a pressure greater than 500 psia. The main reaction is



To suppress the formation of coke, which fouls the catalyst, the reactor feed must contain a substantial fraction of hydrogen at a partial pressure of at least 215 psia. Unfortunately, the hydrogen takes part in a side reaction for the hydrodealkylation of toluene to benzene and methane:



Makeup hydrogen is usually not pure, but contains perhaps 15 mol% methane and 5 mol% ethane. Thus, typically, the reactor effluent contains H_2 , CH_4 , C_2H_6 , C_6H_6 , unreacted C_7H_8 , and C_8H_{10} isomers. As shown in Figure 14.2a, for just the reaction section of the process, this effluent is cooled and partially condensed to 100°F at a pressure of 465 psia. At these conditions, a reasonably good separation is achieved between C_2H_6 and C_6H_6 in the flash drum. Thus, the vapor leaving the flash drum contains most of the H_2 , CH_4 , and C_2H_6 , with most of the aromatic chemicals leaving in the liquid. Because of the large amount of hydrogen in the flash-drum vapor, it is important to recycle this stream to the reactor, rather than sending it to a flare or using it as a fuel. However, if all of the vapor were recycled, methane and ethane would build up in the recycle loop, since no other exit is provided. Before the development of acceptable membranes for the separation of H_2 from CH_4 by gas permeation, part of the vapor stream was customarily purged from the process, as shown in Figure 14.2a, to provide an exit for CH_4 , and C_2H_6 . With the introduction of a suitable membrane in 1979, it became possible to apply membrane separators, as shown in Figure 14.2b.

Table 14.2 is the steady-state material balance of the reaction section of Figure 14.2b for a plant designed to process 7,750 barrels (42 gal/bbl) per operating day of fresh toluene feed. The gas permeation membrane system separates the flash vapor (stream S11) into an H_2 -enriched permeate (S14, the recycled hydrogen), and a methane-enriched retentate (S12, the purge). The flash vapor to the membrane system contains 89.74 mol% H_2 and 9.26 mol% CH_4 . No sweep fluid is necessary. The permeate is enriched to 94.46 mol% in H_2 . The retentate is enriched in CH_4 to 31.18 mol%. The recovery of H_2 in the permeate is 90%. Thus, only 10% of the H_2 in the vapor leaving the flash drum is lost to the purge. Before entering the membrane separator system, the vapor is heated to a

Table 14.1 Industrial Applications of Membrane Separation Processes

1. Reverse osmosis:
Desalinization of brackish water
Treatment of wastewater to remove a wide variety of impurities
Treatment of surface and ground water
Concentration of foodstuffs
Removal of alcohol from beer and wine
2. Dialysis:
Separation of nickel sulfate from sulfuric acid
Hemodialysis (removal of waste metabolites, excess body water, and restoration of electrolyte balance in blood)
3. Electrodialysis:
Production of table salt from seawater
Concentration of brines from reverse osmosis
Treatment of wastewaters from electroplating
Demineralization of cheese whey
Production of ultrapure water for the semiconductor industry
4. Microfiltration:
Sterilization of drugs
Clarification and biological stabilization of beverages
Purification of antibiotics
Separation of mammalian cells from a liquid
5. Ultrafiltration:
Preconcentration of milk before making cheese
Clarification of fruit juice
Recovery of vaccines and antibiotics from fermentation broth
Color removal from Kraft black liquor in paper-making
6. Pre evaporation:
Dehydration of ethanol-water azeotrope
Removal of water from organic solvents
Removal of organics from water
7. Gas permeation:
Separation of CO ₂ or H ₂ from methane and other hydrocarbons
Adjustment of the H ₂ /CO ratio in synthesis gas
Separation of air into nitrogen- and oxygen-enriched streams
Recovery of helium
Recovery of methane from biogas
8. Liquid membranes:
Recovery of zinc from wastewater in the viscose fiber industry
Recovery of nickel from electroplating solutions

temperature of at least 200°F (the dew-point temperature of the retentate) at a pressure of 450 psia (heater not shown). Because the hydrogen content of the feed is reduced in passing through the membrane separator, the retentate becomes more concentrated in the heavier components. Without the heater, undesirable condensation would occur in the separator. The retentate leaves the separator at about the same temperature and pressure as that of heated flash vapor entering the separator. The permeate leaves at

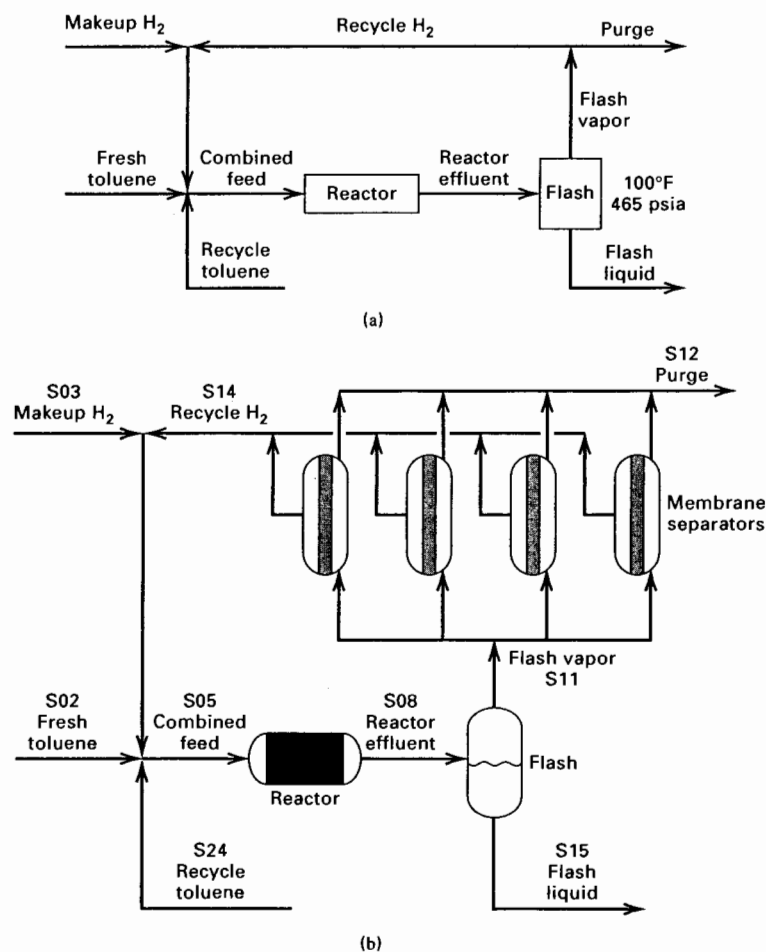


Figure 14.2 Reactor section of process to disproportionate toluene into benzene and xylene isomers. (a) Without a vapor separation step. (b) With a membrane separation step. Note: Heat exchangers, compressors, pump not shown.

Table 14.2 Material Balance for Membrane Separation Process in a Toluene Disproportionation Plant; Flow Rates in lbmol/h for Streams in Reactor Section of Figure 14.2b

Component	S02	S03	S24	S14	S05	S08	S15	S11	S12
Hydrogen		269.0		1,685.1	1,954.1	1,890.6	18.3	1,872.3	187.2
Methane		50.4		98.8	149.3	212.8	19.7	193.1	94.3
Ethane		16.8			16.8	16.8	5.4	11.4	11.4
Benzene			13.1		13.1	576.6	571.8	4.8	4.8
Toluene	1,069.4		1,333.0		2,402.4	1,338.9	1,334.7	4.2	4.2
<i>p</i> -Xylene			8.0		8.0	508.0	507.4	0.6	0.6
Total	1,069.4	336.3	1,354.1	1,783.9	4,543.7	4,543.7	2,457.4	2,086.3	302.4

the much lower pressure of 50 psia and a temperature somewhat lower than 200°F because of gas expansion.

The membrane is an aromatic polyamide polymer consisting of a 0.3-micron-thick, nonporous layer in contact with the feed, and a much thicker porous support backing to give the membrane strength and ability to withstand the pressure differential of $450 - 50 = 400$ psi. This large pressure difference is needed to force the hydrogen through the nonporous membrane, which is in the form of a spiral-wound module made from flat membrane sheets. The average flux of hydrogen through the membrane is 40 scfh (standard ft³/h at 60°F and 1 atm) per ft² of membrane surface area. From the material balance in Table 14.2, the total amount of H₂ transported through the membrane is

$$(1,685.1 \text{ lbmol/h})(379 \text{ scf/lbmol}) = 639,000 \text{ scfh}$$

Thus, the required membrane surface area is $639,000/40 = 16,000 \text{ ft}^2$. The membrane is packaged in pressure-vessel modules of 4,000 ft² each. Thus, four modules in parallel are used, as shown in Figure 14.2b. A disadvantage of the membrane separator in this application is the need to recompress the recycle hydrogen to the reactor inlet pressure. Unlike distillation, where the energy of separation is usually heat, the energy for gas permeation is the shaft work of gas compression.

Membrane separation is an emerging unit operation. Important progress is still being made in the development of efficient membrane materials and the packaging thereof for the processes listed in Table 14.1. Other novel methods for conducting separation with barriers for a wider variety of mixtures are being researched and developed. Applications covering wider ranges of temperature and types of membrane materials are being found. Already, membrane separation processes have found wide application in such diverse industries as the beverage, chemical, dairy, electronic, environmental, food, medical, paper, petrochemical, petroleum, pharmaceutical, and textile industries. Some of these applications are given in Table 1.2 and included in Table 14.1. Often, compared to other separation equipment, membrane separators are more compact, less capital intensive, and more easily operated, controlled, and maintained. However, membrane separators are usually modular in construction, with many parallel units required for large-scale applications, as contrasted with the more common separation techniques, where larger pieces of equipment are designed as plant size becomes larger.

The key to an efficient and economical membrane separation process is the membrane and the manner in which it is packaged and modularized. Desirable attributes of a membrane are (1) good permeability, (2) high selectivity, (3) chemical and mechanical compatibility with the processing environment, (4) stability, freedom from fouling, and reasonable useful life, (5) amenability to fabrication and packaging, and (6) ability to withstand large pressure differences across the membrane thickness. Research and development of membrane processes deals mainly with the discovery of suitable membrane materials and their fabrication.

This chapter discusses types of membrane materials, membrane modules, the theory of transport through membrane materials and modules, and the scale-up of membrane separators from experimental performance data. Emphasis is on dialysis, electrodialysis, reverse osmosis, gas permeation, and pervaporation, but many of the theoretical principles apply as well to emerging, but not yet commercialized, membrane processes such as membrane distillation, membrane gas absorption, membrane stripping, membrane solvent extraction, perstraction, and facilitated transport. The use of membranes in microfiltration and ultrafiltration is not discussed. The status of industrial membrane separa-

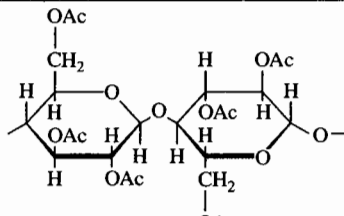
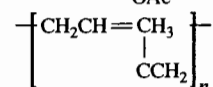
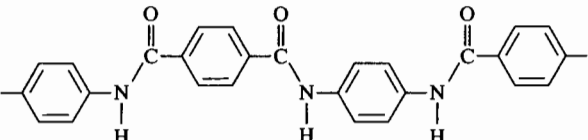
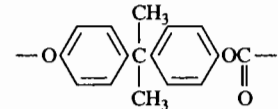
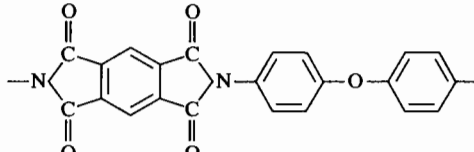
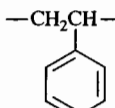
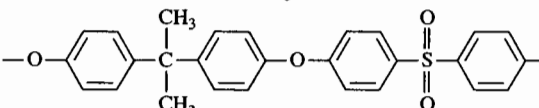
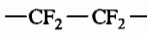
ration systems and directions in research to improve existing applications and make possible new applications are considered in detail by Baker et al. [5] in a study supported by the U.S. Department of Energy (DOE) and by a host of contributors in a recent handbook edited by Ho and Sirkar [6], which includes emerging membrane processes.

14.1 MEMBRANE MATERIALS

Almost all industrial membrane processes are made from natural or synthetic polymers (macromolecules). Natural polymers include wool, rubber, and cellulose. A wide variety of synthetic polymers has been developed and commercialized since 1930. Synthetic polymers are produced by polymerization of a monomer by condensation (step reactions) or addition (chain reactions), or by the copolymerization of two different monomers. The resulting polymer is categorized as having (1) a long linear chain, such as linear polyethylene; (2) a branched chain, such as polybutadiene; (3) a three-dimensional, highly cross-linked structure, such as phenol-formaldehyde; or (4) a moderately cross-linked structure, such as butyl rubber. The linear-chain polymers soften with an increase in temperature, are often soluble in organic solvents, and are referred to as *thermoplastic* polymers. At the other extreme, highly cross-linked polymers do not soften appreciably, are almost insoluble in most organic solvents, and are referred to as *thermosetting* polymers. Of more interest in the application of polymers to membranes is a classification based on the arrangement or conformation of the polymer molecules. At low temperatures, typically below 100°C, idealized polymers can be classified as *glassy* or *crystalline*. The former refers to a polymer that is brittle and glassy in appearance and lacks any crystalline structure (i.e., *amorphous*), whereas the latter refers to a polymer that is brittle, hard, and stiff, with a crystalline structure. If the temperature of a glassy polymer is increased, a point, called the *glass-transition temperature*, T_g , may be reached where the polymer becomes *rubbery*. If the temperature of a crystalline polymer is increased, a point, called the *melting temperature*, T_m , is reached where the polymer becomes a melt. However, a thermosetting polymer never melts. Most polymers have both amorphous and crystalline regions, that is, a certain degree of crystallinity that varies from 5 to 90%, making it possible for some polymers to have both a T_g and a T_m . Membranes made of glassy polymers can operate below or above T_g ; membranes of crystalline polymers must operate below T_m . Table 14.3 lists *repeat units* and values of T_g and/or T_m for several natural and synthetic polymers, from which membranes have been fabricated. Included are crystalline, glassy, and rubbery polymers. Cellulose triacetate is the reaction product of cellulose and acetic anhydride. Cellulose is the most readily available organic raw material in the world. The repeat unit of cellulose is identical to that shown for cellulose triacetate in Table 14.3, except that the acetyl, Ac (CH_3CO) groups are replaced by H. Typically, the number of repeat units (*degree of polymerization*) in cellulose is 1,000 to 1,500, whereas that in cellulose triacetate is around 300. Partially acetylated products are cellulose acetate and cellulose diacetate, with blends of two or three of the acetates being common. The triacetate is highly crystalline, of uniformly high quality, and hydrophobic.

Polyisoprene (natural rubber) is obtained from at least 200 different plants, with many of the rubber-producing countries being located in the Far East. Compared to the other polymers in Table 14.3, polyisoprene has a very low glass-transition temperature. Natural rubber has a degree of polymerization of from about 3,000 to 40,000 and is hard and rigid when cold, but soft, easily deformed, and sticky when hot. Depending on the temperature, it slowly crystallizes. To increase the strength, elasticity and stability of rubber, it is vulcanized with sulfur, a process that introduces cross-links, but still allows unrestricted local motion of the polymer chain.

Table 14.3 Common Polymers Used in Membranes

Polymer	Type	Representative Repeat Unit	Glass Transition Temp., °C	Melting Temp., °C
Cellulose triacetate	Crystalline			300
Polyisoprene (natural rubber)	Rubbery		-70	
Aromatic polyamide	Crystalline			275
Polycarbonate	Glassy		150	
Polyimide	Glassy		310-365	
Polystyrene	Glassy		74-110	
Polysulfone	Glassy		190	
Polytetrafluoroethylene (Teflon)	Crystalline			327

Aromatic polyamides (also called aramids) are high-melting crystalline polymers that have better long-term thermal stability and higher resistance to solvents than do aliphatic polyamides, such as nylon. Some aromatic polyamides are easily fabricated into fibers, films, and sheets. The polyamide structure shown in Table 14.3 is that of Kevlar, a trade name of DuPont.

Polycarbonates, which are characterized by the presence of the -OCOO- group in the chain, are mainly amorphous in structure. The polycarbonate shown in Table 14.3 is an aromatic form, but aliphatic forms also exist. Polycarbonates differ from most other amorphous polymers in that they possess ductility and toughness below T_g . Because polycarbonates are thermoplastic, they can be extruded into various shapes, including films and sheets.

Polyimides are characterized by the presence of aromatic rings and heterocyclic rings containing nitrogen and attached oxygen. The structure shown in Table 14.3 is only one of a number available. Polyimides are tough, amorphous polymers with high resistance to heat and excellent wear resistance. They can be fabricated into a wide variety of forms, including fibers, sheets, and films.

Polystyrene is a linear, amorphous, highly pure polymer of about 1,000 units of the structure shown in Table 14.3. Above a relatively low T_g , which depends on molecular weight, polystyrene becomes a viscous liquid that is easily fabricated by extrusion or injection molding. Like many other polymers, polystyrene can be annealed (heated and then cooled slowly) to convert it to a crystalline polymer with a melting point of 240°C. Styrene monomer can be copolymerized with a number of other organic monomers, including acrylonitrile and butadiene to form ABS copolymers.

Polysulfones are relatively new synthetic polymers, first introduced in 1966. The structure in Table 14.3 is just one of many, all of which contain the SO_2 group, which gives the polymers high strength. Polysulfones are easily spun into hollow fibers.

Polytetrafluoroethylene is a straight-chain, highly crystalline polymer with a very high degree of polymerization of the order of 100,000, which gives it considerable strength. It possesses exceptional thermal stability and can be formed into sheets, films, and tubing.

To be effective for separating a mixture of chemical components, a polymer membrane must possess high *permeance* and a high permeance ratio for the two species being separated by the membrane. The permeance for a given species diffusing through a membrane of given thickness is analogous to a mass transfer coefficient, i.e., the flow rate of that species per unit cross-sectional area of membrane per unit driving force (concentration, partial pressure, etc.). The molar transmembrane flux of species i is

$$N_i = \left(\frac{P_{M_i}}{l_M} \right) (\text{driving force}) = \bar{P}_{M_i} (\text{driving force}) \quad (14-1)$$

where \bar{P}_{M_i} is the permeance, which is defined as the ratio of P_{M_i} , the *permeability*, to l_M , the membrane thickness.

Polymer membranes can be dense or microporous. For dense amorphous membranes, no pores of microscopic dimensions are present, and diffusing species must dissolve into the polymer and then diffuse through the polymer between the segments of the macromolecular chains. Diffusion can be difficult, but highly selective for glassy polymers. If the polymer is partly crystalline, diffusion will occur almost exclusively through the amorphous regions, with the crystalline regions decreasing the diffusion area and increasing the diffusion path.

A microporous membrane contains interconnected pores that are small (on the order of 0.005–20 μm ; 50–200,000 Å), but large in comparison to the size of small molecules. The pores are formed by a variety of proprietary techniques, some of which are described by Baker et al. [5]. Such techniques are especially valuable for producing symmetric, microporous, crystalline membranes. Permeability for microporous membranes is high, but selectivity is low for small molecules. However, when molecules both smaller and larger than the pore size are in the feed to the membrane, the molecules may be separated almost perfectly by size.

Thus, for the separation of small molecules, we seem to be presented with a dilemma. We can have high permeability or a high separation factor, but not both. The beginning of the resolution of this dilemma occurred in 1963 with the fabrication by Loeb and Sourirajan [7] of an asymmetric membrane of cellulose acetate by a novel casting procedure. As shown in Figure 14.3a, the resulting membrane consists of a thin dense skin about 0.1–1.0 μm in thick, called the *permselective* layer, formed over a much thicker microporous layer that provides support for the skin. The flux rate of a species is controlled by the permeance of the very thin permselective skin. From (14-1), the permeance of species i can be high because of the very small value of l_M even though the permeability, P_{M_i} , is

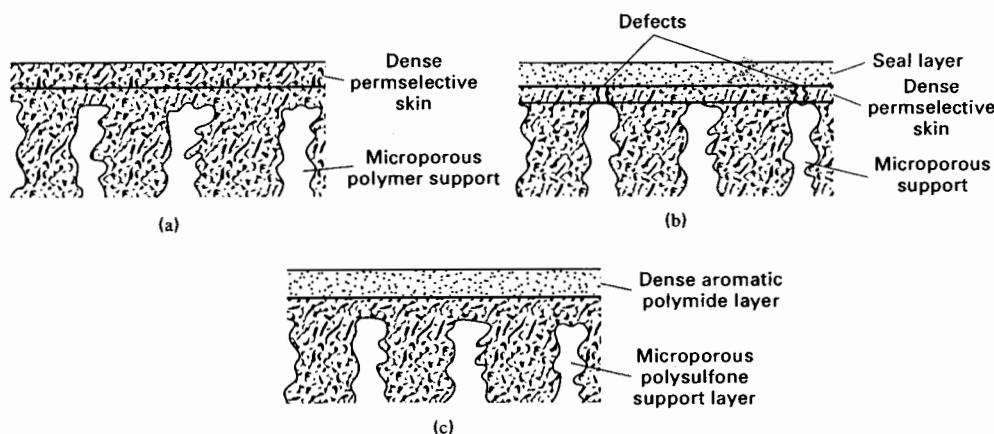


Figure 14.3 Polymer membranes: (a) asymmetric, (b) caulked asymmetric, and (c) typical thin-layer composite.

low because of the absence of pores. When large differences of P_{M_i} exist among molecules, both high permeance and high selectivity can be achieved with asymmetric membranes.

A very thin asymmetric membrane is subject to minute defects or pinholes in the permselective skin, which can render the membrane useless for the separation of a gas mixture. A practical solution to the defect problem for an asymmetric polysulfone membrane was patented by Henis and Tripodi [8] of the Monsanto Company in 1980. They pulled silicone rubber, from a coating on the surface of the skin, into the defects by applying a vacuum. The resulting membrane is sometimes referred to as a *caulked membrane*, as shown in Figure 14.3b.

Another patent by Wrasidlo [9] in 1977, introduced the thin-film composite membrane as an alternative to the asymmetric membrane. In the first application, as shown in Figure 14.3c, a very thin, dense film of polyamide polymer, 250 to 500 Å in thickness, was formed on a thicker microporous polysulfone support. Today asymmetric and thin-film composite membranes are fabricated from a variety of polymers by a variety of techniques.

The application of polymer membranes is generally limited to temperatures below about 200°C and to the separation of mixtures that are chemically inert. When operation at high temperatures and/or with chemically active mixtures is necessary, membranes made of inorganic materials can be used. These include mainly microporous ceramics, metals, and carbon; and dense metals, such as palladium, that allow the selective diffusion of very small molecules such as hydrogen and helium.

Some examples of inorganic membranes are (1) asymmetric microporous α -alumina tubes with 40–100 Å pores at the inside surface and 100,000 Å pores at the outside; (2) microporous glass tubes, the pores of which may or may not be filled with other oxides or the polymerization–pyrolysis product of trichloromethylsilane; (3) silica hollow fibers with extremely fine pores of 3–5 Å; (4) porous ceramic, glass, or polymer materials coated with a thin, dense film of palladium metal that is just a few microns thick; (5) sintered metal; (6) pyrolyzed carbon; and (7) zirconia on sintered carbon. Extremely fine pores (<10 Å) are necessary to separate gas mixtures. Larger pores (>50 Å) may be satisfactory for the separation of large molecules or solid particles from solutions containing small molecules.

EXAMPLE 14.1

A silica-glass membrane of 2 μm thickness and with very fine pores less than 10 Å in diameter has been developed for separating H_2 from CO at a temperature of 500°F. From laboratory data, the membrane permeabilities for hydrogen and carbon monoxide, respectively, are 200,000 and 700 barrer, where the barrer, a commonly used unit for gas permeation, is defined by:

$$1 \text{ barrer} = 10^{-10} \text{ cm}^3 (\text{STP})\text{-cm}/(\text{cm}^2\text{-s-cmHg})$$

where $\text{cm}^3 (\text{STP})/\text{cm}^2\text{-s}$ refers to the volumetric transmembrane flux of the diffusing species in terms of standard conditions of 0°C and 1 atm, cm refers to the membrane thickness, and cmHg refers to the transmembrane partial pressure driving force for the diffusing species.

The barrer unit is named for R. M. Barrer, who published an early article [10] on the nature of diffusion in a membrane, followed later by a widely referenced monograph on diffusion in and through solids [11].

If the transmembrane partial pressure driving forces for H_2 and CO , respectively, are 240 psi and 80 psi, calculate the transmembrane fluxes in $\text{kmol}/(\text{m}^2\text{-s})$. Compare the hydrogen flux to that for hydrogen in the commercial application discussed at the beginning of this chapter.

SOLUTION

At 0°C and 1 atm, 1 kmol of gas occupies $22.42 \times 10^6 \text{ cm}^3$. Also, $2 \mu\text{m}$ thickness $= 2 \times 10^{-4} \text{ cm}$ and $1 \text{ cmHg } \Delta P = 0.1934 \text{ psi}$. Therefore, using (14-1):

$$N_{\text{H}_2} = \frac{(200,000)(10^{-10})(240/0.1934)(10^4)}{(22.42 \times 10^6)(2 \times 10^{-4})} = 0.0554 \frac{\text{kmol}}{\text{m}^2\text{-s}}$$

$$N_{\text{CO}} = \frac{(700)(10^{-10})(80/0.1934)(10^4)}{(22.42 \times 10^6)(2 \times 10^{-4})} = 0.000065 \frac{\text{kmol}}{\text{m}^2\text{-s}}$$

In the application discussed at the beginning of this chapter, the flux of H_2 for the polymer membrane is

$$\frac{(1685.1)(1/2.205)}{(16,000)(0.3048)^2(3600)} = 0.000143 \frac{\text{kmol}}{\text{m}^2\text{-s}}$$

Thus, the flux of H_2 through the ultramicroporous glass membrane is more than 100 times higher than the flux through the dense polymer membrane. Large differences in molar fluxes through different membranes are common. ■

14.2 MEMBRANE MODULES

The asymmetric and thin-film composite polymer membrane materials described in the previous section are available in one or more of the three shapes shown in Figure 14.4a, b, and c. Flat sheets have typical dimensions of 1 m by 1 m by $200 \mu\text{m}$ thick, with a dense skin or thin, dense layer 500 to $5,000 \text{ \AA}$ in thickness. Tubular membranes are typically 0.5 to 5.0 cm in diameter and up to 6 m in length. The thin, dense layer is on either the inside, as shown in Figure 14.4b, or the outside surface of the tube. The porous supporting part of the tube is fiberglass, perforated metal, or other suitable porous material. Very small-diameter hollow fibers, first reported by Mahon [12,13] in the 1960s, are typically $42 \mu\text{m}$ i.d. by $85 \mu\text{m}$ o.d. by 1.2 m long with a 0.1 to $1.0 \mu\text{m}$ -thick dense skin. Hollow fibers, shown in Figure 14.4c, provide a large membrane surface area per unit volume. A honeycomb monolithic element for inorganic oxide membranes is shown in Figure 14.4d. Elements of both hexagonal and circular cross-section are available [14]. The circular flow channels are typically 0.3 to 0.6 cm in diameter, with a 20 to 40 mm-thick membrane layer. The hexagonal element in Figure 14.4d has 19 channels and is 0.85 m long. Both the bulk support and the thin membrane layer are porous, but the pores of the latter can be very small, down to 40 \AA .

The membrane shapes of Figure 14.4 are incorporated into compact commercial modules and cartridges, some of which are shown in Figure 14.5. Flat sheets used in plate-and-frame modules are circular, square, or rectangular in cross-section. The sheets are separated by support plates that channel the permeate. In Figure 14.5a, a feed of brackish water flows across the surface of each membrane sheet in the stack. Pure water is the permeate product, whereas the retentate is a concentrated brine solution.

Flat sheets are also fabricated into spiral-wound modules shown in Figure 14.5b. A laminate, consisting of two membrane sheets separated by spacers for the flow of the feed and permeate, is wound around a central perforated collection tube to form a module that

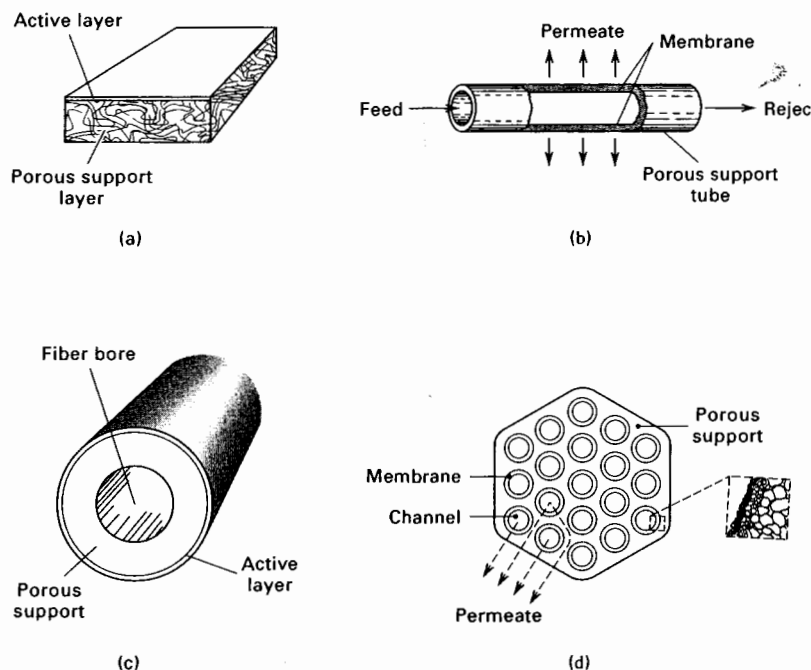


Figure 14.4 Common membrane shapes: (a) flat asymmetric or thin-composite sheet; (b) tubular; (c) hollow fiber; (d) monolithic.

is inserted into a pressure vessel. The feed flows axially in the channels created between the membranes by the porous spacers. Permeate passes through the membrane, traveling inward in a spiral path to the central collection tube. From there, the permeate flows in either axial direction through and out of the central tube. A typical spiral-wound module is 0.1 to 0.3 m in diameter and 3 m long. Six such modules are often placed in series. The four-leaf modification in Figure 14.5c minimizes the pressure drop of the permeate because the permeate travel is less for the same membrane area.

The hollow-fiber module shown in Figure 14.5d, for a gas permeation application, resembles a shell-and-tube heat exchanger. The pressurized feed enters the shell side at one end. While flowing over the fibers toward the other end, permeate passes through the fiber walls into the central fiber channels. Typically the fibers are sealed at one end and embedded into a tube sheet with epoxy resin at the other end. A commercial module might be 1 m long and 0.1 to 0.25 m in diameter and contain more than one million hollow fibers.

A tubular module is shown in Figure 14.5e. This module also resembles a shell-and-tube heat exchanger, but the feed flows through the tubes. Permeate passes through the wall of the tubes into the shell side of the module. Tubular modules contain up to 30 tubes.

The monolithic module in Figure 14.5f contains from 1 to 37 monolithic elements in a module housing. The feed flows through the circular channels and permeate passes through the membrane and porous support and into the open region between elements.

Table 14.4 is a comparison of the characteristics of four of the modules shown in Figure 14.5. The packing density is the membrane surface area per unit volume of module, for which the hollow-fiber membrane modules are clearly superior. Although the plate-and-frame module has a high cost and a moderate packing density, it finds use in all membrane applications except gas permeation. It is the only module widely used for pervaporation. The spiral-wound module is very popular for most applications because of its low cost and reasonable resistance to fouling. Tubular modules are only used for small applications or

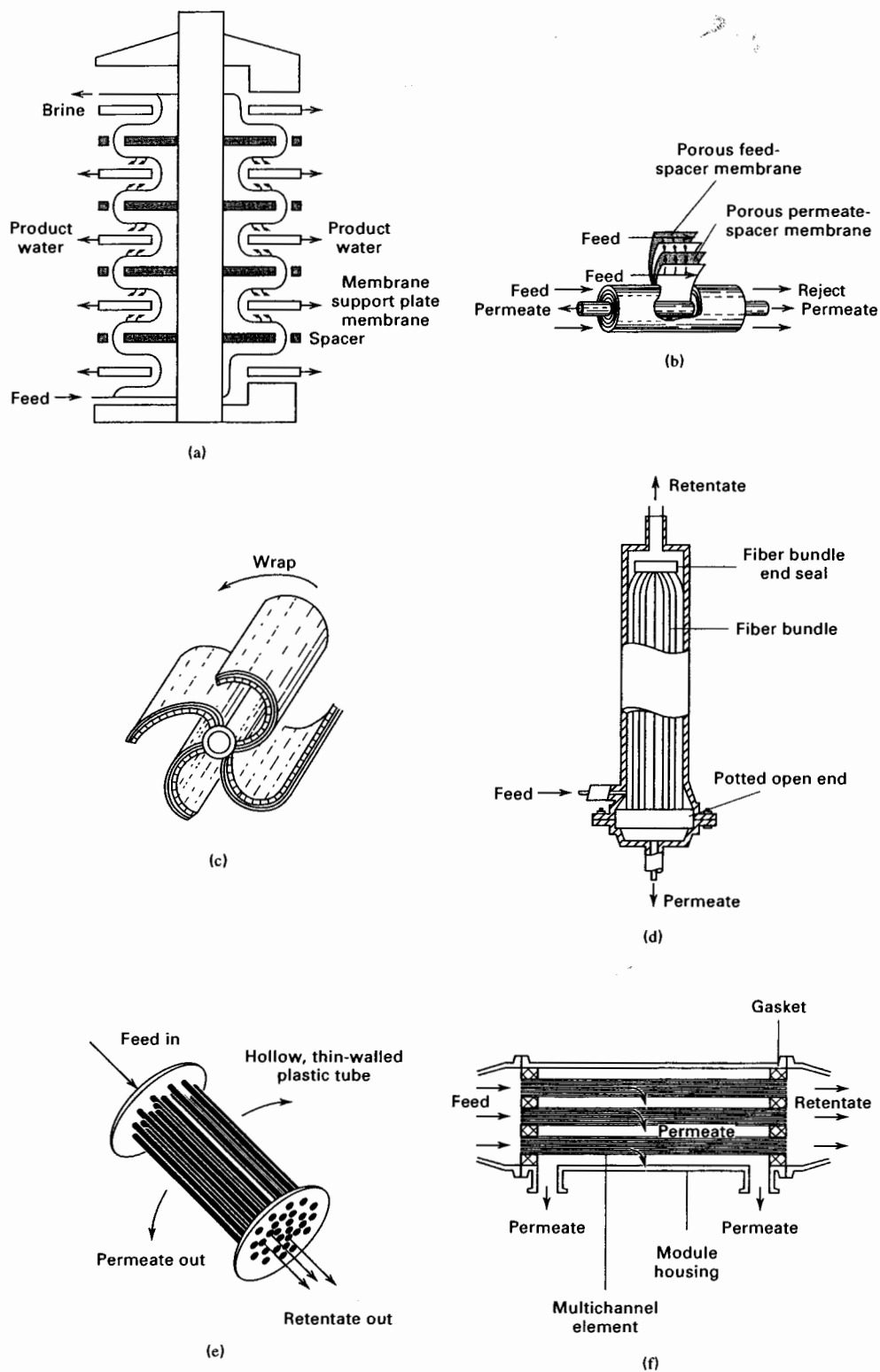


Figure 14.5 Common membrane modules: (a) plate-and frame, (b) spiral-wound, (c) four-leaf spiral-wound, (d) hollow-fiber, (e) tubular, (f) monolithic.

Table 14.4 Typical Characteristics of Membrane Modules

	Plate and Frame	Spiral-Wound	Tubular	Hollow-Fiber
Packing density, m ² /m ³	30 to 500	200 to 800	30 to 200	500 to 9,000
Resistance to fouling	Good	Moderate	Very good	Poor
Ease of cleaning	Good	Fair	Excellent	Poor
Relative cost	High	Low	High	Low
Main applications	D, RO, PV, UF, MF	D, RO, GP, UF, MF	RO, UF	D, RO, GP, UF

Note. D, dialysis; RO, reverse osmosis; GP, gas permeation; PV, pervaporation; UF, ultrafiltration; MF, microfiltration.

when a high resistance to fouling and/or ease of cleaning are essential. Hollow-fiber modules, with a very high packing density and low cost, are popular where fouling does not occur and cleaning is not necessary.

14.3 TRANSPORT IN MEMBRANES

For a given application, the calculation of the required membrane surface area is based on laboratory data for the selected membrane. Although permeation can occur by one or more of the mechanisms discussed in this section, these mechanisms are all consistent with (14-1) in either its permeance form or its permeability form, with the latter being applied more widely. However, because both the driving force and the permeability or permeance depend markedly on the mechanism of transport, it is important to understand the nature of transport in membranes, which is the subject of this section. Applications to dialysis, reverse osmosis, gas permeation, and pervaporation are presented in subsequent sections.

Membranes can be macroporous, microporous, or dense (nonporous). Only microporous or dense membranes are permselective. However, macroporous membranes are widely used to support thin microporous and dense membranes when significant pressure differences across the membrane are necessary to achieve a reasonable throughput. The theoretical basis for transport through microporous membranes is more highly developed than that for dense membranes, so porous-membrane transport is discussed first.

Porous Membranes

Mechanisms for the transport of liquid and gas molecules through a porous membrane are depicted in Figure 14.6a, b, and c. If the pore diameter is large compared to the molecular diameter, and a pressure difference exists across the membrane, bulk or convective flow through the pores occurs, as shown in Figure 14.6a. Such a flow is generally undesirable

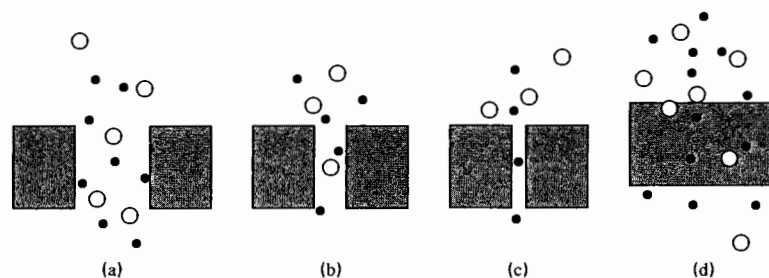


Figure 14.6 Mechanisms of transport in membranes. (Flow is downward.) (a) Bulk flow through pores; (b) diffusion through pores; (c) restricted diffusion through pores; (d) solution-diffusion through dense membranes.

because it is not permselective and, therefore, no separation between components of the feed occurs. If fugacity, activity, chemical potential, concentration, or partial pressure differences exist across the membrane for the various components, but the pressure is the same on both sides of the membrane, permselective diffusion of the components through the pores will take place, effecting a separation as shown in Figure 14.6b. If the pores are of the order of molecular size for at least some of the components in the feed mixture, the diffusion of those components will be restricted (hindered) as shown in Figure 14.6c, resulting in an enhanced separation. Molecules of size larger than the pores will be prevented altogether from diffusing through the pores. This special case is highly desirable and is referred to as *sieving*. Another special case exists for gas diffusion where the pore size and/or pressure (typically a vacuum) is such that the mean free path of the molecules is greater than the pore diameter, resulting in so-called *Knudsen diffusion*, which is dependent on molecular weight.

Bulk Flow

Consider the bulk flow of a fluid, due to a pressure difference, through an idealized straight, cylindrical pore. If the flow is in the laminar regime ($N_{Re} = Dv\rho/\mu < 2,100$), which is almost always the case for flow in small-diameter pores, the flow velocity, v , is given by the Hagen-Poiseuille law [15] as being directly proportional to the transmembrane pressure drop:

$$v = \frac{D^2}{32\mu L} (P_0 - P_L) \quad (14-2)$$

where D is the pore diameter, μ is the viscosity of the fluid, and L is the length of the pore. This law assumes that a parabolic velocity profile exists across the pore radius for the entire length of the pore, that the fluid is Newtonian, and if a gas, that the mean free path of the molecules is small compared to the pore diameter. If the membrane contains n such pores per unit cross-section of membrane surface area normal to flow, the porosity (void fraction) of the membrane is

$$\epsilon = n\pi D^2/4 \quad (14-3)$$

Then the superficial fluid bulk-flow flux (mass velocity), N , through the membrane is

$$N = \frac{\epsilon\rho D^2}{32\mu l_M} (P_0 - P_L) = \frac{n\pi\rho D^4}{128\mu l_M} (P_0 - P_L) \quad (14-4)$$

where l_M is the membrane thickness and ρ and μ are fluid properties.

In real porous membranes, pores may not be cylindrical and straight, making it necessary to modify (14-4). One procedure is that due to Carman and Kozeny, as extended by Ergun [16], where the pore diameter in (14-2) is replaced, as a rough approximation, by the hydraulic diameter:

$$\begin{aligned} d_H &= 4 \left(\frac{\text{Volume available for flow}}{\text{Total pore surface area}} \right) \\ &= \frac{4 \left(\frac{\text{Total pore volume}}{\text{Membrane volume}} \right)}{\left(\frac{\text{Total pore surface area}}{\text{Membrane volume}} \right)} = \frac{4\epsilon}{a} \end{aligned} \quad (14-5)$$

where the membrane volume includes the volume of the pores. The specific surface area, a_v , which is the pore surface area per unit volume of membrane, is

$$a_v = a/(1 - \epsilon) \quad (14-6)$$

Pore length is longer than the membrane thickness and can be represented by $l_M \tau$, where τ is a tortuosity factor >1 . Substituting (14-5), (14-6), and the tortuosity factor into (14-4) gives

$$N = \frac{\rho \epsilon^3 (P_0 - P_L)}{2(1 - \epsilon)^2 \tau a_v^2 \mu l_M} \quad (14-7)$$

In terms of a bulk-flow permeability, (14-7) becomes

$$N = \frac{P_M}{l_M} (P_0 - P_L) \quad (14-8)$$

where

$$P_M = \frac{\rho \epsilon^3}{2(1 - \epsilon)^2 \tau a_v^2 \mu} \quad (14-9)$$

Typically, τ is approximately 2.5, whereas a_v is inversely proportional to the average pore diameter, giving it values over a wide range.

Equation (14-7) may be compared to the following semitheoretical Ergun equation [16], which represents the best fit of experimental data for flow of a fluid through a packed bed:

$$\frac{P_0 - P_L}{l_M} = \frac{150 \mu v_0 (1 - \epsilon)^2}{D_p^2 \epsilon^3} + \frac{1.75 \rho v_0^2 (1 - \epsilon)}{D_p \epsilon^3} \quad (14-10)$$

where D_p is the mean particle diameter and v_0 is the superficial fluid velocity through the membrane. The first term on the right-hand side of (14-10) applies to the laminar flow region and the second to the turbulent region. For a spherical particle:

$$a_v = \pi D_p^2 / (\pi D_p^3 / 6) \text{ or} \quad (14-11)$$

$$D_p = 6/a_v$$

Substitution of (14-11) into (14-10), for just the laminar-flow region, and rearrangement into the bulk-flow flux form gives

$$N = \frac{\rho \epsilon^3 (P_0 - P_L)}{(150/36)(1 - \epsilon)^2 a_v^2 \mu l_M} \quad (14-12)$$

Comparing (14-12) to (14-7), we see that the term (150/36) in (14-12) corresponds to the term (2t) in (14-7). Thus, τ appears to have a value of 2.08, which seems reasonable. Accordingly, (14-12) can be used as a first approximation to the pressure drop for flow through a porous membrane when the pores are not straight cylinders. For gas flow, the density may be taken as the arithmetic average of the densities at the upstream and downstream faces of the membrane.

It is desired to pass water at 70°F through a supported polypropylene membrane, with a skin of 0.003 cm thickness and 35% porosity, at the rate of 200 m³/m²-day. The pores can be considered as straight cylinders of uniform diameter equal to 0.2 micron. If the pressure on the downstream side of the membrane is 150 kPa, estimate the required pressure on the upstream side of the membrane. The pressure drop through the support is negligible.

SOLUTION

Equation (14-4) applies, where in SI units:

$$N/\rho = 200/(24)(3600) = 0.0023 \text{ m}^3/\text{m}^2\text{-s} \quad \epsilon = 0.35$$

$$D_p = 0.2 \times 10^{-6} \text{ m} \quad l_M = 0.00003 \text{ m}$$

$$P_L = 150 \text{ kPa} = 150,000 \text{ Pa} \quad \mu = 0.001 \text{ Pa-s}$$

$$\begin{aligned} \text{From (14-4), } P_0 &= P_L + \frac{32 \mu l_M (N/\rho)}{\epsilon D_p^2} \\ &= 150,000 + \frac{(32)(0.001)(0.00003)(0.00232)}{(0.35)(0.2 \times 10^{-6})^2} = 309,000 \text{ Pa or } 309 \text{ kPa} \end{aligned}$$

Liquid Diffusion

Consider the diffusion of species through the pores of a membrane from a fluid feed to a sweep fluid when identical total pressures but different component concentrations exist on both sides of the membrane. In that case, bulk flow through the membrane due to a pressure difference does not occur and if species diffuse at different rates, a separation can be achieved. If the feed mixture is a liquid of solvent and solutes i , the solute transmembrane flux is given by a modified form of Fick's law:

$$N_i = \frac{D_{e_i}}{l_M} (c_{i_0} - c_{i_L}) \quad (14-13)$$

where D_{e_i} is the effective diffusivity, and c_i is the concentration of i in the liquid in the pores at the two faces of the membrane. In general the effective diffusivity is given by

$$D_{e_i} = \frac{\epsilon D_i}{\tau} K_r \quad (14-14)$$

where D_i is the ordinary molecular diffusion coefficient (diffusivity) of the solute i in the solution, ϵ is the volume fraction of pores in the membrane, τ is the tortuosity, and K_r is a restrictive factor that accounts for the effect of pore diameter, d_p , when the ratio of molecular diameter, d_m , to pore diameter exceeds about 0.01. The restrictive factor is approximated by Beck and Schultz [17] with:

$$K_r = \left[1 - \frac{d_m}{d_p} \right]^4, (d_m/d_p) \leq 1 \quad (14-15)$$

From (14-15), when $(d_m/d_p) = 0.01$, $K_r = 0.96$, but when $(d_m/d_p) = 0.3$, $K_r = 0.24$. When $d_m > d_p$, $K_r = 0$, and the solute cannot diffuse through the pore. This is the sieving effect illustrated in Figure 14.6c. In general, as illustrated in the following example, transmembrane fluxes for liquids through microporous membranes are very small because effective diffusivities are very low.

Beck and Schultz [18] measured effective diffusivities of urea and several different sugars, in aqueous solutions, through microporous membranes of mica, which were especially prepared to give almost straight, elliptical pores of almost uniform size. Based on the following data for a membrane and two solutes, estimate the transmembrane fluxes for the two solutes in $\text{g/cm}^2\text{-s}$ at 25°C . Assume that the aqueous solutions on either side of the membrane are sufficiently dilute that no multicomponent diffusional effects are present.

Membrane:

Material	Microporous mica
Thickness, μm	4.24
Average pore diameter, Angstroms	88.8
Tortuosity, τ	1.1
Porosity, ϵ	0.0233

Solutes (in aqueous solution at 25°C):

Solute	$D_i \times 10^6 \text{ cm}^2/\text{s}$	molecular diameter, $d_m, \text{\AA}$	g/cm^3	
			c_{i_0}	c_{i_L}
1 Urea	13.8	5.28	0.0005	0.0001
2 β -Dextrin	3.22	17.96	0.0003	0.00001

SOLUTION

Calculate the restrictive factor and effective diffusivity from (14-15) and (14-14), respectively. For urea (1):

$$K_r = \left[1 - \left(\frac{5.28}{88.8} \right) \right]^4 = 0.783; D_{e_1} = \frac{(0.0233)(13.8 \times 10^{-6})(0.783)}{1.1} = 2.29 \times 10^{-7} \text{ cm}^2/\text{s}$$

For β -dextrin (2):

$$K_{r_2} = \left[1 - \left(\frac{17.96}{88.8} \right) \right]^4 = 0.405; D_{e_2} = \frac{(0.0233)(3.22 \times 10^{-6})(0.405)}{1.1} = 2.78 \times 10^{-8} \text{ cm}^2/\text{s}$$

Because of the large differences in molecular size, the two effective diffusivities differ by almost an order of magnitude.

Calculate transmembrane fluxes from (14.13) noting the given concentrations are at the two faces of the membranes. Concentrations in the bulk solutions on either side of the membrane will differ from the concentrations at the faces depending upon the magnitudes of the mass-transfer resistances in boundary layers or films adjacent to the two faces of the membrane.

$$\text{For urea: } N_1 = \frac{(2.29 \times 10^{-7})(0.0005 - 0.0001)}{4.24 \times 10^{-4}} = 2.16 \times 10^{-7} \text{ g/cm}^2\text{-s}$$

$$\text{For } \beta\text{-dextrin: } N_2 = \frac{(2.768 \times 10^{-8})(0.0003 - 0.00001)}{(4.24 \times 10^{-4})} = 1.90 \times 10^{-8} \text{ g/cm}^2\text{-s}$$

Note that these fluxes are extremely low. ■

Gas Diffusion

When the mixture on either side of a microporous membrane is a gas, the rate of species diffusion can again be expressed in terms of Fick's law. If pressure and temperature on either side of the membrane are equal and the ideal gas law holds, (14-13) can be written in terms of a partial pressure driving force:

$$N_i = \frac{D_{e_i} c_M}{Pl_M} (p_{i_0} - p_{i_L}) \quad (14-16)$$

where c_M is the total concentration of the gas mixture given as P/RT by the ideal gas law. Thus, (14-16) can be written alternatively as

$$N_i = \frac{D_{e_i}}{RTl_M} (p_{i_0} - p_{i_L}) \quad (14-17)$$

For a gas, diffusion may occur by ordinary diffusion, as with a liquid, and/or in series with Knudsen diffusion when pore diameter is very small and/or total pressure is low. In the Knudsen flow regime, collisions occur primarily between gas molecules and the pore wall, rather than between gas molecules. Thus, in the absence of a bulk flow effect, (14-14) is modified for gas flow:

$$D_{e_i} = \frac{\epsilon}{\tau} \left[\frac{1}{(1/D_i) + (1/D_{K_i})} \right] \quad (14-18)$$

where D_{K_i} is the Knudsen diffusivity, which from the kinetic theory of gases applied to a straight cylindrical pore, is given by

$$D_{K_i} = \frac{d_p \bar{v}_i}{3} \quad (14-19)$$

where \bar{v}_i is the average molecule velocity given by:

$$\bar{v}_i = (8RT/\pi M_i)^{1/2} \quad (14-20)$$

where M is the molecular weight. Combining (14-19) and (14-20):

$$D_{K_i} = 4,850 d_p (T/M_i)^{1/2} \quad (14-21)$$

where D_K is cm^2/s , d_p is cm , and T is K . When Knudsen flow predominates, as it often does for the micropores in membranes, the permeability ratio for species A and B is given from a combination of (14-1), (14-17), (14-18), and (14-21):

$$\frac{P_{M_A}}{P_{M_B}} = \left(\frac{M_B}{M_A} \right)^{1/2} \quad (14-22)$$

Except for gaseous species of widely differing molecular weight, the permeability ratio from (14-22) is not large, and the separation of gases by microporous membranes at low to moderate pressures that are equal on both sides of the membrane to minimize bulk flow is almost always impractical, as illustrated in the following example. However, it is important to note that the separation of the two isotopes of UF_6 by the United States government was accomplished by Knudsen diffusion, with a permeability ratio of only 1.0043, on a large scale at Oak Ridge using thousands of stages and many acres of membrane surface.

A gas mixture of hydrogen (H) and ethane (E) is to be partially separated with a composite membrane having a 1- μm -thick porous skin with an average pore size of 20 Å and a porosity of 30%. The tortuosity can be assumed to be 1.5. The pressure on either side of the membrane is 10 atm and the temperature is 100°C. Estimate the permeabilities of the two components in barrers.

SOLUTION

From (14-1), (14-17), and (14-18), the permeability can be expressed in $\text{gmol-cm}/\text{cm}^2\text{-s-atm}$:

$$P_{M_i} = \frac{\epsilon}{RT\tau} \left[\frac{1}{(1/D_i) + (1/D_K)} \right],$$

where $\epsilon = 0.30$, $R = 82.06 \text{ cm}^3\text{-atm}/\text{mol-K}$, $T = 373 \text{ K}$, and $\tau = 15$

At 100°C, the ordinary diffusivity is given by $D_H = D_E = D_{H,E} = 0.86/P$ in cm^2/s with total pressure P in atm. Thus, at 10 atm, $D_H = D_E = 0.086 \text{ cm}^2/\text{s}$. Knudsen diffusivities are given by (14-21) with pore diameter, d_p , equal to $20 \times 10^{-8} \text{ cm}$.

$$D_{K_H} = 4,850(20 \times 10^{-8})(373/2.016)^{1/2} = 0.0132 \text{ cm}^2/\text{s}$$

$$D_{K_E} = 4,850(20 \times 10^{-8})(373/30.07)^{1/2} = 0.00342 \text{ cm}^2/\text{s}$$

For both components, diffusion is controlled mainly by Knudsen diffusion. For hydrogen:

$$\frac{1}{(1/D_H) + (1/D_{K_H})} = 0.0114 \text{ cm}^2/\text{s}. \text{ For ethane: } \frac{1}{(1/D_E) + (1/D_{K_E})} = 0.00329 \text{ cm}^2/\text{s}.$$

$$P_{M_H} = \frac{0.30(0.0114)}{(82.06)(373)(1.5)} = 7.45 \times 10^{-8} \frac{\text{mol-cm}}{\text{cm}^2\text{-s-atm}}$$

$$P_{M_E} = \frac{0.30(0.00329)}{(82.06)(373)(1.5)} = 2.15 \times 10^{-8} \frac{\text{mol-cm}}{\text{cm}^2\text{-s-atm}}$$

To convert to barrer as defined in Example 14.1, note that

$$76 \text{ cmHg} = 1 \text{ atm and } 22,400 \text{ cm}^3(\text{STP}) = 1 \text{ mol}$$

$$P_{M_H} = \frac{7.45 \times 10^{-8} (22,400)}{(10^{-10})(76)} = 220,000 \text{ barrer}$$

$$P_{M_E} = \frac{2.15 \times 10^{-8} (22,400)}{(10^{-10})(76)} = 63,400 \text{ barrer}$$

Nonporous Membranes

The transport of components through nonporous (dense) solid membranes is the predominant mechanism of membrane separators for reverse osmosis (liquid), gas permeation (gas), and pervaporation (liquid and vapor). As indicated in Figure 14.6d, gas or liquid components absorb into the membrane at the upstream face, diffuse through the solid membrane, and desorb at the downstream face.

Liquid diffusivities are several orders of magnitude less than gas diffusivities, and diffusivities of solutes in solids are a few orders of magnitude less than diffusivities in liquids. Thus, differences between diffusivities in gases and solids are enormous. For example, at 1 atm and 25°C, diffusivities in cm²/s for water are as follows:

Water vapor in air	0.25
Water in ethanol liquid	1.2×10^{-5}
Dissolved water in cellulose acetate solid	1×10^{-8}

As might be expected, small molecules fare better than large molecules for diffusivities in solids. For example, from the *Polymer Handbook* [19], diffusivities in cm²/s for several components in low-density polyethylene at 25°C are

Helium	6.8×10^{-6}
Hydrogen	0.474×10^{-6}
Nitrogen	0.320×10^{-6}
Propane	0.0322×10^{-6}

Regardless of whether a nonporous membrane is used to separate a gas or liquid mixture, the *solution-diffusion model* of Lonsdale, Merten, and Riley [20] is most often applied to analyze experimental permeability data and design membrane separators. This model is based on Fick's law for diffusion through solid nonporous membranes based on the driving force, $c_{i_0} - c_{i_L}$, where the concentrations are those for the solute dissolved in the membrane. The concentrations in the membrane are related to the concentrations or partial pressures in the fluid adjacent to the membrane faces by assuming thermodynamic equilibrium at the fluid-membrane interfaces. This assumption has been validated experimentally by Motanedian et al. [21] for the case of permeation of light gases through dense cellulose acetate membranes at up to 90 atm.

Solution-Diffusion for Liquid Mixtures

Figures 14.7a and b show typical solute concentration profiles for liquid mixtures with porous and nonporous membranes, respectively. Included in these diagrams is the drop in concentration across the membrane and, also, possible drops due to resistances in the fluid boundary layers or films on either side of the membrane. For porous membranes, of the type considered in the previous section, the concentration profile is continuous from the bulk feed liquid to the bulk permeate liquid because liquid is present continuously from one side to the other. The concentration c_{i_0} is the same in the liquid feed just adjacent to the membrane surface and in the liquid just within the entrance of the pore. This is not the case for the nonporous membrane in Figure 14.7b. Solute concentration c'_{i_0} is that in the feed liquid just adjacent to the upstream membrane surface, whereas c_{i_0} is that in the membrane just adjacent to the upstream membrane surface. In general, c_{i_0} is considerably smaller than c'_{i_0} , but the two are related by a thermodynamic equilibrium partition coefficient K_i , defined by

$$K_i = c_{i_0}/c'_{i_0} \quad (14-23)$$

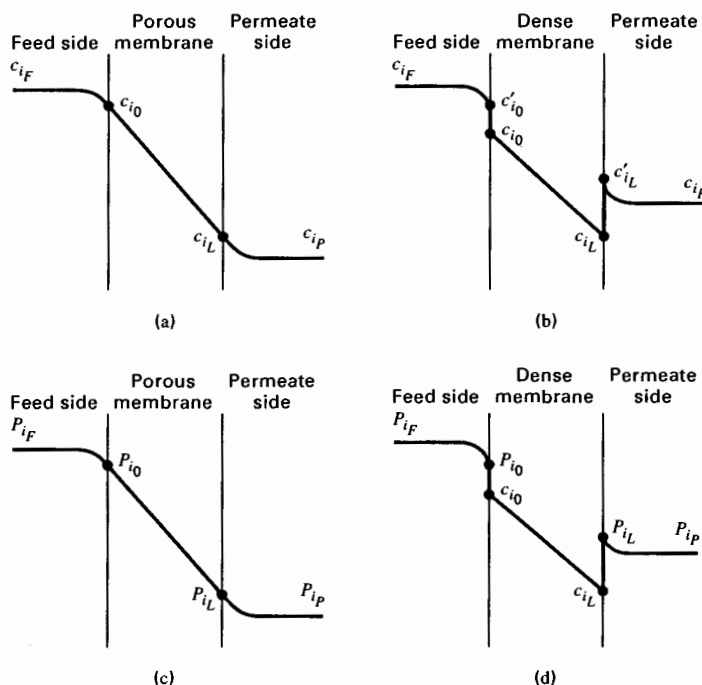


Figure 14.7 Concentration and partial pressure profiles for solute transport through membranes. Liquid mixture with (a) a porous and (b) a nonporous membrane; gas mixture with (c) a porous and (d) a nonporous membrane.

Similarly, at the other face:

$$K_{iL} = c_{iL}/c'_{iL} \quad (14-24)$$

Fick's law applied to the nonporous membrane of Figure 14.7b is:

$$N_i = \frac{D_i}{l_M} (c_{i0} - c_{iL}) \quad (14-25)$$

where D_i is the diffusivity of the solute in the membrane. If (14-23) and (14-24) are combined with (14-25), and the partition coefficient is assumed to be independent of concentration, such that $K_{i0} = K_{iL} = K_i$, we obtain for the flux

$$N_i = \frac{K_i D_i}{l_M} (c'_{i0} - c'_{iL}) \quad (14-26)$$

If the mass-transfer resistances in the two fluid boundary layers or films are negligible:

$$N_i = \frac{K_i D_i}{l_M} (c_{iF} - c_{iP}) \quad (14-27)$$

In (14-26) and (14-27), $K_i D_i$ is the permeability, P_{M_i} , for the solution-diffusion model, where K_i accounts for the solubility of the solute in the membrane and D_i accounts for diffusion through the membrane. Because D_i is generally very small, it is important that the membrane material offers a large value for K_i and/or a small membrane thickness.

Both D_i and K_i , and therefore P_{M_i} , depend on the solute and the membrane. When solutes dissolve in a polymer membrane, it will swell, causing both D_i and K_i to increase.

Table 14.5 Factors That Influence Permeability of Solutes in Dense Polymers

Factor	Value Favoring High Permeability
Polymer density	low
Degree of crystallinity	low
Degree of cross-linking	low
Degree of vulcanization	low
Amount of plasticizers	high
Amount of fillers	low
Chemical affinity of solute for polymer (solubility)	high

Other polymer membrane factors that can influence D_i , K_i , and P_{M_i} are listed in Table 14.5. However, the largest single factor is the chemical structure of the polymer. Because of the many factors involved, it is important to obtain experimental permeability data on the membrane and feed mixture of interest.

Solution-Diffusion for Gas Mixtures

Figures 14.7c and d show typical solute profiles for gas mixtures with porous and nonporous membranes, respectively, including the effect of fluid boundary layer or film mass-transfer resistances. For the porous membrane, a continuous partial pressure profile is shown. For the nonporous membrane, a concentration profile is shown within the membrane where the solute is dissolved in the membrane. Fick's law, given by (14-25), holds for transport through the membrane. Assuming that thermodynamic equilibrium exists at the two fluid-membrane interfaces, the concentrations in Fick's law can be related to the partial pressures adjacent to the membrane faces by Henry's law, which is a linear relation that is most conveniently written for membrane applications as

$$H_{i_0} = c_{i_0}/p_{i_0} \quad (14-28)$$

$$\text{and } H_{i_L} = c_{i_L}/p_{i_L} \quad (14-29)$$

If we assume that H_i is independent of total pressure and that the temperature is the same at both membrane faces:

$$H_{i_0} = H_{i_L} = H_i \quad (14-30)$$

Combining (14-25), (14-28), (14-29), and (14-30), the flux is

$$N_i = \frac{H_i D_i}{l_M} (p_{i_0} - p_{i_L}) \quad (14-31)$$

If the external mass-transfer resistances are neglected, $p_{i_F} = p_{i_0}$ and $p_{i_L} = p_{i_P}$:

$$N_i = \frac{H_i D_i}{l_M} (p_{i_F} - p_{i_P}) = \frac{P_{M_i}}{l_M} (p_{i_F} - p_{i_P}) \quad (14-32)$$

where

$$P_{M_i} = H_i D_i \quad (14-33)$$

Thus, the permeability depends on both the solubility of the gas component in the membrane and the diffusivity of that component in the membrane. An acceptable rate of transport through the membrane can be achieved only by using a very thin membrane and a high pressure on the feed side. The permeability of a gaseous component in a polymer membrane is subject to the factors listed in Table 14.5. Light gases do not interact with the polymer or cause it to swell. Thus, a light-gas-permeant-polymer combination is readily characterized experimentally. Often both solubility and diffusivity are measured. An extensive tabulation is given in the *Polymer Handbook* [19]. Representative data at 25°C are given in Table 14.6. In general, diffusivity decreases and solubility increases with increasing molecular weight of the gas species. The effect of temperature over a modest range of about 50°C can be represented for both solubility and diffusivity by Arrhenius equations. For example,

$$D = D_0 e^{-E_D/RT} \quad (14-34)$$

In general, the modest effect of temperature on solubility may act in either direction. However, an increase in temperature can cause a substantial increase in diffusivity and, therefore, a corresponding increase in permeability. Typical activation energies of diffusion in polymers, E_D , range from 15 to 60 kJ/mol.

The application of Henry's law for rubbery polymers is well accepted, particularly for low-molecular-weight penetrants, but is less accurate for glassy polymers, for which alternative theories have been proposed. Foremost is the dual-mode model first proposed by Barrer and co-workers [22–24] as the result of a comprehensive study of sorption and diffusion in ethyl cellulose. In this model, sorption of the penetrant occurs by ordinary dissolution in the polymer chains, as described by Henry's law, and by Langmuir sorption into holes or sites between chains of glassy polymers. When the downstream pressure is negligible compared to the upstream pressure, the permeability for Fick's law is given by

$$P_{M_i} = H_i D_i + \frac{D_{L_i} a b}{1 + b P} \quad (14-35)$$

Table 14.6 Coefficients for Gas Permeation in Polymers

	Gas Species					
	H ₂	O ₂	N ₂	CO	CO ₂	CH ₄
Low-Density Polyethylene:						
$D \times 10^6$	0.474	0.46	0.32	0.332	0.372	0.193
$H \times 10^6$	1.58	0.472	0.228	0.336	2.54	1.13
$P_M \times 10^{13}$	7.4	2.2	0.73	1.1	9.5	2.2
Polyethylmethacrylate:						
$D \times 10^6$	—	0.106	0.0301	—	0.0336	—
$H \times 10^6$	—	0.839	0.565	—	11.3	—
$P_M \times 10^{13}$	—	0.889	0.170	—	3.79	—
Polyvinylchloride:						
$D \times 10^6$	0.5	0.012	0.0038	—	0.0025	0.0013
$H \times 10^6$	0.26	0.29	0.23	—	4.7	1.7
$P_M \times 10^{13}$	1.3	0.034	0.0089	—	0.12	0.021
Butyl Rubber:						
$D \times 10^6$	1.52	0.081	0.045	—	0.0578	—
$H \times 10^6$	0.355	1.20	0.543	—	6.71	—
$P_M \times 10^{13}$	5.43	0.977	0.243	—	3.89	—

Note. Units: D in cm²/s; H in cm³ (STP)/cm³-Pa; P_M in cm³ (STP)-cm/cm²-s-Pa.

where the second term refers to Langmuir sorption with D_{L_i} = diffusivity of Langmuir sorbed species, P = penetrant pressure, and a, b = Langmuir constants for sorption site capacity and site affinity, respectively.

Koros and Paul [25] found that the dual-mode theory accurately represents data for the sorption of CO_2 in polyethylene terephthalate below its glass-transition temperature of about 85°C . Above that temperature, the rubbery polymer obeys just Henry's law. Mechanisms of diffusion for the Langmuir mode have been suggested by Barrer [26].

The ideal dense polymer membrane has a high permeance, P_M/l_M , for the penetrant molecules and a high separation factor (selectivity) between the components to be separated. The separation factor is defined similarly to relative volatility in distillation:

$$\alpha_{A,B} = \frac{(y_A/x_A)}{(y_B/x_B)} \quad (14-36)$$

where y_i is the mole fraction in the permeate leaving the membrane, corresponding to the partial pressure p_{i_p} in Figure 14.7d, while x_i is the mole fraction in the retentate on the feed side of the membrane, corresponding to the partial pressure p_{i_f} in Figure 14.7d. Unlike the case of distillation, y_i and x_i are not in equilibrium.

For the separation of a binary gas mixture of species A and B in the absence of boundary layer or film mass-transfer resistances, the transport fluxes are given by (14-32):

$$N_A = \frac{H_A D_A}{l_M} (x_A P_F - y_A P_P) \quad (14-37)$$

$$N_B = \frac{H_B D_B}{l_M} (x_B P_F - y_B P_P) \quad (14-38)$$

When no sweep gas is used, the ratio of N_A to N_B is simply the ratio of y_A to y_B in the permeate gas. Thus,

$$\frac{N_A}{N_B} = \frac{y_A}{y_B} = \frac{H_A D_A (x_A P_F - y_A P_P)}{H_B D_B (x_B P_F - y_B P_P)} \quad (14-39)$$

If the downstream (permeate) pressure, P_P , is negligible compared to the upstream pressure, P_F , such that $y_A P_P \ll x_A P_F$ and $y_B P_P \ll x_B P_F$, (14-39) can be rearranged and combined with (14-36) to give an *ideal separation factor*:

$$\alpha_{A,B}^* = \frac{H_A D_A}{H_B D_B} = \frac{P_{M_A}}{P_{M_B}} \quad (14-40)$$

Thus, a high separation factor can be achieved from a high solubility ratio, a high diffusivity ratio, or both. The separation factor depends on both transport phenomena and thermodynamic equilibria.

When the downstream pressure is not negligible, (14-39) can be rearranged to obtain an expression for $\alpha_{A,B}$ in terms of the pressure ratio, $r = P_P/P_F$, and the mole fraction of A on the feed or retentate side of the membrane. Combining (14-36), (14-40), and the definition of r with (14-39):

$$\alpha_{A,B} = \alpha_{A,B}^* \left[\frac{(x_B/y_B) - r\alpha_{A,B}}{(x_B/y_B) - r} \right] \quad (14-41)$$

Because $y_A + y_B = 1$, we can substitute into (14-41) for x_B , the identity:

$$x_B = x_B y_A + x_B y_B$$

Table 14.7 Membrane Separation Factors of Binary Pairs for Two Membrane Materials

	PDMS, Silicon Rubbery Polymer Membrane	PC, Polycarbonate Glassy Polymer Membrane
$P_{M_{He}}$, barrer	561	14
α_{He,CH_4}	0.41	50
α_{He,C_2H_4}	0.15	33.7
$P_{M_{CO_2}}$, barrer	4,550	6.5
α_{CO_2,CH_4}	3.37	23.2
α_{CO_2,C_2H_4}	1.19	14.6
$P_{M_{O_2}}$, barrer	933	1.48
α_{O_2,N_2}	2.12	5.12

to give

$$\alpha_{A,B} = \alpha_{A,B}^* \left[\frac{x_B \left(\frac{y_A}{y_B} + 1 \right) - r \alpha_{A,B}}{x_B \left(\frac{y_A}{y_B} + 1 \right) - r} \right] \quad (14-42)$$

If we combine (14-36) and (14-42) and replace x_B with $1 - x_A$, we obtain for the separation factor:

$$\alpha_{A,B} = \alpha_{A,B}^* \left[\frac{x_A(\alpha_{A,B} - 1) + 1 - r \alpha_{A,B}}{x_A(\alpha_{A,B} - 1) + 1 - r} \right] \quad (14-43)$$

Equation (14-43) is an implicit equation for $\alpha_{A,B}$, in terms of the pressure ratio, r , and x_A , that is readily solved for $\alpha_{A,B}$ by the formula for a quadratic equation. In the limit when $r = 0$, (14-43) reduces to $\alpha_{A,B} = \alpha_{A,B}^* = (P_{M_A}/P_{M_B})$. Many experimental investigators report values of $\alpha_{A,B}^*$. For example, Table 14.7, taken from the *Membrane Handbook* [6], gives data at 35°C for various binary pairs with polydimethyl siloxane (PDMS), a rubbery polymer, and bisphenol-A-polycarbonate (PC), a glassy polymer. For the rubbery polymer, permeabilities are high, but separation factors are low. The opposite is true for the glassy polymer. For a given feed composition, the separation factor places a definite limit on the degree of separation that can be achieved.

EXAMPLE 14.5

Air can be separated into nitrogen-enriched and oxygen-enriched streams by gas permeation with a number of different dense polymer membranes. In all cases, the membrane is more permeable to oxygen. A total of 20,000 scfm of air is compressed, cooled, and treated to remove moisture and compressor oil prior to being sent to a membrane separator at 150 psia and 78°F. Assume the composition of the air is 79 mol% N_2 and 21 mol% O_2 . A low-density polyethylene membrane in the form of a thin-film composite is being considered with solubilities and diffusivities given in Table 14.6. If the membrane skin is 0.2 μm thick, calculate the material balance and area in ft^2 for the membrane as a function of the cut (fraction of feed permeated). Assume a pressure of 15 psia on the permeate side with perfect mixing on both sides of the membrane, such that compositions on both sides are uniform and equal to exit compositions. Neglect pressure drop and mass transfer resistances external to the membrane. Comment on the practicality of the membrane for making a reasonable separation.

SOLUTION

Assume standard conditions are 0°C and 1 atm (359 ft³/lbmol)

$$n_F = \text{Feed flow rate} = \frac{20,000}{359} (60) = 3,343 \text{ lbmol/h}$$

For the low-density polyethylene membrane, from Table 14.6, and applying (14-33), letting A = O₂ and B = N₂:

$$\begin{aligned} P_{M_B} &= H_B D_B = (0.228 \times 10^{-6})(0.32 \times 10^{-6}) \\ &= 0.073 \times 10^{-12} \text{ cm}^3 (\text{STP})\text{-cm/cm}^2\text{-s-Pa} \end{aligned}$$

or, in American engineering units,

$$P_{M_B} = \frac{(0.073 \times 10^{-12})(2.54 \times 12)(3600)(101,300)}{(22,400)(454)(14.7)} = 5.43 \times 10^{-12} \frac{\text{lbmol-ft}}{\text{ft}^2\text{-h-psia}}$$

$$\text{Similarly, for oxygen: } P_M = 16.2 \times 10^{-12} \frac{\text{lbmol-ft}}{\text{ft}^2\text{-h-psia}}$$

Permeance values are based on a 0.2-μm-thick membrane skin (0.66 × 10⁻⁶ ft)

$$\text{From (14-1), } \bar{P}_{M_i} = P_{M_i}/l_M$$

$$\bar{P}_{M_B} = 5.43 \times 10^{-12}/0.66 \times 10^{-6} = 3.58 \times 10^{-6} \text{ lbmol/ft}^2\text{-h-psia}$$

$$\bar{P}_{M_A} = 16.2 \times 10^{-12}/0.66 \times 10^{-6} = 24.55 \times 10^{-6} \text{ lbmol/ft}^2\text{-h-psia}$$

Material balance equations:

For N₂

$$x_{F_B} n_F = y_{P_B} n_P + x_{R_B} n_R \quad (1)$$

where n = flow rate in lbmol/h and subscripts F , P , and R refer, respectively, to the feed, permeate, and retentate. Let

$$\theta = \text{cut} = n_P/n_F, \text{ then } (1 - \theta) = n_R/n_F$$

Substituting the definition of θ in (1) gives

$$x_{R_B} = \frac{x_{F_B} - y_{P_B} \theta}{1 - \theta} = \frac{0.79 - y_{P_B} \theta}{1 - \theta} \quad (2)$$

Similarly, for O₂,

$$x_{R_A} = \frac{0.21 - y_{P_A} \theta}{1 - \theta} \quad (3)$$

Separation factor:

From the definition of the separation factor, (14-36), since both fluid sides are well mixed:

$$\alpha_{A,B} = \frac{y_{P_A}/x_{R_A}}{(1 - y_{P_A})/(1 - x_{R_A})} \quad (4)$$

Transport equations:

The transport of A and B through the membrane of area A_M , with partial pressures at exit conditions because of perfect mixing, can be written as:

$$y_{P_B} n_P = A_M \bar{P}_{M_B} (x_{R_B} P_R - y_{P_B} P_P) \quad (5)$$

$$y_{P_A} n_P = A_M \bar{P}_{M_A} (x_{R_A} P_R - y_{P_A} P_P) \quad (6)$$

where A_M is the membrane area normal to flow, n_P , through the membrane. The ratio of (6) to (5) is y_{P_A}/y_{P_B} , and subsequent manipulations lead to (14-43), where

$$r = P_P/P_R = 15/150 = 0.1$$

$$\text{and } \alpha_{A,B}^* = \alpha_{O_2,N_2} = \bar{P}_{M_{O_2}}/\bar{P}_{M_{N_2}} = (10.7 \times 10^{-6})/(3.5 \times 10^{-6}) = 2.99$$

From (14-43):

$$\alpha_{A,B} = \alpha = 2.99 \left[\frac{x_{R_A}(\alpha - 1) + 1 - 0.299}{x_{R_A}(\alpha - 1) + 1 - 0.1} \right] \quad (7)$$

Equations (3), (4), and (7) contain four unknowns: x_{R_A} , y_{P_A} , θ , and $\alpha_{A,B} = \alpha$. The variable θ is bounded between 0 and 1, so values of θ are selected in that range. The other three variables are computed in the following manner. Combine (3), (4), and (7) to eliminate α and x_{R_A} . Solve the resulting nonlinear equation for y_{P_A} . Then solve (3) for x_{R_A} and (4) for α . Solve (6) for the membrane area, A_M . Alternatively, the three equations can be solved simultaneously with a computer program such as Mathcad. The following results are obtained:

θ	x_{R_A}	y_{P_A}	$\alpha_{A,B}$	A_M, ft^2
0.01	0.208	0.406	2.602	22,000
0.2	0.174	0.353	2.587	462,000
0.4	0.146	0.306	2.574	961,000
0.6	0.124	0.267	2.563	1,488,000
0.8	0.108	0.236	2.555	2,035,000
0.99	0.095	0.211	2.548	2,567,000

Note that the separation factor remains almost constant, varying by only 2% with a value of about 86% of the ideal value. The maximum oxygen content of the permeate (40.6 mol%) occurs with the smallest amount of permeate ($\theta = 0.01$). The maximum nitrogen content of the retentate (90.5 mol%) occurs with the largest amount of permeate ($\theta = 0.99$). With a retentate equal to 60 mol% of the feed ($\theta = 0.4$), the nitrogen content of the retentate has been increased only from 79 to 85.4 mol%. Furthermore, the membrane area requirements are very large. The low-density polyethylene membrane is not very practical. To achieve a more reasonable separation, say with $\theta = 0.6$ and a retentate of 95 mol% N_2 , it is advisable to use a membrane with an ideal separation factor of 5 in a membrane module that approximates crossflow or countercurrent flow of permeate and retentate with no mixing and a much higher permeance for oxygen. For higher purities, a membrane cascade of two or more stages should be considered. These alternatives are developed in the next two subsections. ■

Module Flow Patterns

In Example 14.5, perfect mixing was assumed on both sides of the membrane. Three other idealized flow patterns, shown in Figure 14.8, have received considerable attention; all assume no mixing and are comparable to the idealized flow patterns used to design heat exchangers. These patterns are (b) countercurrent flow; (c) cocurrent flow; and (d) crossflow. For a given cut, θ , the flow pattern can significantly affect the degree of separation and the membrane area. For flow patterns (b) to (d), fluid on the feed or retentate side of the membrane flows along and parallel to the upstream surface of the membrane. For countercurrent and cocurrent flow, permeate fluid at a given location on the downstream side of the membrane consists of fluid that has just passed through the membrane at that location plus the permeate fluid flowing to that location. For the crossflow case, there is no flow of permeate fluid along the membrane surface. The permeate fluid that has just passed through the membrane at a given location is the only fluid there. For a given

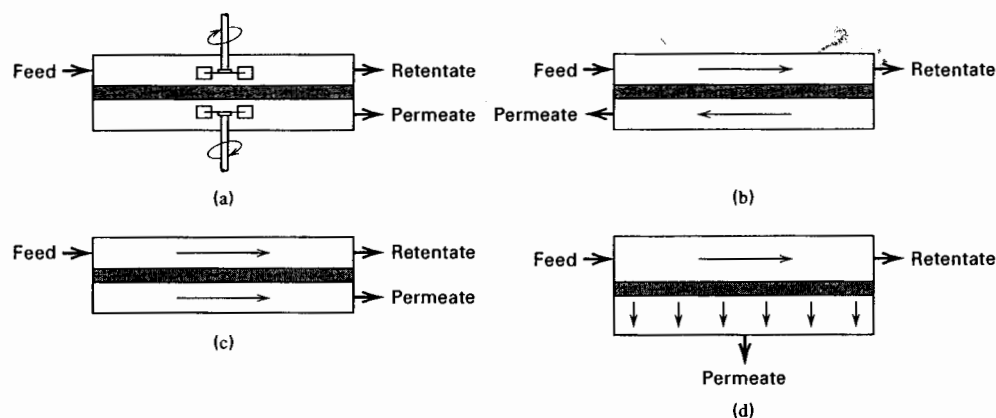


Figure 14.8 Idealized flow patterns in membrane modules: (a) perfect mixing; (b) countercurrent flow; (c) cocurrent flow; (d) crossflow.

module geometry, it is not always obvious which idealized flow pattern to assume. This is particularly true for the spiral-wound module of Figure 14.5b. If the permeation rate is high, the fluid issuing from the downstream side of the membrane may continue to flow perpendicularly to the membrane surface until it finally mixes with the bulk permeate fluid flowing past the surface. In that case, the idealized crossflow pattern might be appropriate. Hollow-fiber modules may be designed to approximate idealized countercurrent, cocurrent, or crossflow patterns. The module shown in Figure 14.5d is approximated by a countercurrent flow pattern.

Walawender and Stern [27] present solution methods for all four flow patterns of Figure 14.8 under the assumptions of a binary feed with constant pressure ratio, r , and constant ideal separation factor, $\alpha_{A,B}^*$. Exact analytical solutions are possible for the perfect mixing case (as shown in Example 14.5) and for the crossflow case, but numerical solutions are necessary for the countercurrent and cocurrent flow cases. A reasonably simple, but approximate, analytical solution for the crossflow case, derived by Naylor and Backer [28], is presented here.

Consider a membrane module with the crossflow pattern shown in Figure 14.9. The feed passes across the upstream membrane surface in plug flow with no longitudinal mixing. The pressure ratio, $r = P_P/P_F$, and the ideal separation factor, $\alpha_{A,B}^*$, are assumed constant.

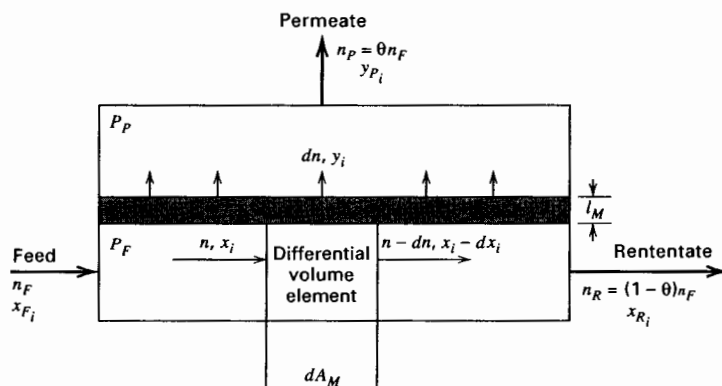


Figure 14.9 Crossflow model for membrane module.

Boundary layer or film mass-transfer resistances external to the membrane are assumed negligible. At the differential element, the local mole fractions in the retentate and permeate, respectively, are x_i and y_i , and the penetrant molar flux is dn/dA_M . Also, the local separation factor is given by (14-43) in terms of the local x_A , r , and $\alpha_{A,B}^*$. An alternative expression for the local permeate composition in terms of y_A , x_A , and r , is obtained by combining (14-36) and (14-41).

$$\frac{y_A}{1 - y_A} = \alpha_{A,B}^* \left[\frac{x_A - r y_A}{(1 - x_A) - r(1 - y_A)} \right] \quad (14-44)$$

A material balance for A around the differential volume element gives:

$$y_A dn = d(nx_A) = x_A dn + n dx_A \quad \text{or} \quad \frac{dn}{n} = \frac{dx_A}{y_A - x_A} \quad (14-45)$$

If (14-36) is combined with (14-45) to eliminate y_A , we obtain

$$\frac{dn}{n} = \left[\frac{1 + (\alpha - 1)x_A}{x_A(\alpha - 1)(1 - x_A)} \right] dx_A \quad (14-46)$$

where $\alpha = \alpha_{A,B}$.

In the solution to Example 14.5, it was noted that $\alpha = \alpha_{A,B}$ is relatively constant over the entire range of cut, θ . Such is generally the case when the pressure ratio, r , is small. If the assumption of constant $\alpha = \alpha_{A,B}$ is made in (14-46) and integration is carried out from the intermediate location of the differential element to the final retentate, that is, from n to n_R and from x_A to x_{R_A} , the result is

$$n = n_R(1 - \theta) \left[\left(\frac{x_A}{x_{R_A}} \right)^{\left(\frac{1}{\alpha-1} \right)} \left(\frac{1 - x_{R_A}}{1 - x_A} \right)^{\left(\frac{\alpha}{\alpha-1} \right)} \right] \quad (14-47)$$

The mole fraction of A in the final permeate and the total membrane surface area are obtained by integrating the values obtained from solving (14-44) to (14-46):

$$y_{P_A} = \int_{x_{F_A}}^{x_{R_A}} y_A dn / \theta n_F \quad (14-48)$$

By combining (14-48) with (14-46), (14-47), and the definition of α , the integral in n can be transformed to an integral in x_A , which when integrated gives

$$y_{P_A} = x_{R_A}^{\left(\frac{1}{1-\alpha} \right)} \left(\frac{1 - \theta}{\theta} \right) \left[(1 - x_{R_A})^{\left(\frac{\alpha}{\alpha-1} \right)} \left(\frac{x_{F_A}}{1 - x_{F_A}} \right)^{\left(\frac{\alpha}{\alpha-1} \right)} - x_{R_A}^{\left(\frac{\alpha}{\alpha-1} \right)} \right] \quad (14-49)$$

where $\alpha = \alpha_{A,B}$ can be estimated from (14-43) by using $x_A = x_{F_A}$.

The differential rate of mass transfer of A across the membrane is given by

$$y_A dn = \frac{P_{M_A} dA_M}{l_M} [x_A P_F - y_A P_P] \quad (14-50)$$

from which the total membrane surface area can be obtained by integration:

$$A_M = \int_{x_{R_A}}^{x_{F_A}} \frac{l_M y_A dn}{P_{M_A} (x_A P_F - y_A P_P)} \quad (14-51)$$

For the conditions of Example 14.5, compute exit compositions for a spiral-wound module that approximates crossflow.



SOLUTION

From Example 14.5: $\alpha_{A,B}^* = 2.99$; $r = 0.1$; $x_{F_A} = 0.21$

From (14-43), using $x_A = x_{F_A}$; $\alpha_{A,B} = 2.603$

An overall module material balance for O_2 (A) gives

$$x_{F_A} n_F = x_{R_A} (1 - \theta) n_F + y_{P_A} \theta n_F \quad \text{or} \quad x_{R_A} = \frac{(x_{F_A} - y_{P_A} \theta)}{1 - \theta} \quad (1)$$

Solving (1) and (14-49) simultaneously with a program such as Mathcad gives the following results:

θ	x_{R_A}	y_{P_A}	Stage α_S
0.01	0.208	0.407	2.61
0.2	0.168	0.378	3.01
0.4	0.122	0.342	3.74
0.6	0.0733	0.301	5.44
0.8	0.0274	0.256	12.2
0.99	0.000241	0.212	1,120.

Comparing these results to those of Example 14.5, we see that for crossflow, the permeate is richer in oxygen and the retentate is richer in nitrogen. Thus, for a given cut, θ , crossflow is more efficient than perfect mixing.

Also included in the preceding table is the calculated degree of separation for the stage, α_S , defined on the basis of the mole fractions in the permeate and retentate exiting the stage by

$$(\alpha_{A,B})_S = \alpha_S = \frac{(y_{P_A}/x_{R_A})}{(1 - y_{P_A})/(1 - x_{R_A})} \quad (2)$$

Recall that the ideal separation factor, $\alpha_{A,B}^*$, for this example is 2.99. Also, if (2) is applied to the perfect mixing case of Example 14.5, it is found that α_S is 2.603 for $\theta = 0.01$ and decreases slowly with increasing θ until at $\theta = 0.99$, $\alpha_S = 2.548$. Thus, for perfect mixing, $\alpha_S < \alpha^*$ for all θ . Such is not the case for crossflow. In the table, $\alpha_S < \alpha^*$ for $\theta > 0.2$, and α_S increases with increasing θ . For $\theta = 0.6$, α_S is almost twice α^* . ■

Calculations of the degree of separation of a binary mixture in a membrane module utilizing cocurrent or countercurrent flow patterns involve the numerical solution of ordinary differential equations. Derivation of these equations and FORTRAN computer codes for their solution are given by Walawender and Stern [27]. A representative solution is shown in Figure 14.10 for the separation of air (20.9 mol% O_2) for conditions of $\alpha^* = 5$, $r = 0.2$. For a given cut, θ , it is seen that the best separation is achieved with countercurrent flow. The curve for cocurrent flow lies between those for crossflow and perfect mixing. The perfect mixing case for binary mixtures is extended to multicomponent mixtures by Stern et al. [29], who present an iterative procedure. As with crossflow, countercurrent flow also offers the possibility of a separation factor for the stage, α_S , defined by (2) earlier, that can be considerably greater than α^* .

Cascades

A single membrane module or a number of such modules arranged in parallel or in series without recycle constitutes a single-stage membrane separation process. The extent to which a feed mixture can be separated in a single stage is limited and, as shown in the previous subsection, is determined by the separation factor, α . This factor depends, in

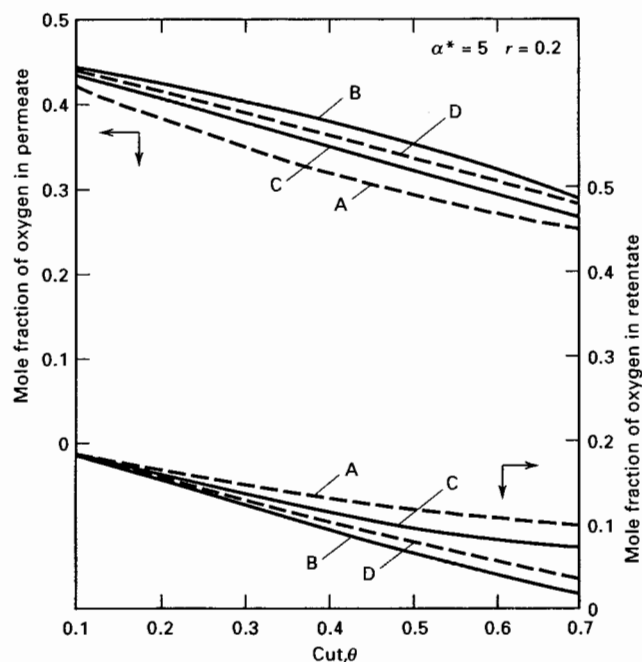


Figure 14.10 Effect of membrane module flow pattern on degree of separation of air. A, perfect mixing; B, countercurrent flow; C, cocurrent flow; D, crossflow.

turn, on the module flow pattern, the permeability ratio (ideal separation factor), the cut, θ , and the driving force for mass transfer through the membrane. To achieve a higher degree of separation than possible with a single stage, a countercurrent cascade of stages, such as are used in distillation, absorption, stripping, and liquid-liquid extraction, or a hybrid process that couples a membrane separator with another separation operation, such as distillation or adsorption, can be applied.

A countercurrent recycle cascade of membrane separators, similar to a distillation column, is shown in Figure 14.11. The feed enters at stage F, somewhere near the middle of the column. Permeate is enriched in components of high permeability in an enriching section, while the retentate is enriched in components of low permeability in a stripping section. The final permeate is withdrawn from stage 1, while the final retentate is withdrawn

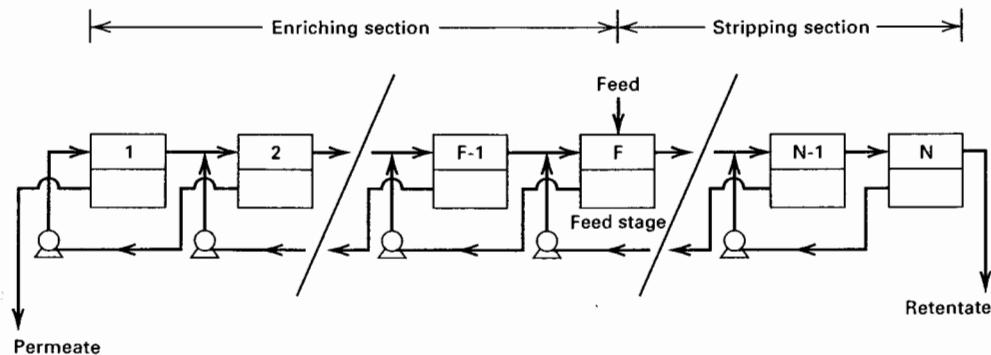


Figure 14.11 Countercurrent recycle cascade of membrane separators.

from stage N . For a cascade, additional factors that affect the degree of separation of the feed are the number of stages and the recycle ratio (permeate recycle rate/permeate product rate). As discussed by Hwang and Kammermeyer [30], it is best to manipulate the cut and reflux rate at each stage so as to force the compositions of the two streams entering each stage to be identical. For example, the composition of retentate leaving Stage 1 would be identical to the composition of permeate leaving Stage 3. This corresponds to the least amount of entropy production for the cascade and, thus, the highest second-law efficiency. Such a cascade is referred to as ideal. Calculation methods for cascades are discussed by Hwang and Kammermeyer [30] and utilize the single-stage methods that depend upon the module flow pattern, as discussed in the previous section. The calculations are best carried out with a computer program, but results for a binary mixture can be conveniently displayed on a McCabe–Thiele type diagram in terms of the mole fraction in the permeate leaving each stage, y_i , versus the mole fraction in the retentate leaving each stage, x_i . For a membrane cascade, the equilibrium curve becomes the selectivity curve in terms of the separation factor for the stage, α_s .

In Figure 14.11, it is assumed the pressure drop on the upstream side of the membrane is negligible. Thus, only the permeate must be pumped, if a liquid, or compressed, if a gas, to be sent to the next stage. In the case of gas permeation, compression costs can be high. Thus, membrane cascades for gas permeation are often limited to just two or three stages, with the most common configurations shown in Figure 14.12. Compared to a single stage, the two-stage stripping cascade is designed to obtain a more pure retentate, whereas a more purer permeate is the goal of the two-stage enriching cascade. The addition of the premembrane stage, shown in Figure 14.12c, may be attractive when the feed concentration is low in the component to be passed preferentially through the membrane, the desired permeate purity is high, the separation factor is low, and/or a high recovery of the more permeable component is desired. An example of the application of the enrichment cascades is given by Spillman [31] for the removal of carbon dioxide from natural gas (assumed to be methane) using cellulose acetate membranes in spiral-wound modules that approximate

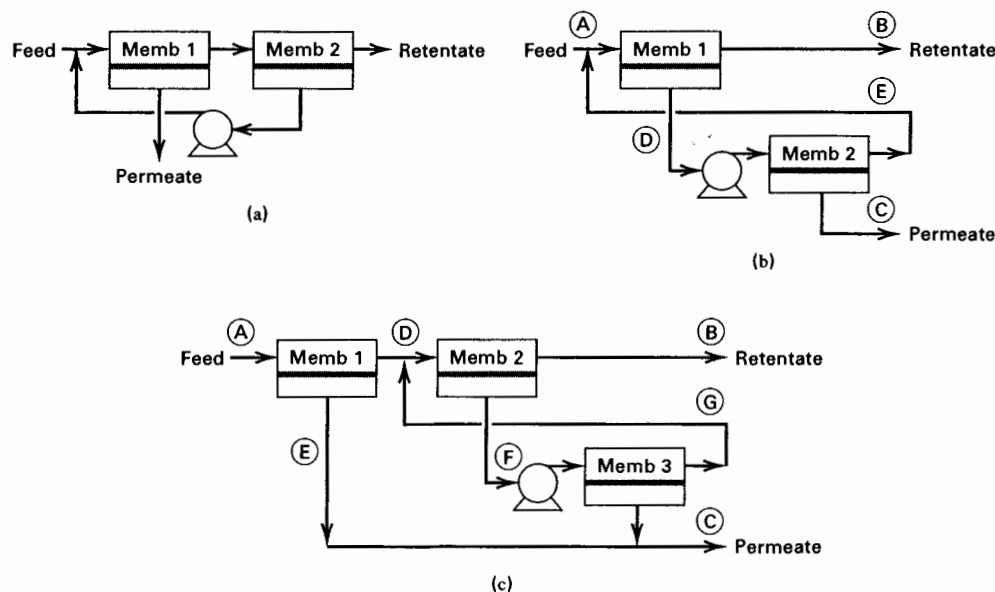


Figure 14.12 Common recycle cascades. (a) Two-stage stripping cascade. (b) Two-stage enriching cascade. (c) Two-stage enriching cascade with additional premembrane stage.

Table 14.8 Separation of N₂ and CH₄ with Membrane Cascades

Case 1: Single Membrane Stage:

	Stream		
	A Feed	B Retentate	C Permeate
Composition (mole%)			
CH ₄	93.0	98.0	63.4
CO ₂	7.0	2.0	36.6
Flow rate (MM/SCFD)	20.0	17.11	2.89
Pressure (psig)	850	835	10

Case 2: Two-Stage Enriching Cascade (Figure 14.12b):

	Stream				
	A	B	C	D	E
Composition (mole%)					
CH ₄	93.0	98.0	18.9	63.4	93.0
CO ₂	7.0	2.0	81.1	36.6	7.0
Flow rate (MM/SCFD)	20.00	18.74	1.26	3.16	1.90
Pressure (psig)	850	835	10	10	850

Case 3: Two-Stage Enriching Cascade with Premembrane Stage (Figure 14.12c):

	Stream						
	A	B	C	D	E	F	G
Composition (mole%)							
CH ₄	93.0	98.0	49.2	96.1	56.1	72.1	93.0
CO ₂	7.0	2.0	50.8	3.9	43.9	27.9	7.0
Flow rate (MM/SCFD)	20.00	17.95	2.05	19.39	1.62	1.44	1.01
Pressure (psig)	850	835	10	840	10	10	850

Note. MM, million.

crossflow. The ideal separation factor, $\alpha_{\text{CO}_2, \text{CH}_4}^*$ is 21. Results of computer calculations are given in Table 14.8 for a single stage, a two-stage enriching cascade (Figure 14.12b), and a two-stage enriching cascade with an additional premembrane stage. Carbon dioxide flows through the membrane faster than methane. In all three cases, the feed is 20 million (MM) scfd of 7 mol% CO₂ in methane at 850 psig (about 865 psia) and the retentate is 98 mol% in methane. For each stage, the downstream membrane pressure is 10 psig (about 25 psia). In Table 14.8, for all three cases, stream A is the feed, stream B is the final retentate, and stream C is the final permeate. Case 1 achieves a 90.2% recovery of methane. Case 2 increases that recovery to 98.7%. Case 3 achieves an intermediate recovery of 94.6%. The following degrees of separation are computed from data given in Table 14.8:

Case	α_S for Membrane Stage		
	1	2	3
1	28	—	—
2	28	57	—
3	20	19	44

We can also compute overall degrees of separation 3, giving values of 210 and 51, respectively.

Concentration Polarization

Thus far, all of the resistance to mass transfer has been in the membrane. Thus, concentrations in the fluid at the membrane have been assumed equal to the respective concentrations on the other side of the membrane. When mass-transfer resistance in the fluid is negligible, concentration or partial pressure gradients are negligible adjacent to the membrane surfaces, as was illustrated in Fig. 1. For a given bulk fluid concentrations, the presence of the membrane offers a resistance for mass transfer across the membrane and, therefore, a depletion or enrichment of species in the boundary layer or film adjacent to the membrane is referred to as *concentration polarization*.

In general, the solution-diffusion mechanism for mass transfer involves diffusion in the gas boundary layers or film adjacent to the membrane. If transfer resistances are negligible and $P_{i_F} = P_{i_0}$, concentration polarization is commonly neglected. In liquid boundary layers and films can be slow, concentration polarization is neglected in membrane processes that involve liquid and pervaporation. The need to consider the effect of concentration polarization is of particular importance in reverse osmosis, where the goal is to increase the salt flux.

Consider a membrane process of the type in Fig. 1. In a steady-state, rates of mass transfer of a penetrating species i are given as follows:

$$N_i = k_{i_F}(c_{i_F} - c_{i_0}) = \frac{P_{M_i}}{l_M}(c_{i_0} - c_{i_L})$$

If these three equations are combined to eliminate c_{i_0} and c_{i_L} , we obtain

$$N_i = \frac{c_{i_F} - c_{i_F}}{\frac{1}{k_{i_F}} + \frac{l_M}{P_{M_i}} + \frac{1}{k_{i_P}}}$$

where k_{i_F} and k_{i_P} are mass-transfer coefficients for the fluid and permeate boundary layers or films. The three terms in the denominator represent the resistances to the mass flux. In general, the mass-transfer coefficients are functions of flow properties, flow channel geometry, and flow regime. In laminar flow regime, a long entry region may exist where the velocity profile is not fully developed. With the distance, L , from the entry of the membrane, the flow becomes fully developed. This is complicated by fluid velocities that change between the two fluids.

Typical mass-transfer coefficients for channel flow can be estimated using the empirical film-model correlation [32]:

$$N_{Sh} = k_i d_H / D_i = a N_{Re}^b N_{Sc}^c$$

where

$$N_{Re} = d_H v \rho / \mu$$

$$N_{Sc} = \mu / \rho D_i$$

 d_H = hydraulic diameter v = velocityThe constants a , b , and d are as follows:

Flow Regime	Flow Channel Geometry	d_H	a	b	d
Turbulent, ($N_{Re} > 10,000$)	Circular tube	D	0.023	0.8	0
	Rectangular channel	$2hw/(h+w)$	0.023	0.8	0
Laminar, ($N_{Re} < 2,100$)	Circular tube	D	1.86	0.33	0.33
	Rectangular channel	$2hw/(h+w)$	1.62	0.33	0.33

where

 w = width of channel h = height of channel L = length of channel

A dilute solution of solute A in solvent B is passed through a tubular membrane separator, with the feed flowing through the tubes. At a certain location, the solute concentrations are 5.0×10^{-2} kmol/m³ and 1.5×10^{-2} kmol/m³, respectively, on the feed and permeate sides. The permeance of the membrane for solute A is 7.3×10^{-5} m/s. If the tube-side Reynolds number is 15,000, the feed-side solute Schmidt number is 500, the diffusivity of the feed-side solute is 6.5×10^{-5} cm²/s, and the inside diameter of the tube is 0.5 cm, estimate the flux of the solute through the membrane if the mass-transfer resistance on the permeate side of the membrane is negligible.

SOLUTION

The flux of the solute is given by a modification of (14-53):

$$N_A = \frac{c_{A_F} - c_{A_P}}{\frac{1}{k_{A_F}} + \frac{1}{\bar{P}_{M_A}} + 0}$$

$$c_{A_F} - c_{A_P} = 5 \times 10^{-2} - 1.5 \times 10^{-2} = 3.5 \times 10^{-2} \text{ kmol/m}^3 \quad (1)$$

$$\bar{P}_{M_A} = 7.3 \times 10^{-5} \text{ m/s}$$

From (14-54) for turbulent flow in a tube, since $N_{Re} > 10,000$:

$$k_{A_F} = 0.023 \frac{D_A}{D} N_{Re}^{0.8} N_{Sc}^{0.33} = 0.023 \left(\frac{6.5 \times 10^{-5}}{0.5} \right) (15,000)^{0.8} (500)^{0.33}$$

$$= 0.051 \text{ cm/s or } 5.1 \times 10^{-4} \text{ m/s}$$

$$\text{From (1), } N_A = \frac{3.5 \times 10^{-2}}{\frac{1}{5.1 \times 10^{-4}} + \frac{1}{7.3 \times 10^{-5}}} = 2.24 \times 10^{-6} \text{ kmol/s} \cdot \text{m}^2$$

The fraction of the total resistance due to the membrane is

$$\frac{\frac{1}{7.3 \times 10^{-5}}}{\frac{1}{5.1 \times 10^{-4}} + \frac{1}{7.3 \times 10^{-5}}} = 0.875 \text{ or } 87.5\%$$

14.4 DIALYSIS AND ELECTRODIALYSIS

In a dialysis membrane separation process, shown in Figure 14.13, the feed is a liquid, at pressure P_1 , containing solvent, solutes of type A, and solutes of type B and/or insoluble, but dispersed, colloidal matter. A sweep liquid or wash of the same solvent is fed at pressure P_2 to the other side of the membrane. The membrane is thin with micropores of a size such that solutes of type A can pass through by a concentration driving force. Solute of type B are larger in molecular size than those of type A and pass through the membrane only with difficulty or not at all. This transport of solutes A and B through the membrane is called dialysis. Colloids do not pass through the membrane. With pressure $P_1 = P_2$, the solvent may also pass through the membrane, but by a concentration driving force acting in the opposite direction. The transport of the solvent is called osmosis. By elevating P_1 above P_2 , solvent osmosis can be reduced or eliminated. The products of a dialysis unit (dialyzer) are a liquid *diffusate* (permeate) containing solvent, solutes of type A, and smaller amounts of solutes of type B; and a *dialysate* (retentate) of the solvent and remaining solutes of types A and B, and colloidal matter. Ideally, the dialysis unit would enable a perfect separation between solutes of type A and solutes of type B and any colloidal matter. However, at best only a fraction of the solutes of type A are recovered in the diffusate, even when solutes of type B do not pass through the membrane.

For example, when dialysis is used to recover sulfuric acid from an aqueous stream containing sulfate salts, the following results are obtained, as reported by Chamberlin and Vromen [33]:

	Streams in		Streams out	
	Feed	Wash	Dialysate	Diffusate
Flow rate, gph	400	400	420	380
H ₂ SO ₄ , g/L	350	0	125	235
CuSO ₄ , g/L as Cu	30	0	26	2
NiSO ₄ , g/L as Ni	45	0	43	0

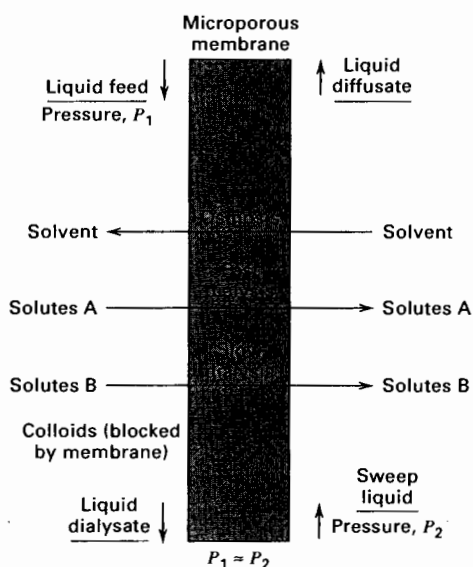


Figure 14.13 Dialysis.

Thus, about 64% of the H_2SO_4 is recovered in the diffusate, accompanied by only about 6% of the CuSO_4 , and essentially no NiSO_4 .

Dialysis is closely related to other membrane processes that use other driving forces for separating liquid mixtures, including (1) reverse osmosis, which depends upon a transmembrane pressure difference for solute and/or solvent transport; (2) electrodialysis and electroosmosis, which depend upon a transmembrane electrical potential difference for solute and solvent transport, respectively; and (3) thermal osmosis, which depends upon a transmembrane temperature difference for solute and solvent transport.

Dialysis is attractive when the concentration differences for the main diffusing solutes are large and the permeability differences between those solutes and the other solute(s) and/or colloids is large. Although dialysis has been known since the work of Graham in 1861 [34], commercial applications of dialysis do not rival reverse osmosis and gas permeation. Nevertheless, dialysis has been applied to a number of separations, including (1) recovery of sodium hydroxide from a 17–20 wt% caustic viscose liquor contaminated with hemicellulose to produce a pure diffusate of 9–10 wt% caustic; (2) recovery of chromic, hydrochloric, and hydrofluoric acids from contaminating metal ions; (3) recovery of sulfuric acid from aqueous solutions containing nickel sulfate; (4) removal of alcohol from beer to produce a reduced-alcohol beer; (5) recovery of nitric and hydrofluoric acids from spent stainless-steel pickle liquor; (6) removal of mineral acids from organic compounds; (7) removal of low-molecular-weight contaminants from polymers; and (8) purification of pharmaceuticals. Also of great importance is hemodialysis, in which urea, creatine, uric acid, phosphates, and chlorides are removed from blood without removing essential higher-molecular-weight compounds and blood cells. This dialysis device is called an artificial kidney.

Typical microporous membrane materials used in dialysis are hydrophilic, including cellulose, cellulose acetate, various acid-resistant polyvinyl copolymers, polysulfones, and polymethylmethacrylate, typically less than 50 μm thick and with pore diameters of 15 to 100 Å. The most common membrane modules are plate-and-frame and hollow-fiber. Compact hollow-fiber hemodialyzers, which are widely used, typically contain several thousand 200- μm -diameter fibers with a wall thickness of 20–30 μm and a length of 10–30 cm. Dialysis membranes can be thin because pressures on either side of the membrane are essentially equal.

At a differential location in a dialyzer, the rate of mass transfer of solute across the dialysis membrane is given by

$$dn_i = K_i(c_{iF} - c_{iP}) dA_M \quad (14-55)$$

where K_i is the overall mass-transfer coefficient, which is given in terms of the individual coefficients from (14-53):

$$\frac{1}{K_i} = \frac{1}{k_{iF}} + \frac{l_M}{P_{M_i}} + \frac{1}{k_{iP}} \quad (14-56)$$

The determination of the membrane area is made by integrating (14-55) taking into account the module flow patterns, the bulk concentration gradients, and the individual mass-transfer coefficients in (14-56).

One of the oldest membrane materials for use with aqueous solutions is porous cellophane, for which solute permeability is given by (14-14) with $P_{M_i} = D_e$ and $\bar{P}_{M_i} \cdot l_M$. In the presence of a solution, cellophane will swell to about twice its dry thickness. The wet thickness should be used for l_M . Typical values of parameters given in (14-13) to (14-15) for commercial cellophane are as follows:

Wet thickness = l_M = 0.004 to 0.008 cm;

Tortuosity = τ = 3 to 5;

porosity = ϵ = 0.45 to 0.60

pore diameter = D = 30 to 50 Å

If solute does not interact with the membrane material, the diffusivity, D_e , in (14-14) is the ordinary molecular diffusion coefficient, which depends only on solute and solvent properties. However, the membrane may have a profound effect on the solute diffusivity if any of a number of membrane-solute interactions occur, including covalent, ionic, and hydrogen bonding; physical adsorption and chemisorption; and membrane polymer flexibility. Thus, it is preferred to measure \bar{P}_M experimentally using process fluids.

Although the transport of solvents, such as water, which usually occurs in a direction opposite to the solute, could be formulated in terms of Fick's law, it is more common to measure the solvent flux and report the so-called *water-transport number*, which is the ratio of the water flux to the solute flux, with a negative value indicating transport of solvent in the same direction as the solute. The membrane can also interact with the solvent and even curtail solvent transport. Ideally, the water transport number should be a small value less than +1.0. The ideal experimental dialyzer is a batch cell with a variable-speed stirring mechanism on both sides of the membrane so that external mass transfer resistances, $1/k_{if}$ and $1/k_{ip}$ in (14-56), are made negligible. Stirrer speeds greater than 2,000 rpm may be required.

A common dialyzer is the plate-and-frame type of Figure 14.5a. However, for dialysis applications, the frames are arranged vertically. A typical unit might contain 100 square frames, each 0.75×0.75 m on 0.6-cm spacing, equivalent to 56 m^2 of membrane surface. The dialysis rate for sulfuric acid might be 5 lb/day-ft^2 . More recently developed dialysis units utilize hollow fibers of 200- μm inside diameter, 16- μm wall thickness, and 28-cm length packed into a heat-exchanger-type module to give 22.5 m^2 of membrane area in a volume that might be one-tenth of the volume of an equivalent plate-and-frame unit.

In a plate-and-frame dialyzer, the flow pattern is nearly countercurrent. Because total flow rates change little and solute concentrations are typically small, it is common to estimate the solute transport rate by assuming a constant overall mass-transfer coefficient with a log-mean concentration driving force. Thus, from (14-55):

$$n_i = K_i A_M (\Delta c_i)_{LM} \quad (14-57)$$

where K_i is given by (14-56).

EXAMPLE 14.8

A countercurrent-flow, plate-and-frame dialyzer is to be sized to process $0.78 \text{ m}^3/\text{h}$ of an aqueous solution of 300 kg/m^3 of H_2SO_4 and smaller amounts of copper and nickel sulfates. A wash water rate of $1.0 \text{ m}^3/\text{h}$ is to be used, and it is desired to recover 30% of the acid at 25°C . From batch laboratory experiments with an acid-resistant vinyl membrane, in the absence of external mass-transfer resistances, a permeance of 0.025 cm/min for the acid and a water transport number of +1.5 are measured. Membrane transport of copper and nickel sulfates is negligible. For these flow rates, experience with plate-and-frame dialyzers indicates that flow will be laminar and the combined external liquid-film mass-transfer coefficients will be 0.020 cm/min . Determine the membrane area required in m^2 .

SOLUTION

$$m_{\text{H}_2\text{SO}_4} \text{ in feed} = 0.78(300) = 234 \text{ kg/h}$$

$$m_{\text{H}_2\text{SO}_4} \text{ transferred} = 0.3(234) = 70 \text{ kg/h}$$

$$m_{\text{H}_2\text{O}} \text{ transferred to dialysate} = 1.5(70) = 105 \text{ kg/h}$$

$$m_{\text{H}_2\text{O}} \text{ in entering wash} = 1.0(1,000) = 1,000 \text{ kg/h}$$

$$m_P \text{ leaving} = 1,000 - 105 + 70 = 965 \text{ kg/h}$$

For mixture densities, assume aqueous sulfuric acid solutions and use the appropriate table in *Perry's Chemical Engineers' Handbook*:

$$\rho_F = 1,175 \text{ kg/m}^3 \quad \rho_R = 1,114 \text{ kg/m}^3 \quad \rho_P = 1,045 \text{ kg/m}^3$$

$$m_F = 0.78(1,175) = 917 \text{ kg/h} \quad m_R \text{ leaving} = 917 + 105 - 70 = 952 \text{ kg/h}$$

Sulfuric acid concentrations:

$$c_F = 300 \text{ kg/m}^3 \quad c_{\text{wash}} = 0 \text{ kg/m}^3$$

$$c_R = \frac{(234 - 70)}{952} (1,114) = 192 \text{ kg/m}^3 \quad c_P = \frac{70}{965} (1,045) = 76 \text{ kg/m}^3$$

The log mean driving force for H_2SO_4 with countercurrent flow of feed and wash:

$$(\Delta c)_{\text{LM}} = \frac{(c_F - c_P) - (c_R - c_{\text{wash}})}{\ln \left(\frac{c_F - c_P}{c_R - c_{\text{wash}}} \right)} = \frac{(300 - 76) - (192 - 0)}{\ln \left(\frac{300 - 76}{192 - 0} \right)} = 208 \text{ kg/m}^3$$

The driving force is almost constant in the membrane module, varying only from 224 to 192 kg/m^3 .

From (14-56),

$$K_{\text{H}_2\text{SO}_4} = \frac{1}{\frac{1}{P_M} + \left(\frac{1}{k} \right)_{\text{combined}}} = \frac{1}{\frac{1}{0.025} + \frac{1}{0.020}} = 0.0111 \text{ cm/min or } 0.0067 \text{ m/h}$$

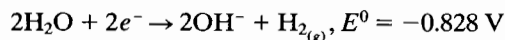
From (14-57), using mass units instead of molar units:

$$A_M = \frac{m_{\text{H}_2\text{SO}_4}}{K_{\text{H}_2\text{SO}_4} (\Delta c_{\text{H}_2\text{SO}_4})_{\text{LM}}} = \frac{70}{0.0067(208)} = 50 \text{ m}^2$$

Electrodialysis

Electrodialysis began in the early 1900s as a modification to dialysis by the addition of electrodes and direct current to increase the rate of dialysis in electrolyte solutions. However, since the 1940s, electrodialysis has developed into a membrane separation process that differs from dialysis in many ways. Today, electrodialysis refers to an electrolytic process for separating an aqueous electrolyte feed solution into a concentrate or brine and a dilute or desalted water (dilate) by means of an electric field and ion-selective membranes. A typical electrodialysis process is shown in Figure 14.14, where the four ion-selective membranes shown are of two types arranged in an alternating-series pattern. The cation-selective membranes (C) carry a negative charge, and thus attract and pass positively charged ions (cations), while retarding negative ions. The anion-selective membranes (A) carry a positive charge that attracts and permits passage of negative ions (anions). Both types of membranes are impervious to water. The net result is that both anions and cations are concentrated in compartments 2 and 4, from which concentrate is withdrawn, and ions are depleted in compartment 3, from which the dilute is withdrawn. Compartment pressures are essentially equal. Compartments 1 and 5 are bounded on the far sides by the anode and cathode, respectively. A direct-current voltage is applied (e.g. with a battery or direct-current generator) across the anode and cathode, causing current to flow by metallic conduction of electrons through wiring from the anode to the cathode and then through the cell by ionic conduction from the cathode back to the anode. Both electrodes are chemically neutral metals, with the anode being typically stainless steel and the cathode typically platinum-coated tantalum, niobium, or titanium. Thus, the electrodes are neither oxidized nor reduced.

But half reactions must occur at the two electrodes. Typically, the most easily oxidized species is oxidized at the anode and the most easily reduced species is reduced at the cathode. With inert electrodes, the result at the cathode is the reduction of water by the half reaction



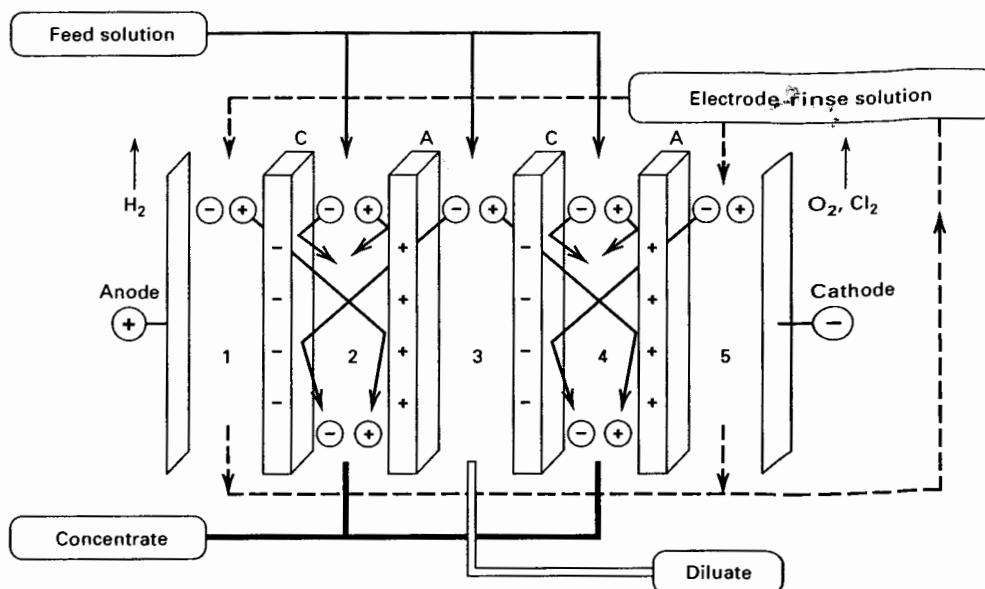
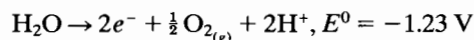
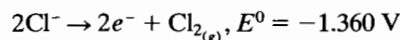


Figure 14.14 Schematic diagram of the electrodialysis process. C, cation transfer membrane; A, anion transfer membrane. [Adapted from W. S. W. Ho and K. K. Sirkar, editors, "Membrane Handbook," Van Nostrand Reinhold, New York (1992).]

The oxidation half reaction at the anode is

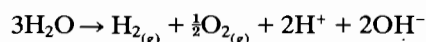


or, if chloride ions are present:

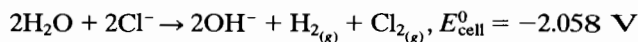


where the electrode potentials are the standard values at 25°C for one molar solutions of ions and partial pressures of one atmosphere for the gaseous products. Values of E^0 can be corrected for nonstandard conditions by the Nernst equation.

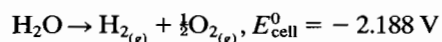
The corresponding overall cell reactions are:



or



The net reaction for the first case is



The electrode rinse solution that circulates through compartments 1 and 5 is typically acidic to neutralize the OH ions formed in compartment 1 and prevent precipitation of compounds such as CaCO_3 and $\text{Mg}(\text{OH})_2$.

The most widely used ion-exchange membranes for electrodialysis, first reported by Juda and McRae [35] in 1950, are (1) cation-selective membranes containing negatively charged groups fixed to a polymer matrix, and (2) anion-selective membranes containing positively charged groups fixed to a polymer matrix. The former, shown schematically in Figure 14.15, includes fixed anions, mobile cations (called counterions), and mobile anions

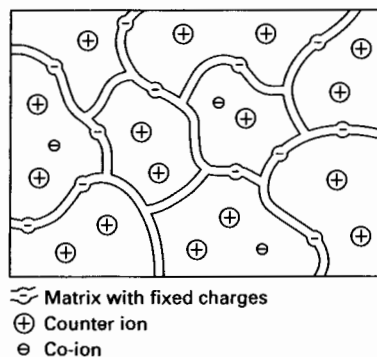


Figure 14.15 Cation-exchange membrane. [From H. Strathmann, *Sep. and Purif. Methods*, **14**(1), 41–66 (1985) with permission.]

(called co-ions). The latter are almost completely excluded from the polymer matrix by electrical repulsion, called the Donnan effect. For perfect exclusion, only cations are transferred through the membrane. In practice, the exclusion is better than 90%.

A typical cation-selective membrane is made of polystyrene cross-linked with divinylbenzene and sulfonated to produce fixed sulfonate, $-\text{SO}_3^-$, anion groups. A typical anion-selective membrane of the same polymer contains quaternary ammonium groups such as $-\text{NH}_3^+$. Membranes are 0.2–0.5 mm in thickness and reinforced with a screen to provide mechanical stability. The membranes, which are made in flat sheets, contain 30 to 50% water and have a network of pores too small to permit water transport.

A cell pair or unit cell consists of one cation-selective membrane and one anion-selective membrane. Although Figure 14.14 shows an electrodialysis system with two cell pairs, a commercial electrodialysis system is a large stack of membranes patterned after a plate and frame configuration that, according to Applegate [2] and the *Membrane Handbook* [6], may contain 100 to 600 cell pairs. In a stack, membranes of from 0.4 to 1.5 m^2 surface area each are separated by from 0.5 to 2 mm with spacer gaskets. The total voltage or electrical potential applied across the cell includes (1) the electrode potentials discussed earlier, (2) overvoltages due to gas formation at the two electrodes, (3) the voltage required to overcome the ohmic resistance of the electrolyte in each compartment, (4) the voltage required to overcome the resistance in each membrane, and (5) the voltage required to overcome concentration polarization effects caused by mass-transfer resistances in the electrolyte solutions adjacent to the membrane surface. For large stacks, the latter three voltage increments predominate and depend upon the current density (amps flowing through the stack per unit surface area of membranes). A typical voltage drop across a cell pair is 0.5–1.5 V. Current densities are in the range of 5–50 mA/cm^2 . Thus, a stack of 400 membranes (200 unit cells) of 1 m^2 surface area each might require 200 V at 100 A. Typically 50 to 90% of brackish water is converted to potable water, depending on concentrate recycle.

As the current density is increased for a given membrane surface area, the concentration-polarization effect increases. A schematic diagram of this effect for a single cation-selective membrane is shown in Figure 14.16, where c_m refers to cation concentrations in the membrane, c_b refers to bulk electrolyte cation concentrations, and superscripts c and d refer to concentrate side and dilute side, respectively. The maximum or limiting current density is reached when c_m^d reaches zero. Typically, an electrodialysis cell is operated at 80% of the limiting current density, which is determined by experiment. The corresponding cell voltage or resistance is also determined experimentally.

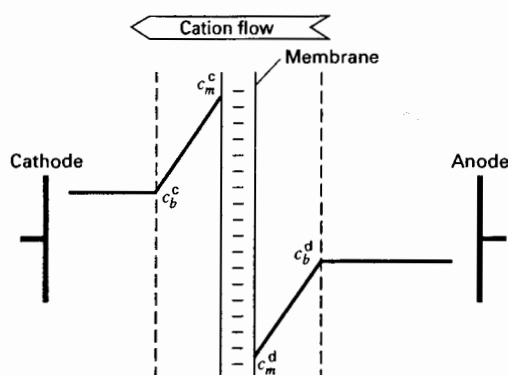


Figure 14.16 Concentration-polarization effects for a cation-exchange membrane. [From H. Strathmann, *Sep. and Purif. Methods*, 14(1), 41–66 (1985) with permission.]

The amounts of gases formed at the electrodes at the two ends of the stack are governed by *Faraday's law of electrolysis*. During electrolysis, one Faraday (96,520 coulombs) of electricity reduces at the cathode and oxidizes at the anode an equivalent of oxidizing and reducing agent corresponding to the transfer of 6.023×10^{23} (Avogadro's number) electrons through wiring from the anode to the cathode. In general, it takes a very large quantity of electricity to form appreciable quantities of gases in an electrodialysis process.

Of more importance in the design or operation of an electrodialysis process are the membrane area and electrical energy requirements as discussed by Applegate [2] and Strathmann [36]. The membrane area is estimated from the current density, rather than from a permeability, and mass-transfer resistances by applying Faraday's law:

$$A_M = \frac{zFQ\Delta c}{i\xi} \quad (14-58)$$

where

A_M = total area of all cell pairs, m^2

z = electrochemical valence of the ions being transported through the membranes

F = Faraday's constant (96,520 amp-s/equivalent)

Q = volumetric flow rate of the diluate (potable water), m^3/s

Δc = difference between feed and diluate ion concentration in equivalents/ m^3

i = current density, amps/ m^2 of a cell pair, usually about 80% of i_{max}

ξ = current efficiency < 1.00

The last variable accounts for the fact that not all of the current is effective in transporting the selected ions through the membranes. Inefficiencies are caused by a Donnan exclusion of less than 100%, some transfer of water through the membranes, current leakage through manifolds, etc.

Power consumption is given by

$$P = IE \quad (14-59)$$

where

P = power, W, I = electric current flow through the stack, and E = voltage across the stack.

The electrical current flow is given by a rearrangement of (14-58):

$$I = \frac{zFQ\Delta c}{n\xi} \quad (14-60)$$

where n is the number of cell pairs.

The main application of electrodialysis is to the desalinization of brackish water in the salt concentration range of 500 to 5,000 ppm (mg/L). Below this range, ion exchange is more economical, whereas above this range, to 50,000 ppm, reverse osmosis is preferred. However, electrodialysis cannot produce water with a very low dissolved solids content because of the high electrical resistance of dilute solutions. Other applications include recovery of nickel and copper from electroplating rinse water; deionization of cheese whey, fruit juices, wine, milk, and sugar molasses; separation of salts, acids, and bases from organic compounds; and recovery of organic compounds from their salts. Bipolar membranes, prepared by laminating a cation-selective membrane and an anion-selective membrane back-to-back, can be used to produce sulfuric acid and sodium hydroxide from a sodium sulfate solution.

EXAMPLE 14-8

Estimate membrane area and electrical energy requirements for an electrodialysis process to reduce the salt (NaCl) of 24,000 m³/day of brackish water from 1,500 mg/L to 300 mg/L with a 50% conversion. Assume each membrane has a surface area of 0.5 m² and each stack contains 300 cell pairs. A reasonable current density is 5 mA/cm² and the current efficiency is 0.8 (80%).

Solution

Use (14-58) to estimate membrane area, with $z = 1$.

$$\begin{aligned} F &= 96,520 \text{ A/equiv} & Q &= (24,000)(0.5)/(24)(3,600) = 0.139 \text{ m}^3/\text{s} \\ \text{MW}_{\text{NaCl}} &= 58.5 & i &= 5 \text{ mA/cm}^2 = 50 \text{ A/m}^2 \\ \Delta c &= (1,500 - 300)/58.5 = 20.5 \text{ mmol/L or } 20.5 \text{ mol/m}^3 = 20.5 \text{ equiv/m}^3 \\ A_M &= \frac{(1)(96,520)(0.139)(20.5)}{(50)(0.8)} = 6,876 \text{ m}^2 \end{aligned}$$

Each stack contains 300 cell pairs with a total area of $0.5(300) = 150 \text{ m}^2$. Therefore, number of stacks = $6,876/150 = 46$ in parallel

From (14-60), electrical current flow is given by

$$I = \frac{(1)(96,500)(0.139)(20.5)}{(300)(0.8)} = 1,146 \text{ A or } I/\text{stack} = 1,146/46 = 25 \text{ A.}$$

To obtain the electrical power, we need to know the average voltage drop across each cell pair. Assume a value of 1 V. From (14-59):

$$P = (1,146)(1)(300) = 344,000 \text{ W} = 344 \text{ kW}$$

Additional energy is required to pump feed, recycle concentrate, and electrode rinse.

It is also instructive to estimate the amount of feed that would be electrolyzed (say, as water to hydrogen and oxygen gases) at the electrodes. From the half-cell reactions presented earlier, half a molecule of H₂O is electrolyzed for each electron or, 0.5 mol H₂O is electrolyzed for each faraday of electricity.

1,146 amps = 1,146 coulombs/s or $(1,146)(3,600)(24) = 99,010,000$ coulombs/day or $99,010,000/96,520 = 1,026$ faradays/day. This electrolyzes $(0.5)(1,026) = 513$ mol/day of water. The feed rate is 12,000 m³/day, or

$$\frac{(12,000)(10^6)}{18} = 6.7 \times 10^8 \text{ mol/day}$$

Therefore, the amount of water electrolyzed is negligible. ■

14.5 REVERSE OSMOSIS

Osmosis, from the Greek word for “push,” refers to the passage of a solvent, such as water, through a dense membrane that is permeable to the solvent (A), but not the solute(s) (B) (e.g., inorganic ions). The first recorded account of osmosis was given in 1748 by Nollet, whose experiments were conducted with water, an alcohol, and an animal-bladder membrane. The important aspects of osmosis are illustrated by example in Figure 14.17, where all solutions are at 25°C. In the initial condition (a), seawater of approximately 3.5 wt% dissolved salts and at 101.3 kPa is on the left side of the membrane, while pure water at the same pressure is on the right side. The dense membrane is permeable to water, but not to the dissolved salts. By osmosis, water passes from the right side to the seawater on the left side, causing dilution with respect to dissolved salts. At equilibrium, the condition of Figure 14.17b is reached, wherein some pure water still resides on the right side and seawater, less concentrated in salt, resides on the left side. The pressure, P_1 , on the left side is now greater than the pressure, P_2 , on the right side, with the difference, π , referred to as the *osmotic pressure*.

The process of osmosis is not useful as a separation process because the solvent is transferred in the wrong direction, resulting in mixing rather than separation. However, the direction of transfer of solvent through the membrane can be reversed, as shown in Figure 14.17c by applying a pressure, P_1 , on the left side of the membrane, that is higher than the sum of the osmotic pressure and the pressure, P_2 , on the right side: that is, $P_1 - P_2 > \pi$. Now water in the seawater is transferred to the pure water, and the seawater becomes more concentrated in dissolved salts. This phenomenon, called *reverse osmosis*, can be used to partially remove a solvent from a solute-solvent mixture. As discussed later, an important factor in developing a reverse osmosis separation process is the osmotic pressure, π , of the feed mixture. In general, as discussed in more detail later, π is proportional to the solute concentration.

In a reverse osmosis (RO) membrane separation process, as shown in Figure 14.18, the feed is a liquid at high pressure, P_1 , containing solvent (e.g., water) and solubles (e.g., inorganic salts and, perhaps, colloidal matter). No sweep liquid is used, but the other side of the membrane is maintained at a much lower pressure, P_2 . A dense membrane, such as an acetate or aromatic polyamide, is used that is permselective for the solvent. To withstand the large pressure differential, the membrane must be thick. Accordingly, asymmetric or thin-wall composite membranes, having a thin, dense skin or layer on a thick, porous support, are used. The products of reverse osmosis are a permeate of almost pure solvent and a retentate of solvent-depleted feed. However, a perfect separation between the solvent and solute is not achieved, since only a fraction of the solvent in the feed is transferred to the permeate.

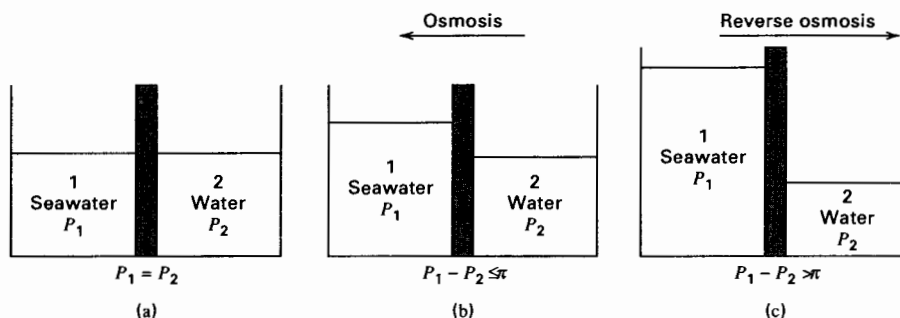


Figure 14.17 Osmosis and reverse osmosis phenomena. (a) Initial condition. (b) At equilibrium after osmosis. (c) Reverse osmosis.

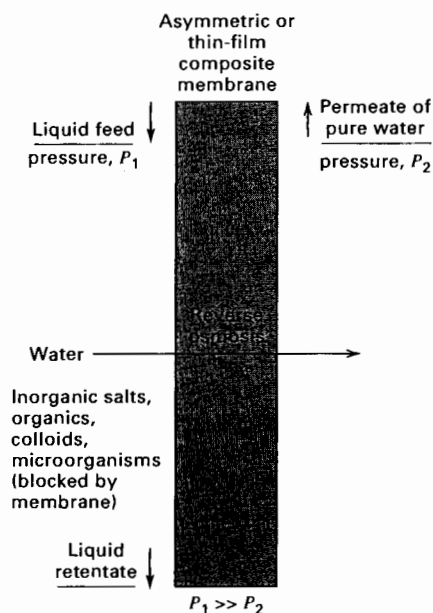


Figure 14.18 Reverse osmosis.

Reverse osmosis is applied to the desalinization and purification of seawater, brackish water, and wastewater. Prior to 1980, multistage flash distillation was the main process for the desalinization of water. By 1990, this situation was dramatically reversed, making RO the dominant process for new construction. The dramatic shift from a thermally driven process to a more economical pressure-driven process was made possible through the development by Loeb and Sourirajan [7] of an asymmetric membrane that allows pressurized water to pass through at a high rate, while almost preventing transmembrane flows of dissolved salts, organic compounds, colloids, and microorganisms. Today more than 1,000 RO desalting plants are producing more than 750,000,000 gallons per day of potable water worldwide.

According to Baker et al. [5], the use of RO to desalinize water is accomplished mainly with spiral-wound and hollow-fiber membrane modules utilizing cellulose triacetate, cellulose diacetate, and aromatic polyamide membrane materials. Cellulose acetates are susceptible to biological attack, and acidic or basic hydrolysis back to cellulose, making it necessary to chlorinate the feed water and control the pH within the range of 4.5 to 7.5. Polyamides are not susceptible to biological attack and resist hydrolysis in the pH range of 4 to 11. However, polyamides are attacked by chlorine.

The preferred membrane for the desalinization of seawater, which contains about 3.5 wt% dissolved salts and has an osmotic pressure of 350 psia, is a spiral-wound, multileaf module of polyamide thin-film composite operating at a feed pressure of 800 to 1,000 psia. With a transmembrane water flux of 9 gal/ft²-day (0.365 m³/m²-day), this module can recover 45% of the water at a purity of about 99.95 wt%. A typical cylindrical module is 8 inches in diameter by 40 inches long, containing 365 ft² (33.9 m²) of membrane surface. Such modules resist fouling by colloidal and particulate matter, but the seawater must be treated with sodium bisulfate to remove oxygen and/or chlorine.

For the desalinization of brackish water containing less than 0.5 wt% dissolved salts, hollow-fiber modules of high packing density, and containing fibers of cellulose acetates or aromatic polyamides, are used if fouling is not serious. Because the osmotic pressure is much lower (<50 psi), feed pressures can be less than 250 psia. Transmembrane fluxes may be as high as 20 gal/ft²-day.

Other uses of reverse osmosis, usually on a smaller scale than the desalinization of water to produce potable water, include (1) the treatment of industrial wastewater to remove heavy metal ions, nonbiodegradable substances, and other components of commercial value; (2) the treatment of rinse water from electroplating processes to obtain a metal ion concentrate and a permeate that can be reused as a rinse; (3) the separation of sulfites and bisulfites from effluents in pulp and paper processes; (4) the treatment of wastewater in dyeing processes; (5) the recovery of constituents having food value from wastewaters in food processing plants (e.g. lactose, lactic acid, sugars, and starches); (6) the treatment of municipal water to remove inorganic salts, low-molecular-weight organic compounds, viruses, and bacteria; (7) the dewatering of certain food products such as coffee, soups, tea, milk, orange juice, and tomato juice; and (8) the concentration of amino acids and alkaloids. In such applications, membranes must have chemical, mechanical, and thermal stability to be competitive with other processes.

As with all membrane processes where the fluid feed being separated is a liquid, three resistances to mass transfer must be considered: the membrane resistance and the two fluid-film or boundary-layer resistances on either side of the membrane. If the permeate is pure solvent, then there is no film resistance on that side of the membrane.

Although the driving force for the transport of water through the dense membrane is the concentration or activity difference in and across the membrane, common practice is to use a driving force based on osmotic pressure. Consider the reverse osmosis process of Figure 14.17c. At equilibrium, solvent chemical potentials or fugacities on the two sides of the membrane must be equal. Thus,

$$f_A^{(1)} = f_A^{(2)} \quad (14-61)$$

From definitions in Table 2.2, rewrite (14-61) in terms of activities:

$$a_A^{(1)} f_A^0(T, P_1) = a_A^{(2)} f_A^0(T, P_2) \quad (14-62)$$

For pure solvent, A, $a_A^{(2)} = 1$. For seawater, $a_A^{(1)} = x_A^{(1)} \gamma_A^{(1)}$. Substitution into (14-62) gives

$$f_A^0(T, P_2) = x_A^{(1)} \gamma_A^{(1)} f_A^0(T, P_1) \quad (14-63)$$

Standard-state, pure-component fugacities f^0 increase with increasing pressure. Thus, if $x_A^{(1)} \gamma_A^{(1)} < 1$, then from (14-63), $P_1 > P_2$. The pressure difference $P_1 - P_2$ is shown as a hydrostatic-head difference in Figure 14.17b. This difference, which can be observed experimentally, is the osmotic pressure, π .

To relate π to solvent or solute concentration, we apply the Poynting correction of (2-28), which for an incompressible liquid of specific volume, v_A , gives

$$f_A^0(T, P_2) = f_A^0(T, P_1) \exp \left[\frac{v_{A_L}(P_1 - P_2)}{RT} \right] \quad (14-64)$$

Substitution of (14-63) into (14-64) gives

$$\pi = P_1 - P_2 = -\frac{RT}{v_{A_L}} \ln(x_A^{(1)} \gamma_A^{(1)}) \quad (14-65)$$

Thus, osmotic pressure is a thermodynamic quantity that replaces activity.

For a mixture, on the feed or retentate side of the membrane, that is dilute in the solute, $\gamma_A^{(1)} = 1$. Also, $x_A^{(1)} = 1 - x_B^{(1)}$ and $\ln(1 - x_B^{(1)}) \approx -x_B^{(1)}$. Substitution into (14-65) gives

$$\pi = P_1 - P_2 = RT x_B^{(1)} / v_{A_L} \quad (14-66)$$

Finally, since $x_B^{(1)} \approx n_B/n_A$, $n_A v_{A_L} = V$, and $n_B/V = c_B$, (14-66) becomes

$$\pi \approx RT c_B \quad (14-67)$$

which was cited in Exercise 1.8. For applications to the reverse osmosis of seawater, Applegate [2] suggests the approximate expression

$$\pi = 1.12T \sum \bar{m}_i \quad (14-68)$$

where π is in psia, T is in K, and $\sum \bar{m}_i$ is the summation of molalities of all dissolved ions and nonionic species in the solution in mol/L. More exact expressions for π are developed by Stoughton and Lietzke [38].

In the general case, when reverse osmosis takes place with solute on each side of the membrane, then at equilibrium, $(P_1 - \pi_1) = (P_2 - \pi_2)$. Accordingly, as discussed by Merten [37], the driving force for the transport of solvent through the membrane is $\Delta P - \Delta\pi$, and the rate of mass transport is

$$N_{H_2O} = \frac{P_{M_{H_2O}}}{l_M} (\Delta P - \Delta\pi) \quad (14-69)$$

where

ΔP = hydraulic pressure difference across the membrane

$$= P_{\text{feed}} - P_{\text{permeate}}$$

$\Delta\pi$ = osmotic pressure difference across the membrane

$$\pi_{\text{feed}} - \pi_{\text{permeate}}$$

Often, $\pi_{\text{permeate}} \approx 0$ because the permeate is almost pure solvent.

The flux of solute (e.g., salt) is given by (14-26) in terms of membrane concentrations, and thus is independent of the ΔP across the membrane. Accordingly, the higher the ΔP , the purer the permeate water. Alternatively, the flux of salt may be expressed for ease of application in terms of *salt passage*, SP , defined by

$$SP = (c_{\text{salt}})_{\text{permeate}} / (c_{\text{salt}})_{\text{feed}} \quad (14-70)$$

Values of SP decrease with increasing ΔP . *Salt rejection* is given by $SR = 1 - SP$.

For brackish water of 1,500 mg/L as NaCl, at 25°C, (14-68) predicts $\pi = 17.1$ psia. For seawater of 35,000 mg/L as NaCl, at 25°C, (14-68) predicts $\pi = 385$ psia, while Stoughton and Lietzke [38] give 368 psia. From (14-69), ΔP must be greater than $\Delta\pi$ for reverse osmosis to occur. For the desalinization of brackish water by RO, ΔP is typically 400–600 psi, while for seawater, it is 800–1,000 psi. To prevent membrane fouling and scaling, feed water pretreatment, consisting of prefiltration, flocculation, and chemical treatment, is required.

Concentration polarization is particularly important on the feed side of the reverse-osmosis membrane. This effect is illustrated in Figure 14.19, where typical concentrations are shown for water, c_w , and salt, c_s . Because of the high pressure, the activity of water on the feed side is somewhat higher than that of near-pure water on the permeate side, thus providing the necessary driving force for water transport through the membrane. The flux of water to the membrane carries with it salt by bulk flow. However, because the salt cannot readily penetrate the membrane, the concentration of the salt in the liquid adjacent to the surface of the membrane, c_{s_i} , is greater than that in bulk of the feed, c_{s_f} . This difference causes mass transfer of salt by diffusion from the membrane surface back to the bulk feed. The back rate of salt diffusion depends on the mass-transfer coefficient for the film or boundary layer on the feed side. The lower the mass-transfer coefficient, the higher the value of c_{s_i} . The value of c_{s_i} is important because it fixes the osmotic pressure, and thus influences the driving force for water transport according to (14-69).

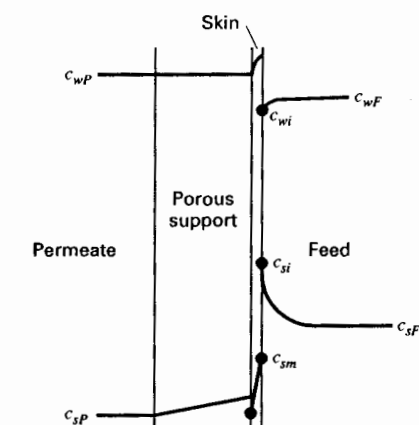


Figure 14.19 Concentration-polarization effects in reverse osmosis.

Consider steady-state transport of water with back-diffusion of salt. A salt balance at the upstream membrane surface gives

$$N_{H_2O}c_{sF}(SP) = k_s(c_{s_i} - c_{s_F}) \quad (14-71)$$

Solving for c_{s_i} gives

$$c_{s_i} = c_{s_F} \left(1 + \frac{N_{H_2O}(SP)}{k_s} \right) \quad (14-72)$$

Values of k_s are estimated from (14-54). The concentration-polarization effect is seen to be most significant for high water fluxes and low mass-transfer coefficients.

Pressure drop on the feed side of the membrane is also important because, by (14-69), it causes a reduction in the driving force for water transport. Because of the complex geometries used for both spiral-wound and hollow-fiber modules, it is best to estimate pressure drops from experimental data. Feedside pressure drops for spiral-wound modules and hollow-fiber modules range from 43 to 85 and 1.4 to 4.3 psi, respectively [6].

A schematic diagram of a typical reverse osmosis process for the desalinization of water is shown in Figure 14.20. The source of feed water may be a well or surface water, which is pumped through a series of pretreatment steps to ensure a long membrane life. Of particular importance is pH adjustment. The pretreated water is then fed by a high-pressure-discharge pump to an appropriate parallel-and-series network of reverse osmosis modules of the spiral-wound or hollow-fiber type. The concentrate, which leaves the membrane system at a high pressure that is 10–15% lower than the inlet pressure, is then routed through a power-recovery turbine, which reduces the net power consumption of the process by 25 to 40% while reducing the pressure of the concentrate to an appropriate low level. The permeate, which may be 99.95 wt% pure water and about 50% of the feed water, is sent to a series of posttreatment steps before it is ready to drink.

EXAMPLE 14.9

At a certain location in a spiral-wound membrane, the bulk conditions on the feed side are 1.8 wt% NaCl, 25°C, and 1,000 psia, while bulk conditions on the permeate side are 0.05 wt% NaCl, 25°C, and 50 psia. For the particular membrane being used, the permeance values are 1.1×10^{-5} g/cm²·s·atm for H₂O and 16×10^{-6} cm/s for the salt. If mass-transfer resistances are negligible on each side of the membrane, calculate the flux of water in gal/ft²·day and the flux of salt in g/ft²·day.

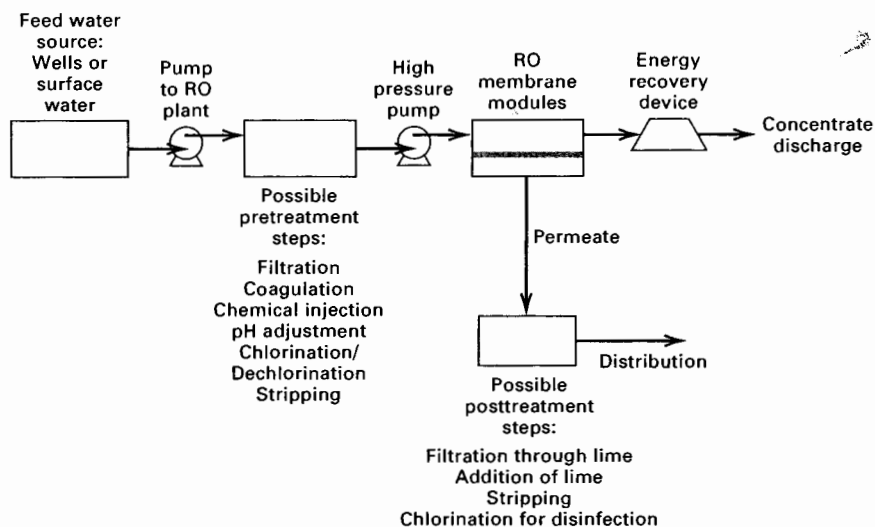


Figure 14.20 Reverse osmosis process.

SOLUTION

Bulk salt concentrations are approximately

$$\frac{1.8(1,000)}{58.5(98.2)} = 0.313 \text{ mol/L on feed side}$$

$$\frac{0.05(1,000)}{58.5(99.95)} = 0.00855 \text{ mol/L on permeate side}$$

For water transport, using (14-68) for osmotic pressure, noting that dissolved NaCl gives 2 ions per molecule:

$$\Delta P = (1,000 - 50)/14.7 = 64.6 \text{ atm}$$

$$\pi_{\text{feedside}} = 1.12(298)(2)(0.313) = 209 \text{ psia} = 14.2 \text{ atm}$$

$$\pi_{\text{permeate side}} = 1.12(298)(2)(0.00855) = 5.7 \text{ psia} = 0.4 \text{ atm}$$

$$\Delta P - \Delta \pi = 64.6 - (14.2 - 0.4) = 50.8 \text{ atm}$$

$$P_{M_{H_2O}}/l_M = 1.1 \times 10^{-5} \text{ g/cm}^2\text{-s-atm}$$

From (14-69),

$$N_{H_2O} = (1.1 \times 10^{-5})(50.8) = 0.000559 \text{ g/cm}^2\text{-s or}$$

$$\frac{(0.000559)(3,600)(24)}{(454)(8.33)(1.076 \times 10^{-3})} = 11.9 \text{ gal/ft}^2\text{-day}$$

For salt transport:

$$\Delta c = 0.313 - 0.00855 = 0.304 \text{ mol/L or } 0.000304 \text{ mol/cm}^3$$

$$P_{M_{NaCl}}/l_M = 16 \times 10^{-6} \text{ cm/s}$$

From (14-26):

$$N_{NaCl} = 16 \times 10^{-6}(0.000304) = 4.86 \times 10^{-9} \text{ mol/cm}^2\text{-s}$$

$$\text{or } \frac{(4.86 \times 10^{-9})(3,600)(24)(58.5)}{1.076 \times 10^{-3}} = 0.95 \text{ g/ft}^2\text{-day}$$

We see that the flux of salt is very much smaller than the flux of water. ■

14.6 GAS PERMEATION

In gas permeation (GP), shown in Figure 14.21, the feed gas, at high pressure P_1 , contains some low-molecular-weight species (MW < 50) to be separated from small amounts of higher-molecular-weight species. Usually a sweep gas is not used, but the other side of the membrane is maintained at a much lower pressure, P_2 , often near ambient pressure. The membrane, often dense but sometimes microporous, is permselective for certain of the low-molecular-weight species in the feed gas, shown in Figure 14.21 as the A species. If the membrane is dense, these species are absorbed at the surface and then transported through the membrane by one or more mechanisms. Thus, permselectivity depends on both membrane absorption and the membrane transport rate. Usually all mechanisms are formulated in terms of a partial pressure or fugacity driving force using the solution-diffusion model of (14-32). The products are a permeate that is enriched in the A species and a retentate that is enriched in B. A near-perfect separation is generally not achievable. If the membrane is microporous, as for example in high-temperature applications, pore size is extremely important because it is usually necessary to block the passage of species B. Otherwise, unless molecular weights of A and B differ appreciably, only a very modest separation is achievable, as was discussed in connection with Knudsen diffusion, (14-22).

Since the early 1980s, applications of GP with dense polymeric membranes have increased dramatically. Applications include (1) separation of hydrogen from methane; (2) adjustment of H_2 -to- CO ratio in synthesis gas; (3) O_2 enrichment of air; (4) N_2 enrichment of air; (5) removal of CO_2 ; (6) drying of natural gas and air; (7) removal of helium; and (8) removal of organic solvents from air.

Gas permeation must compete with distillation at cryogenic conditions, absorption, and pressure-swing adsorption. Some of the advantages of gas permeation, as cited by Spillman and Sherwin [39], are low capital investment, ease of installation, ease of operation, absence of rotating parts, high process flexibility, low weight and space requirements, and low environmental impact. In addition, if the feed gas is already at so high a pressure that a gas compressor is not needed, then no utilities are required.

Since 1986, the most rapidly developing application for GP has been air separation, for which available membranes have separation factors for O_2 with respect to N_2 of 3 to 7.

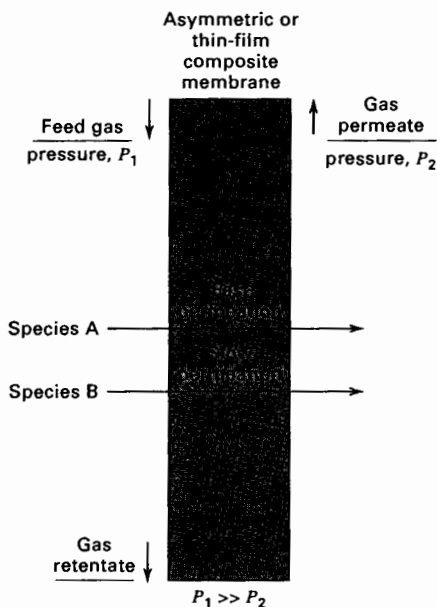


Figure 14.21 Gas permeation.

However, product purities are economically limited to a retentate of 95–99% N_2 and a permeate of 30–45% O_2 . Thus, the largest application of GP for air separation is the production of nitrogen rather than oxygen.

Gas permeation also competes very favorably with other separation processes for hydrogen recovery because of the high separation factors achieved. For example, the rate of permeation of hydrogen through a typical dense polymer membrane is more than 30 times that for nitrogen. A typical GP process might achieve a 95% recovery of 90% pure hydrogen from a feed gas containing 60% hydrogen.

Early applications of GP used dense (nonporous) membranes of cellulose acetates and polysulfones, which are still predominant, although polyimides, polyamides, polycarbonates, polyetherimides, sulfonated polysulfones, Teflon, polystyrene, and silicone rubber are also finding applications for temperatures to at least 70°C. Although plate-and-frame and tubular modules can be used for gas permeation, almost all large-scale applications use spiral-wound or hollow-fiber modules because of their higher packing density. Commercial membrane modules for gas permeation are available from more than 20 suppliers. Feed-side pressure is typically 300 to 500 psia, but is as high as 1,650 psia. Typical refinery applications involve feed-gas flow rates of 20 million scfd, but flow rates as large as 300 million scfd have been reported [40]. When the feed gas contains condensables, it may be necessary to preheat the gas prior to entry into the membrane system to prevent condensation on the membrane as the retentate becomes richer in the high-molecular-weight species. For high-temperature applications where polymers cannot be used, membranes of glass, carbon, and inorganic oxides are available, but are limited in their selectivity.

For dense membranes, external mass-transfer resistances or concentration polarization effects are generally negligible, and (14-32) with a partial-pressure driving force can be used to compute the rate of species transport through the membrane. As discussed earlier in the subsection on module flow patterns, the appropriate partial-pressure driving force depends on the flow pattern. Cascades of the type discussed earlier are used to increase the degree of separation.

Progress is being made in the development of a method for the prediction of permeability of gases in glassy and rubbery homopolymers, random copolymers, and block copolymers. Teplyakov and Meares [41] present correlations at 25°C for the diffusion coefficient, D , and solubility, S , applied to 23 different gases for 30 different polymers. Predicted values for glassy polyvinyltrimethylsilane (PVTMS) and rubbery polyisoprene are listed in Table 14.9. Typically, D and S agree with experimental data to within $\pm 20\%$ and $\pm 30\%$, respectively.

Gas permeation separators are claimed to be relatively insensitive to changes in feed flow rate, feed composition, and loss of membrane surface area [42]. This claim is tested in the following example.

EXAMPLE 14.10

The feed to a membrane separator consists of 500 lbmol/h of a mixture of 90% H_2 (H) and 10% CH_4 (M) at 500 psia. Permeance values based on a partial-pressure driving force are

$$\bar{P}_{M_H} = 3.43 \times 10^{-4} \text{ lbmol/h-ft}^2\text{-psi and } \bar{P}_{M_M} = 5.55 \times 10^{-5} \text{ lbmol/h-ft}^2\text{-psi}$$

The flow patterns in the separator are such that the permeate side is well mixed and the feed side is in plug flow. The pressure on the permeate side is constant at 20 psia and there is no pressure drop on the feed side.

- (a) Compute the membrane area and permeate purity if 90% of the hydrogen is transferred to the permeate.
- (b) For the membrane area determined in part (a), calculate the permeate purity and hydrogen recovery if
 - (1) the feed rate is increased by 10%.
 - (2) the feed composition is reduced to 85% H_2 .
 - (3) 25% of the membrane area becomes inoperative

Table 14.9 Predicted Values of Diffusivity and Solubility of Light Gases in a Glassy and a Rubbery Polymer

Permeant	$D \times 10^{11}$, m ² /s	$S \times 10^4$, gmol/m ³ -Pa	P_M , barrer
Polyvinyltrimethylsilane (Glassy Polymer)			
He	470	0.18	250
Ne	87	0.26	66
Ar	5.1	1.95	30
Kr	1.5	6.22	29
Xe	0.29	20.6	18
Rn	0.07	69.6	15
H ₂	160	0.54	250
O ₂	7.6	1.58	37
N ₂	3.8	0.84	9
CO ₂	4.0	13.6	160
CO	3.7	1.28	14
CH ₄	1.9	3.93	22
C ₂ H ₆	0.12	30.2	10
C ₃ H ₈	0.01	98.1	2.8
C ₄ H ₁₀	0.001	347	1.2
C ₂ H ₄	0.23	17.8	12
C ₃ H ₆	0.038	77.6	9
C ₄ H ₈ (1)	0.0052	293	4.5
C ₂ H ₂	0.58	16.8	32
C ₃ H ₄ (m)	0.17	138.1	70
C ₄ H ₆ (e)	0.053	318.5	50
C ₃ H ₄ (a)	0.15	186.5	83
C ₄ H ₆ (b)	0.03	226.1	20
Polyisoprene (Rubber-like Polymer)			
He	213	0.06	35
Ne	77.4	0.08	18
Ar	14.6	0.58	25
Kr	7.2	1.78	25
Xe	2.7	5.68	45
Rn	1.2	18.7	64
H ₂	109	0.17	54
O ₂	18.4	0.47	26
N ₂	12.2	0.26	10
CO ₂	12.6	3.80	140
CO	12.1	0.38	14
CH ₄	8.0	1.14	27
C ₂ H ₆	3.3	8.13	79
C ₃ H ₈	1.6	25.4	123
C ₄ H ₁₀	1.5	86.4	390
C ₂ H ₄	4.3	4.84	62
C ₃ H ₆	2.7	20.3	163
C ₄ H ₈ (1)	1.5	73.3	333
C ₂ H ₂	5.7	4.64	80
C ₃ H ₄ (m)	4.1	35.3	433
C ₄ H ₆ (e)	2.9	79.6	690
C ₃ H ₄ (a)	4.5	47.4	640
C ₄ H ₆ (b)	3.4	40.0	410

Note. m, methylacetylene; e, ethylacetylene; a, allene; b, butadiene.

SOLUTION

The following independent equations apply to all parts of this example. Component material balances:

$$n_{i_F} = n_{i_R} + n_{i_P}, \quad i = H, M \quad (1,2)$$

$$\text{Dalton's law of partial pressures: } P_k = p_{H_k} + p_{M_k}, \quad k = F, R, P \quad (3,4,5)$$

$$\text{Partial pressure-mole relations: } p_{H_k} = P_k n_{H_k} / (n_{H_k} + n_{M_k}), \quad k = F, R, P \quad (6,7,8)$$

Solution-diffusion transport rates are obtained using (14-32), assuming a log-mean partial-pressure driving force based on the exiting permeate partial pressures on the downstream side of the membrane because of the assumption of perfect mixing on that side:

$$n_{i_P} = \bar{P}_{M_i} A_M \left[\frac{p_{i_F} - p_{i_R}}{\ln \left(\frac{p_{i_F} - p_{i_P}}{p_{i_R} - p_{i_P}} \right)} \right], \quad i = H, M \quad (9,10)$$

Thus, we have a system of 10 equations in the following 18 variables:

$$\begin{array}{cccccc} A_M & n_{H_F} & n_{M_F} & P_F & P_R & P_P \\ \bar{P}_{M_H} & n_{H_R} & n_{M_R} & p_{H_F} & p_{H_R} & p_{H_P} \\ \bar{P}_{M_M} & n_{H_P} & n_{M_P} & p_{M_F} & p_{M_R} & p_{M_P} \end{array}$$

Thus, eight variables must be fixed. For all parts of this example, the following five variables are fixed:

$$\begin{array}{l} \bar{P}_{M_H} \text{ and } \bar{P}_{M_M} \text{ given above} \\ P_F = 500 \text{ psia} \quad P_R = 500 \text{ psia} \quad P_P = 20 \text{ psia} \end{array}$$

For each part, three additional variables must be fixed.

(a)

$$\begin{array}{l} n_{H_F} = 0.9(500) = 450 \text{ lbmol/h} \\ n_{M_F} = 0.1(500) = 50 \text{ lbmol/h} \\ n_{H_P} = 0.9(450) = 405 \text{ lbmol/h} \end{array}$$

Solving Equations (1)–(10) above, using a PC program such as MathCad, we obtain

$$\begin{array}{l} A_M = 3,370 \text{ ft}^2 \\ n_{M_P} = 20.0 \text{ lbmol/h} \quad n_{H_R} = 45.0 \text{ lbmol/h} \quad n_{M_R} = 30.0 \text{ lbmol/h} \\ p_{H_F} = 450 \text{ psia} \quad p_{M_F} = 50 \text{ psia} \quad p_{H_R} = 300 \text{ psia} \\ p_{M_R} = 200 \text{ psia} \quad p_{H_P} = 19.06 \text{ psia} \quad p_{M_P} = 0.94 \text{ psia} \end{array}$$

(b) Calculations are made in a similar manner using Equations (1)–(10). Results for parts (1), (2), and (3) are:

		Part		
		(1)	(2)	(3)
Fixed:				
	n_{H_F} , lbmol/h	495	425	450
	n_{M_F} , lbmol/h	55	75	50
	A_M , ft ²	3,370	3,370	2,528
Calculated, in lbmol/h:				
	n_{H_P}	424.2	369.6	338.4
	n_{M_P}	18.2	25.9	11.5
	n_{H_R}	70.8	55.4	111.6
	n_{M_R}	36.8	49.1	38.5
Calculated, in psia:				
	p_{H_F}	450	425	450
	p_{M_F}	50	75	50
	p_{H_R}	329	265	372
	p_{M_R}	171	235	128
	p_{H_P}	19.18	18.69	19.34
	p_{M_P}	0.82	1.31	0.66

From the above results, the following are computed:

		Part			
		(a)	(b1)	(b2)	(b3)
	Mol% H ₂ in permeate	95.3	95.9	93.5	96.7
	% H ₂ recovery in permeate	90	85.7	87.0	75.2

From these results, we see that when the feed rate is increased by 10% (part b1), the hydrogen recovery drops about 5%, but the permeate purity is maintained. When the feed composition is reduced from 90% to 85% hydrogen (part b2), the hydrogen recovery decreases by about 3% and the permeate purity decreases by about 2%. With 25% of the membrane area inoperative (part b3), the hydrogen recovery decreases by about 17%, but the permeate purity is about 1% higher. Overall, percentage changes in hydrogen recovery and purity are less than the percentage changes in feed flow rate, feed composition, and membrane area, thus tending to confirm the insensitivity of gas permeation separators to changes in operating conditions. ■

14.7 PERVAPORATION

As shown in Figure 14.22, pervaporation (PV) differs from dialysis, reverse osmosis, and gas permeation in that the phase state on one side of the membrane is different from that on the other side. The feed to the membrane module is a liquid mixture (e.g., an alcohol–water azeotrope) at a pressure, P_1 , that is usually ambient or elevated high enough to maintain a liquid phase as the feed is depleted of species A and B to produce the product retentate. A composite membrane is used that is selective for species A, but species B usually has some finite permeability. The dense, thin membrane film is in contact with the liquid side. The retentate is enriched in species B. Generally, a sweep fluid is not used on the other side of the membrane, but a pressure, P_2 , is maintained at or below the dew point of the permeate, making it vapor. Often, P_2 is a vacuum. Vaporization may occur near the downstream face of the membrane, such that the membrane can be considered to operate with two zones, a liquid-phase zone and a vapor-phase zone, as shown in Figure 14.22.

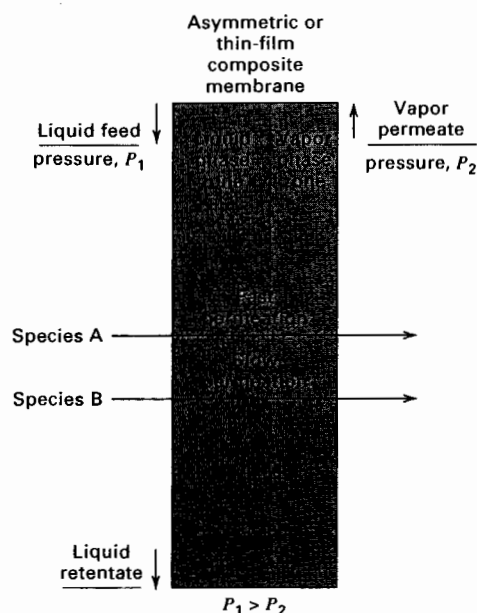


Figure 14.22 Pervaporation.

Alternatively, the vapor phase may only exist on the permeate side of the membrane. The vapor permeate is enriched in species A. Overall permeabilities of species A and B depend upon their solubilities in and diffusion rates through the membrane. Generally, the solubilities cause the membrane to swell.

The term pervaporation is a combination of the two words, *permselective* and *evaporation*. It was first reported in 1917 by Kober [43], who studied several experimental techniques for removing water from albumin/toluene solutions. Although the economic potential of PV was shown by Binning et al. [44] in 1961, commercial applications were delayed until the mid-1970s, when adequate membrane materials first became available. Major commercial applications now include (1) dehydration of ethanol; (2) dehydration of other organic alcohols, ketones, and esters; and (3) removal of organics from water. The separation of organic mixtures is receiving much attention.

Pervaporation is best applied when the feed solution is dilute in the main permeant because sensible heat of the feed mixture provides the enthalpy of vaporization of the permeant. If the feed is rich in the main permeant, a number of membrane stages may be needed, with a small amount of permeant produced per stage and reheating of the retentate between stages. Even when only one membrane stage is sufficient, the feed may be heated before entering the membrane module.

Many pervaporation separation schemes have been proposed [6], with three of the more important ones shown in Figure 14.23. A hybrid process for integrating distillation with pervaporation to produce 99.5 wt% ethanol from a feed of 60 wt% ethanol is shown in Figure 14.23a. The feed is sent to a distillation column operating at near-ambient pressure, where a bottoms product of nearly pure water and an ethanol-rich distillate of 95 wt% is produced. The distillate purity is limited because of the 95.6 wt% ethanol in water azeotrope. The distillate is sent to a pervaporation step where a permeate of 25 wt% alcohol and a retentate of 99.5 wt% ethanol is produced. The permeate vapor is condensed under vacuum and recycled to the distillation column. The vacuum is sustained with a vacuum pump. The dramatic difference in separability of the pervaporation membrane as compared to vapor-liquid equilibrium for distillation is shown in Figure 14.24, taken from Wesslein et

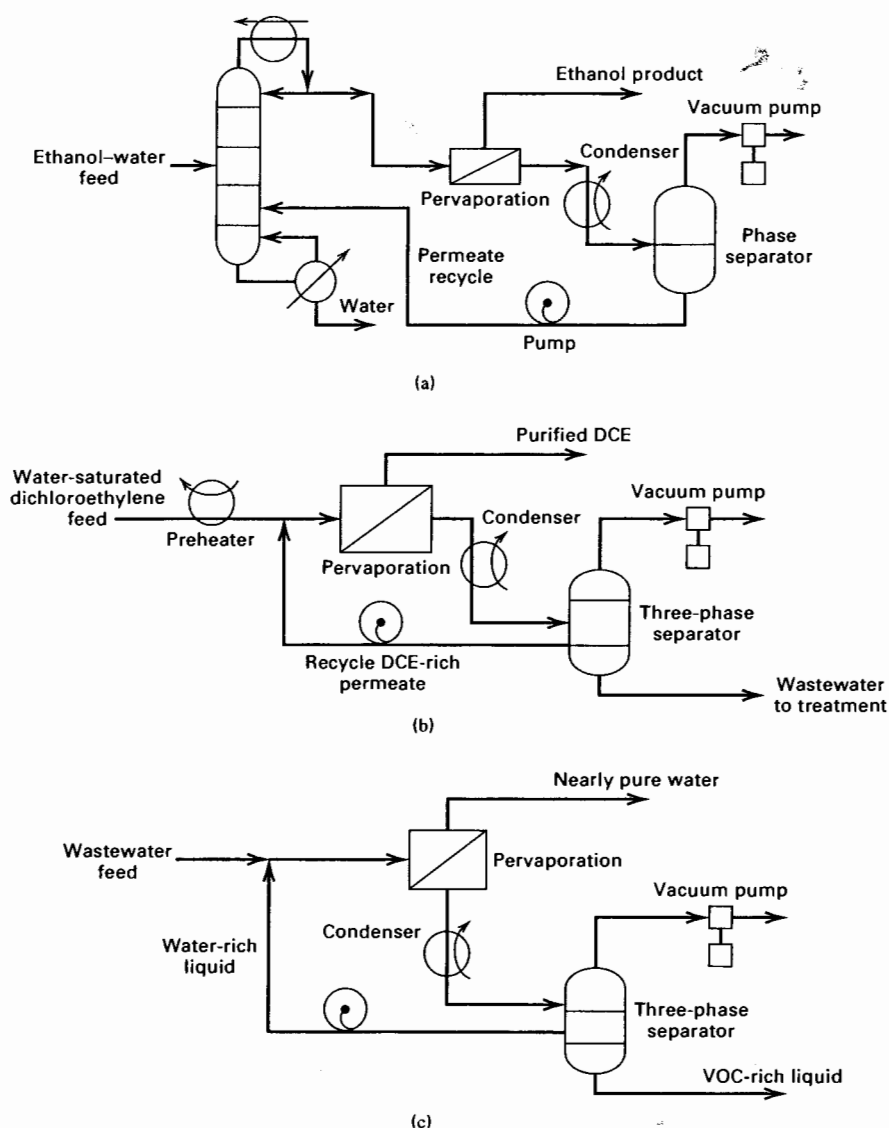


Figure 14.23 Pervaporation processes. (a) Hybrid process for removal of water from ethanol. (b) Dehydration of dichloroethylene. (c) Removal of volatile organic compounds (VOCs) from wastewater.

al. [45]. For pervaporation, the compositions refer to a liquid feed (abscissa) and a vapor permeate (ordinate) at 60°C for a polyvinylalcohol (PVA) membrane and a vacuum of 15 torr. For this membrane, there is no limitation on ethanol purity and the separation index is very high for feeds containing more than 90 wt% ethanol.

A pervaporation process for dehydrating dichloroethylene (DCE) is shown in Figure 14.23b. The liquid feed, which is DCE saturated with water (0.2 wt%), is preheated to 90°C at 0.7 atm and sent to a PVA membrane system, which produces a retentate of almost pure DCE (<10 ppm H₂O) and a permeate vapor of 50 wt% DCE under vacuum. Following condensation, the two resulting liquid phases are separated, with the DCE-rich phase recycled back to the membrane system and the water-rich phase sent to an air stripper, steam stripper, adsorption unit, or hydrophobic pervaporation membrane system for residual DCE removal.

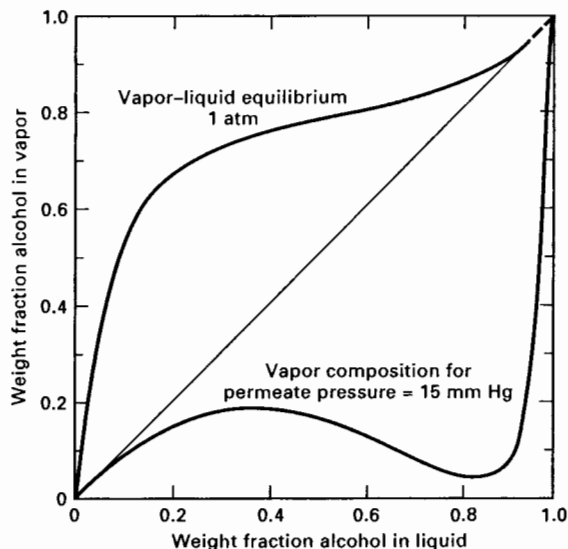


Figure 14.24 Comparison of ethanol-water separabilities.
[From M. Wesslein et al., *J. Membrane Sci.*, **51**, 169 (1990).]

Pervaporation can be used for the removal of VOCs (e.g., toluene and trichloroethylene) from wastewater by pervaporation with hollow-fiber modules of silicone rubber, as shown in Figure 14.23c. The retentate is almost pure water (<5 ppb of VOCs) and the permeate, after condensation, is (1) a water-rich phase that is recycled to the membrane system and (2) a nearly pure VOC phase.

A pervaporation module typically operates adiabatically with the enthalpy of vaporization supplied by sensible enthalpy of the feed. Consider the pervaporation of a binary liquid mixture of components A and B. Assume constant pure-component liquid specific heats, and ignore heat of mixing. For an enthalpy datum temperature of T_0 , an enthalpy balance, in terms of mass flow rates, m , liquid sensible heats, and heats of vaporization, gives

$$\begin{aligned}
 (m_{A_F} C_{P_A} + m_{B_F} C_{P_B})(T_F - T_0) \\
 &= [(m_{A_F} - m_{A_P}) C_{P_A} + (m_{B_F} - m_{B_P}) C_{P_B}](T_R - T_0) \\
 &\quad + (m_{A_P} C_{P_A} + m_{B_P} C_{P_B})(T_P - T_0) + m_{A_P} \Delta H_{A_P}^{\text{vap}} \\
 &\quad + m_{B_P} \Delta H_{B_P}^{\text{vap}}
 \end{aligned} \tag{14-73}$$

where enthalpies of vaporization are evaluated at T_P . After collection of terms, (14-73) reduces to

$$\begin{aligned}
 (m_{A_F} C_{P_A} + m_{B_F} C_{P_B})(T_F - T_R) &= (m_{A_P} C_{P_A} + m_{B_P} C_{P_B})(T_P - T_R) \\
 &\quad + (m_{A_P} \Delta H_{A_P}^{\text{vap}} + m_{B_P} \Delta H_{B_P}^{\text{vap}})
 \end{aligned} \tag{14-74}$$

The temperature of the permeate, T_P , is the permeate dew point at the permeate vacuum upstream of the condenser. The retentate temperature is computed from (14-74).

Membrane selection is critical in the commercial application of PV, when used in the presence of organic compounds. For water permeation, hydrophilic membrane materials are preferred. For example, a three-layer membrane is often used for the dehydration of ethanol, with water being the main permeating species. The support layer is porous polyester, which is cast on a microporous polyacrylonitrile or polysulfone membrane. The final

layer, which provides the separation, is dense PVA of 0.1 μm in thickness. This composite combines chemical and thermal stability with adequate permeability. Hydrophobic membranes, such as silicone rubber and Teflon, are preferred when organics are the permeating species.

Commercial membrane modules for PV are almost exclusively of the plate-and-frame type because of the ease of using gasketing materials that are resistant to organic solvents and the ease of providing heat exchange for evaporation and high-temperature operation. However, considerable interest is evident in the use of hollow-fiber modules for the removal of VOCs from wastewater. Because feeds are generally clean and operation is at low pressure, membrane fouling and damage can be minimal, resulting in useful membrane lives of 2–4 years.

Various models for the transport of a permeant through a membrane by pervaporation have been proposed, based on the solution-diffusion model. They all assume equilibrium between the upstream liquid and the upstream membrane surface, and between the downstream vapor and the other side of the membrane. Transport through the membrane follows Fick's law with a concentration gradient of the permeant in the membrane as the driving force. However, because of the phase change and nonideal-solution effects in the liquid feed, simple equations like (14-55) for dialysis and (14-32) for gas permeation do not apply to pervaporation.

A particularly convenient PV model is that of Wijmans and Baker [46]. They express the driving force for permeation in terms of a partial vapor pressure difference. Because pressures on the both sides of the membrane are low, the gas phase follows the ideal gas law. Therefore, at the upstream membrane surface (1), permeant activity for component i is expressed as

$$a_i^{(1)} = f_i^{(1)} / f_i^{(0)} = p_i^{(1)} / P_i^s(1) \quad (14-75)$$

where P_i^s is the vapor pressure at the feed temperature. The liquid on the upstream side of the membrane is generally nonideal. Thus, from Table 2.2:

$$a_i^{(1)} = \gamma_i^{(1)} x_i^{(1)} \quad (14-76)$$

Combining (14-75) and (14-76):

$$p_i^{(1)} = \gamma_i^{(1)} x_i^{(1)} P_i^s(1) \quad (14-77)$$

On the downstream vapor side of the membrane (2), the partial pressure is

$$p_i^{(2)} = y_i^{(2)} P_P^{(2)} \quad (14-78)$$

Thus, the driving force can be expressed as $(\gamma_i^{(1)} x_i^{(1)} P_i^s(1) - y_i^{(2)} P_P^{(2)})$

The corresponding permeant flux, after dropping unnecessary superscripts, is

$$N_i = \frac{P_{M_i}}{l_M} (\gamma_i x_i P_i^s - y_i P_P) \quad (14-79)$$

or

$$N_i = \bar{P}_{M_i} (\gamma_i x_i P_i^s - y_i P_P) \quad (14-80)$$

where γ_i and x_i refer to the feed-side liquid, P_i^s is the vapor pressure at the feed-side temperature, y_i is the mole fraction in the permeant vapor, and P_P is the total permeant pressure.

Unlike gas permeation where P_{M_i} depends mainly on the permeant, the polymer, and temperature, the permeability for pervaporation depends additionally on the concentrations of permeants in the polymer, which can be large enough to cause polymer swelling and

cross-diffusion effects. For a binary system it is best to back-calculate and correlate the permeant flux with feed composition at a given feed temperature and permeate pressure. Because of these nonideal effects, the selectivity can be a strong function of feed concentration and permeate pressure, causing inversion of selectivity in some cases, as illustrated in the following example.

EXAMPLE 14.11

Wesslein et al. [45] present the following experimental data for the pervaporation of liquid mixtures of ethanol (1) and water (2) at a feed temperature of 60°C for a permeate pressure of 76 mmHg, using a commercial polyvinylalcohol membrane:

wt% ethanol		Total Permeation Flux kg/m ² ·h
Feed	Permeate	
8.8	10.0	2.48
17.0	16.5	2.43
26.8	21.5	2.18
36.4	23.0	1.73
49.0	22.5	1.46
60.2	17.5	0.92
68.8	13.0	0.58
75.8	9.0	0.40

At 60°C, vapor pressures are 352 and 149 mmHg for ethanol and water, respectively. Liquid-phase activity coefficients at 60°C for the ethanol (1)–water (2) system are given by the van Laar equations:

$$\ln \gamma_1 = 1.6276 \left[\frac{0.9232x_2}{1.6276x_1 + 0.9232x_2} \right]^2$$

$$\ln \gamma_2 = 0.9232 \left[\frac{1.6276x_1}{1.6276x_1 + 0.9232x_2} \right]^2$$

Calculate values of permeance for water and ethanol from (14-80).

SOLUTION

For the first row of data, the mole fractions in the feed mixture (x_i) and the permeate (y_i), using molecular weights of 46.07 and 18.02 for ethanol and water, respectively, are

$$x_1 = \frac{0.088/46.07}{\frac{0.088}{46.07} + \frac{(1.0 - 0.088)}{18.02}} = 0.0364$$

$$x_2 = 1.0 - 0.0364 = 0.9636$$

$$y_1 = \frac{0.10/46.07}{\frac{0.10}{46.07} + \frac{0.90}{18.02}} = 0.0416$$

$$y_2 = 1.0 - 0.0416 = 0.9584$$

The activity coefficients for the feed mixture are

$$\gamma_1 = \exp \left\{ 1.6276 \left[\frac{0.9232(0.9636)}{1.6276(0.0364) + 0.9232(0.9636)} \right]^2 \right\} = 4.182$$

$$\gamma_2 = \exp \left\{ 0.9232 \left[\frac{1.6276(0.0364)}{1.6276(0.0364) + 0.9232(0.9636)} \right]^2 \right\} = 1.004$$

From the given total mass flux, the component molar fluxes are

$$N_1 = \frac{(2.48)(0.10)}{46.07} = 0.00538 \frac{\text{kmol}}{\text{h} - \text{m}^2}$$

$$N_2 = \frac{(2.48)(0.90)}{18.02} = 0.1239 \frac{\text{kmol}}{\text{h} - \text{m}^2}$$

From (14-80), the permeance values are

$$\bar{P}_{M_1} = \frac{0.00538}{(4.182)(0.0364)(352) - (0.0416)(76)} = 0.000107 \frac{\text{kmol}}{\text{h} - \text{m}^2 - \text{mmHg}}$$

$$\bar{P}_{M_2} = \frac{0.1239}{(2.004)(1.0 - 0.0364)(149) - (1.0 - 0.0416)(76)} = 0.001739 \frac{\text{kmol}}{\text{h} - \text{m}^2 - \text{mmHg}}$$

Results for the other feed conditions are computed in a similar manner:

wt% Ethanol		Activity Coefficient in Feed		Permeance, kmol/h-m ² -mmHg	
Feed	Permeate	Ethanol	Water	Ethanol	Water
8.8	10.0	4.182	1.004	1.07×10^{-4}	1.74×10^{-3}
17.0	16.5	3.489	1.014	1.02×10^{-4}	1.62×10^{-3}
26.8	21.5	2.823	1.038	8.69×10^{-5}	1.43×10^{-3}
36.4	23.0	2.309	1.077	6.14×10^{-5}	1.17×10^{-3}
49.0	22.5	1.802	1.158	4.31×10^{-5}	1.10×10^{-3}
60.2	17.5	1.477	1.272	1.87×10^{-5}	8.61×10^{-4}
68.8	13.0	1.292	1.399	7.93×10^{-6}	6.98×10^{-4}
75.8	9.0	1.177	1.539	3.47×10^{-6}	6.75×10^{-4}

The PVA membrane is hydrophilic. Thus, as the concentration of ethanol in the feed liquid increases, the sorption of feed liquid by the membrane decreases, resulting in a reduction of polymer swelling. The preceding results show that as swelling is reduced, the permeance of ethanol decreases more rapidly than that of water, thus increasing the selectivity for water. For example, the selectivity for water can be defined as

$$\alpha_{2,1} = \frac{(100 - w_1)_P / (w_1)_P}{(100 - w_1)_F / (w_1)_F}$$

where w_1 = weight fraction of ethanol. For the cases of 8.8 and 75.8 wt% ethanol in the feed, the selectivities for water are, respectively, 0.868 (more selective for ethanol) and 31.7 (more selective for water). ■

SUMMARY

1. The separation of liquid and gas mixtures with membranes is an emerging separation operation. Applications greatly accelerated in the 1980s. The products of separation are the retentate and the permeate.
2. The key to an efficient and economical membrane separation process is the membrane. It must have good permeability, high selectivity, stability, freedom from fouling, and a long life (2 or more years).
3. Commercialized membrane separation processes include dialysis, electrodialysis, reverse osmosis, gas permeation, and pervaporation.

4. Most membranes for commercial separation processes are natural or synthetic, glassy or rubbery polymers. However, for high-temperature ($>200^{\circ}\text{C}$) or operations with chemically reactive mixtures, ceramics, metals, and carbon find applications.
5. To achieve high permeability and selectivity, dense, nonporous membranes are preferred. For mechanical integrity, membranes of 0.1 to 1.0 mm in thickness are incorporated as a surface layer or film onto or as part of a much thicker asymmetric or composite membrane.
6. To achieve a high surface area per unit volume, membranes are fabricated into spiral-wound or hollow-fiber modules. Less surface is available in plate-and-frame, tubular, and monolithic modules.
7. Permeation through a membrane can occur by a variety of mechanisms. For a microporous membrane, the mechanisms include bulk flow (with no selectivity), liquid diffusion, gas diffusion, Knudsen diffusion, restrictive diffusion (including sieving), and surface diffusion. For a nonporous membrane, a solution-diffusion mechanism, involving absorption, diffusion, and desorption, is commonly assumed.
8. Flow patterns in membrane modules have a profound effect on overall permeation rates. Idealized flow patterns for which theory has been developed include perfect mixing, countercurrent flow, cocurrent flow, and crossflow.
9. To overcome the limit of separation in a single membrane-module stage, modules can be arranged in series and/or parallel cascades.
10. In gas permeation, boundary-layer or film mass-transfer resistances on either side of the membrane are usually negligible compared to the membrane resistance. For the membrane separation of liquid mixtures, however, the external mass-transfer effects, referred to as concentration polarization, can be significant.
11. For most membrane separators, the component mass-transfer fluxes through the membrane can be formulated as the product of two terms: concentration, partial pressure, fugacity, or activity driving force; and a permeance \bar{P}_{M_i} , which is the ratio of the permeability, P_{M_i} , to the membrane thickness, l_M .
12. In the dialysis of a liquid mixture, small solutes of type A are separated from the solvent and larger solutes of type B with a microporous membrane. The driving force is the concentration difference across the membrane. The transport of solvent can be minimized by adjusting the pressure difference across the membrane to equal the osmotic pressure.
13. In electrodialysis, a series of alternating cation- and anion-selective membranes are used with a direct-current voltage across an outer anode and an outer cathode to concentrate an electrolyte.
14. In reverse osmosis, the solvent of a liquid mixture is selectively transported through a dense membrane. By this means, seawater can be desalinated. The driving force for transport of the solvent through the membrane is the fugacity difference, which is commonly expressed in terms of $\Delta P - \Delta\pi$, where π is the osmotic pressure.
15. In gas permeation, mixtures of gases are separated by differences in permeation rates through dense membranes. The driving force for each component is its partial pressure difference, Δp_i , across the membrane. Both the permeance and permeability depend on the absorptivity of the membrane for the particular gas species (usually as a Henry's law constant) and the diffusivity of the species through the membrane. Thus, $P_{M_i} = H_i D_i$.
16. In pervaporation, a liquid mixture is separated with a dense membrane by pulling a vacuum on the permeate side of the membrane so as to evaporate the permeate. The driving force may be approximated as a fugacity difference expressed by $(\gamma_i x_i P_i^s - y_i P_P)$. The permeability can vary greatly with concentration because of membrane swelling.

1. I
2. I
3. I
64(9)
4. I
Prog
5. I
and
and l
ment
6. I
Nost
7. I
38, S
8. F
9. V
10. E
11. E
Lona
12. N
13. N
14. F
39, 2
15. B
nome
16. E
17. B
18. B
273 (I
19. B
3rd e
20. L
Sci., 5
21. M
Tanio
brane.
22. B
329 (I
23. B
24. B
197 (I

EXI

Sectic

14.1
rator

(a) A

(b) C

(c) L

(d) E

REFERENCES

1. Lonsdale, H.K., *J. Membrane Sci.*, **10**, 81 (1982).
2. Applegate, L.E., *Chem. Eng.*, **91**(12), 64–89 (1984).
3. Havens, G.G., and D.B. Guy, *Chem. Eng. Progress Symp. Series*, **64**(90), 299 (1968).
4. Bollinger, W.A., D.L. MacLean, and R.S. Narayan, *Chem. Eng. Progress*, **78**(10), 27–32 (1982).
5. Baker, R.W., E.L. Cussler, W. Eykamp, W.J. Koros, R.L. Riley, and H. Strathmann, *Membrane Separation Systems—A Research and Development Needs Assessment*, Report DE 90-011770, Department of Commerce, NTIS, Springfield, VA (1990).
6. Ho, W.S.W., and K.K. Sirkar, Eds., *Membrane Handbook*, Van Nostrand Reinhold, New York (1992).
7. Loeb, S., and S. Sourirajan, *Advances in Chemistry Series*, Vol. 38, *Saline Water Conversion II* (1963).
8. Henis, J.M.S., and M.K. Tripodi, U.S. Patent 4,230,463 (1980).
9. Wrasidlo, W. J., U.S. Patent 3,951,815 (1977).
10. Barrer, R.M., *J. Chem. Soc.*, 378–386 (1934).
11. Barrer, R. M., *Diffusion in and through Solids*, Cambridge Press, London (1951).
12. Mahon, H. I., U.S. Patent 3,228,876 (1966).
13. Mahon, H. I., U.S. Patent 3,228,877 (1966).
14. Hsieh, H.P., R.R. Bhave, and H.L. Fleming, *J. Membrane Sci.*, **39**, 221–241 (1988).
15. Bird, R.B., W.E. Stewart, and E.N. Lightfoot, *Transport Phenomena*, John Wiley and Sons, New York, pp 42–47 (1960).
16. Ergun, S., *Chem. Eng. Progress*, **48**, 89–94 (1952).
17. Beck, R.E., and J.S. Schultz, *Science*, **170**, 1302–1305 (1970).
18. Beck, R.E., and J.S. Schultz, *Biochim. Biophys. Acta*, **255**, 273 (1972).
19. Brandrup, J., and E.H. Immergut, Eds., *Polymer Handbook*, 3rd ed., John Wiley and Sons, New York (1989).
20. Lonsdale, H.K., U. Merten, and R.L. Riley, *J. Applied Polym. Sci.*, **9**, 1341–1362 (1965).
21. Motamedian, S., W. Pusch, G. Sendelbach, T.-M. Tak, and T. Tanioka, *Proceedings of the 1990 International Congress on Membranes and Membrane Processes*, Chicago, Vol. II, pp. 841–843.
22. Barrer, R.M., J.A. Barrie, and J. Slater, *J. Polym. Sci.*, **23**, 315–329 (1957).
23. Barrer, R.M., and J.A. Barrie, *J. Polym. Sci.*, **23**, 331–344 (1957).
24. Barrer, R.M., J.A. Barrie, and J. Slater, *J. Polym. Sci.*, **27**, 177–197 (1958).
25. Koros, W.J., and D.R. Paul, *J. Polym. Sci., Polym. Physics Edition*, **16**, 1947–1963 (1978).
26. Barrer, R.M., *J. Membrane Sci.*, **18**, 25–35 (1984).
27. Walawender, W.P., and S.A. Stern, *Separation Sci.*, **7**, 553–584 (1972).
28. Naylor, R.W., and P.O. Backer, *AIChE J.*, **1**, 95–99 (1955).
29. Stern, S.A., T.F. Sinclair, P.J. Gareis, N.P. Vahldieck, and P.H. Mohr, *Ind. Eng. Chem.*, **57**(2), 49–60 (1965).
30. Hwang, S.-T., and K.L. Kammermeyer, *Membranes in Separations*, Wiley-Interscience, New York, pp. 324–338 (1975).
31. Spillman, R.W., *Chem. Eng. Progress*, **85**(1), 41–62 (1989).
32. Strathmann, H., "Membrane and Membrane Separation Processes," in Vol. A16, *Ullmann's Encyclopedia of Industrial Chemistry*, VCH, FRG, p. 237, (1990).
33. Chamberlin, N.S., and B.H. Vroman, *Chem. Engr.* **66**(9), 117–122 (1959).
34. Graham, T., *Phil. Trans. Roy. Soc. London*, **151**, 183–224 (1861).
35. Juda, W., and W.A. McRae, *J. Amer. Chem. Soc.*, **72**, 1044 (1950).
36. Strathmann, H., *Sep. and Purif. Methods*, **14**(1), 41–66 (1985).
37. Merten, U., *Ind. Eng. Chem. Fundamentals*, **2**, 229–232 (1963).
38. Stoughton, R.W., and M.H. Lietzke, *J. Chem. Eng. Data*, **10**, 254–260 (1965).
39. Spillman, R.W., and M.B. Sherwin, *Chemtech*, 378–384 (June 1990).
40. Schell, W.J., and C.D. Houston, *Chem. Eng. Progress*, **78**(10), 33–37 (1982).
41. Teplyakov, V., and P. Meares, *Gas Sep. and Purif.*, **4**, 66–74 (1990).
42. Rosenzweig, M.D., *Chem. Eng.*, **88**(24), 62–66 (1981).
43. Kober, P.A., *J. Am. Chem. Soc.*, **39**, 944–948 (1917).
44. Binning, R.C., R.J. Lee, J.F. Jennings, and E.C. Martin, *Ind. Eng. Chem.*, **53**, 45–50 (1961).
45. Wesslein, M., A. Heintz, and R.N. Lichtenthaler, *J. Membrane Sci.*, **51**, 169 (1990).
46. Wijmans, J.G., and R.W. Baker, *J. Membrane Sci.*, **79**, 101–113 (1993).
47. Rautenbach, R., and R. Albrecht, *Membrane Processes*, John Wiley and Sons, New York (1989).
48. Rao, M.B., and S. Sircar, *J. Membrane Sci.*, **85**, 253–264 (1993).

EXERCISES

Section 14.1

14.1 Explain, as completely as you can, how membrane separations differ from:

- (a) Absorption and stripping
- (b) Distillation
- (c) Liquid–liquid extraction
- (d) Extractive distillation

14.2 For the commercial application of membrane separators discussed at the beginning of this chapter, calculate the permeabilities of hydrogen and methane in barrer.

14.3 A new asymmetric polyimide polymer membrane has been developed for the separation of N_2 from CH_4 . At 30°C, permeance values are 50,000 and 10,000 barrer/cm for N_2 and CH_4 , respectively. If this new membrane is used to perform the separation in Figure 14.25, determine the mem-

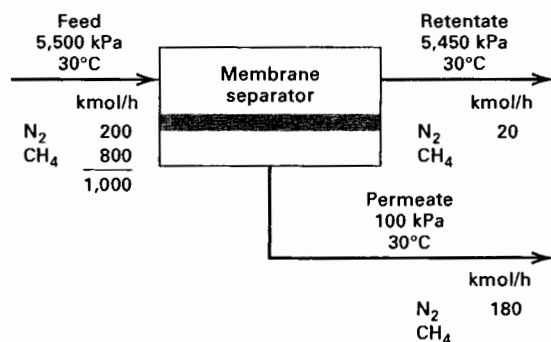


Figure 14.25 Data for Exercise 14.3.

brane surface area required in m^2 , and the $kmol/h$ of CH_4 in the permeate. Base the driving force for diffusion through the membrane on the arithmetic average of the partial pressures of the entering feed and the exiting retentate, with the permeate-side partial pressures at the exit condition.

Section 14.2

14.4 A hollow-fiber module has 4,000 ft^2 of membrane surface area based on the inside diameter of the fibers, which are $42 \mu m$ i.d. $\times 85 \mu m$ o.d. $\times 1.2$ m long each. Determine:

- The number of hollow fibers in the module.
- The diameter of the module, assuming the fibers are on a square spacing of $120 \mu m$ center-to-center.
- The membrane surface area per unit volume of module (packing density) m^2/m^3 . Compare your result with that in Table 14.4.

14.5 A typical spiral-wound module made from a flat sheet of membrane material is 0.3 m in diameter and 3 m long. If the packing density (membrane surface area/unit module volume) is $500 m^2/m^3$, determine the center-to-center spacing of the membrane in the spiral, assuming a collection tube 1 cm in diameter.

14.6 A monolithic membrane element, of the type shown in Figure 14.4d, contains 19 flow channels that are 0.5 cm in inside diameter by 0.85 m long. If nine of these elements are placed into a cylindrical module of the type shown in Figure 14.5, determine reasonable values for:

- Module volume in m^3 .
- Packing density in m^2/m^3 . Compare your value with values for other membrane modules given in Table 14.4.

Section 14.3

14.7 Water at $70^\circ C$ is to be passed through a porous polyethylene membrane of 25% porosity with an average pore diameter of 0.3 micron and an average tortuosity of 1.3. The

(1 μm thick membrane)
pressures on the downstream and upstream sides of the membrane are 125 and 500 kPa, respectively. Estimate the flow rate of water through the membrane in $m^3/m^2 \cdot day$.

14.8 A porous glass membrane, with an average pore diameter of 40 \AA , is to be used to separate light gases at $25^\circ C$ under conditions where Knudsen flow may be dominant. The downstream pressure is 15 psia, while the upstream pressure is not greater than 120 psia. The membrane has been calibrated with pure helium gas, giving a constant permeability of 117,000 barrer over the operating pressure range. Experiments with pure CO_2 over the pressure range give a permeability of 68,000 barrer.

Assuming that helium is in Knudsen flow, predict the permeability of CO_2 . Is the value in agreement with the experimental value? If not, suggest an explanation. Reference: Kammermeyer, K., and L.O. Rutz, *C.E.P. Symp. Ser.*, 55 (24), 163–169 (1959).

14.9 Two mechanisms for the transport of gas components through a porous membrane that are not discussed in Section 14.3 or illustrated in Figure 14.6 are (1) partial condensation in the pores by some components of the gas mixture to the exclusion of other components and subsequent transport of the condensed molecules through the pore, and (2) selective adsorption on pore surfaces of certain components of the gas mixture and subsequent surface diffusion across the pores. In particular, Rao and Sircar [48] have found that the latter mechanism provides a potentially attractive means for separating hydrocarbons from hydrogen for low-pressure gas streams. In porous carbon membranes with continuous pores 4–15 \AA in diameter, little pore void space is available for the Knudsen diffusion of hydrogen when the hydrocarbons are selectively adsorbed.

Typically, the membranes are not more than $5 \mu m$ in thickness. Measurements at 295.1 K of permeabilities for five pure components and a mixture of the five components are as follows:

Component	Permeability, barrer		
	As a Pure Gas	In the Mixture	mol% in the Mixture
H_2	130	1.2	41.0
CH_4	660	1.3	20.2
C_2H_6	850	7.7	9.5
C_3H_8	290	25.4	9.4
nC_4H_{10}	155	112.3	19.9
			100.0

A refinery waste gas mixture of the preceding composition is to be processed through such a porous carbon membrane. If the pressure of the gas is 1.2 atm and an inert sweep gas is used on the permeate side such that partial pressures of feed gas components on that side are close to zero, determine the permeate composition on a sweep-gas-free basis when

the composition on the upstream-pressure side of the membrane is that of the feed gas. Explain why the component permeabilities differ so drastically between experiments with the pure gas and the gas mixture.

14.10 A mixture of 60 mol% propylene and 40 mol% propane at a flow rate of 100 lbmol/h and at 25°C and 300 psia is to be separated with a polyvinyltrimethylsilane polymer (see Table 14.9 for permeabilities). The membrane skin is 0.1 μm thick, and spiral-wound modules are used with a pressure of 15 psia on the permeate side. Calculate the material balance and membrane area in m^2 as a function of the cut (fraction of feed permeated) for:

- Perfect mixing flow pattern.
- Crossflow pattern.

14.11 Repeat part (a) of Exercise 14.10 for a two-stage stripping cascade and a two-stage enriching cascade, as shown in Figure 14.12. However, select just one set of reasonable cuts for the two stages of each case so as to produce 40 lbmol/h of final retentate.

14.12 Repeat Example 14.7 with the following changes:

Tube-side Reynolds number = 25,000

Tube inside diameter = 0.4 cm

Permeate-side mass transfer coefficient = 0.06 cm/s

How important is concentration polarization?

Section 14.4

14.13 An aqueous process stream of 100 gal/h at 20°C contains 8 wt% Na_2SO_4 and 6 wt% of a high-molecular-weight substance (A). This stream is processed in a continuous countercurrent flow dialyzer using a pure water sweep of the same flow rate. The membrane is a microporous cellophane with pore volume = 50%, wet thickness = 0.0051 cm, tortuosity = 4.1, and pore diameter = 31 Å. The molecules to be separated have the following properties:

	Na_2SO_4	A
Molecular weight	142	1,000
Molecular diameter, Å	5.5	15.0
Diffusivity, $\text{cm}^2/\text{s} \times 10^5$	0.77	0.25

Calculate the membrane area in m^2 for only a 10% transfer of A through the membrane, assuming no transfer of water. What is the percent recovery of the Na_2SO_4 in the diffusate? Use log-mean concentration driving forces and assume that the mass-transfer resistances on each side of the membrane are each 25% of the total mass-transfer resistances for Na_2SO_4 and A.

14.14 A dialyzer is to be used to separate 300 L/h of an aqueous solution containing 0.1 M NaCl and 0.1 M HCl. Laboratory experiments with the microporous membrane to

be used give the following values for the overall mass transfer coefficient K_i in (14-57), for a log-mean concentration driving force:

	K_i , cm/min
Water	0.0025
NaCl	0.021
HCl	0.055

Determine the membrane area in m^2 for 90, 95, and 98% transfer of HCl to the diffusate. For each of the three cases, determine the complete material balance in kmol/h. A sweep of 300 L/h can be assumed.

14.15 A total of 86,000 gal/day of an aqueous solution of 3,000 ppm of NaCl is to be desalinated to 400 ppm by electrodialysis, with a 40% conversion. The process will be conducted in four stages, with three stacks of 150 cell pairs in each stage. The fractional desalination will be the same in each stage and the expected current efficiency is 90%. The applied voltage for the first stage is 220 V. Each cell pair has an area of 1,160 cm^2 . Calculate the current density in mA/cm^2 , the current in A, and the power requirement in kW for the first stage. Reference: Mason, E.A., and T.A. Kirkham, *C.E.P. Symp. Ser.*, **55**(24), 173–189 (1959).

Section 14.5

14.16 A reverse osmosis plant is being used to treat 30,000,000 gal/day of seawater at 20°C containing 3.5 wt% dissolved solids to produce 10,000,000 gal/day of potable water with 500 ppm of dissolved solids, and the balance as brine containing 5.25 wt% dissolved solids. The feed-side pressure is 2,000 psia, while the permeate pressure is 50 psia. A single stage of spiral-wound membranes is used that approximates crossflow. If the total membrane area is 2,000,000 ft^2 , estimate the permeance for water and the salt passage.

14.17 A reverse osmosis process is to be designed to handle a feed flow rate of 100 gal/min. Three designs have been proposed, differing in the % recovery of potable water from the feed:

Design 1: A single stage consisting of four units in parallel to obtain a 50% recovery

Design 2: Two stages in series with respect to the retentate (four units in parallel followed by two units in parallel)

Design 3: Three stages in series with respect to the retentate (four units in parallel followed by two units in parallel followed by a single unit)

Draw the three designs and determine the percent recovery of potable water for designs 2 and 3.

14.18 The production of paper involves a pulping step to break down wood chips into cellulose and lignin. In the Kraft process, an aqueous pulping feed solution, known as white

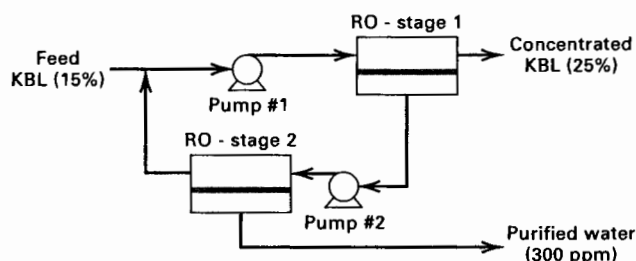


Figure 14.26 Data for Exercise 14.18.

liquor, is used that consists of dissolved inorganic chemicals such as sodium sulfide and sodium hydroxide. Following removal of the pulp (primarily cellulose), a solution known as weak (Kraft) black liquor (KBL) is left, which is regenerated to recover white liquor for recycle. In the conventional process, a typical 15 wt% (dissolved solids) KBL is concentrated to 45 to 70 wt% by multieffect evaporation. It has been suggested that reverse osmosis might be used to perform an initial concentration to perhaps 25 wt%. Higher concentrations may not be feasible because of the very high osmotic pressure, which at 180°F and 25 wt% solids is estimated to be 1,700 psia. The osmotic pressure for other conditions can be scaled with (14-68) using wt% instead of molality.

A two-stage RO process, shown in Figure 14.26, has been proposed to carry out this initial concentration for a feed rate of 1,000 lb/h at 180°F. A feed pressure of 1,756 psia is used for the first stage to yield a permeate of 0.4 wt% solids. The feed pressure to the second stage is 518 psia to produce water of 300 ppm dissolved solids and a retentate of 2.6 wt% solids. Permeate-side pressure for both stages is 15 psia. Equation (14-69) can be used to estimate membrane area, where the permeance for water can be taken as 0.0134 lb/ft²-hr-psi in conjunction with an arithmetic-mean osmotic pressure for plug flow on the feed side. Complete the material balance for the process and estimate the required membrane areas for each stage. Reference: Gottschlich, D.E., and D.L. Roberts. Final Report DE91004710, SRI International, Menlo Park, CA, Sept. 28, 1990.

Section 14.6

14.19 Gas permeation can be used to recover VOCs from air at low pressures using a membrane material that is highly selective for the VOCs. In a typical application, 1,500 scfm (0°C, 1 atm) of air containing 0.5 mol% acetone (A) is fed to a spiral-wound membrane module system at 40°C and 1.2 atm. A liquid-ring vacuum pump on the permeate side establishes a pressure of 4 cmHg. A silicone rubber, thin-composite membrane with a 2 μm-thick skin gives permeabilities of 4 barrer for air and 20,000 barrer for acetone.

If the retentate is to contain 0.05 mol% acetone and the permeate is to contain 5 mol% acetone, determine the membrane area required in m², assuming crossflow. References: (1) Peinemann, K.-V., J.M. Mohr, and R.W. Baker, *C.E.P. Symp. Series*, **82**(250), 19-26 (1986); (2) Baker, R.W., N.

Yoshioka, J.M. Mohr, and A.J. Khan, *J. Membrane Sci.*, **31**, 259-271 (1987).

14.20 The separation of air into nitrogen and oxygen is widely practiced. Cryogenic distillation is most economical for processing 100 to 5,000 tons of air per day, while pressure-swing-adsorption is favorable for 20 to 50 tons/day. For small-volume users requiring less than 10 tons/day, gas permeation finds applications where for a single stage, either an oxygen-enriched air (40 mol% oxygen) or 98 mol% nitrogen can be produced. It is desired to produce 5 ton/day (2,000 lb/ton) of 40 mol% oxygen and nitrogen, ideally of 90 mol% purity, by gas permeation. Assume pressures of 500 psia (feed side) and 20 psia (permeate). Two companies, who can supply the membrane modules, have provided the following data:

	Company A	Company B
Module type	Hollow-fiber	Spiral-wound
\bar{P}_M for O ₂ , barrer/μm	15	35
$P_{M_{O_2}}/P_{M_{N_2}}$	3.5	1.9

Determine the required membrane area in m² for each company. Assume that both module types approximate cross-flow.

14.21 A joint venture has been underway for several years to develop a membrane process to separate CO₂ and H₂S from high-pressure sour natural gas. Typical feed and product conditions are:

	Feed Gas	Pipeline Gas
Pressure, psia	1,000	980
Composition, mol%:		
CH ₄	70	97.96
H ₂ S	10	0.04
CO ₂	20	2.00

To meet these conditions, the following hollow-fiber membrane material targets have been established:

	Selectivity
CO ₂ -CH ₄	50
H ₂ S-CH ₄	50

where selectivity is the ratio of permeabilities.

$$P_{M_{CO_2}} = 13.3 \text{ barrer,}$$

and membrane skin thickness is expected to be 0.5 μm.

Make calculations to show whether the targets can realistically meet the pipeline gas conditions in a single stage with a reasonable membrane area. Assume a feed gas flow rate of 10 × 10³ scfm (0°C, 1 atm) with crossflow.

Reference: Stam, H., in *Future Industrial Prospects of*

Membrane Processes, L. Cecille and J.-C. Toussaint, Eds., Elsevier Applied Science, London, pp. 135–152 (1989).

Section 14.7

14.22 Pervaporation is to be used to separate ethyl acetate (EA) from water. The feed rate is 100,000 gal/day of water containing 2.0 wt% EA at 30°C and 20 psia. The membrane is dense polydimethylsiloxane with a 1 μm -thick skin in a spiral-wound module that approximates crossflow. The permeate pressure is 3 cmHg. The total measured membrane flux at these conditions is 1.0 L/m²-h with a separation factor given by (14-36) of 100 for EA with respect to water. A retentate of 0.2 wt% EA is desired for a permeate of 45.7 wt% EA. Determine the required membrane area in m² and estimate the temperature drop of the feed. Reference: Blume, I., J.G. Wijans, and R.W. Baker, *J. Membrane Sci.*, **49**, 253–286 (1990).

14.23 For a temperature of 60°C and a permeate pressure of 15.2 mmHg, Wesslein et al. [45] measured a total permeation flux of 1.6 kg/m²-h for a 17.0 wt% ethanol in water

feed, giving a permeate of 12 wt% ethanol. Otherwise, conditions were those of Example 14.11. Calculate the permeances of ethyl alcohol and water for these conditions. Also, calculate the selectivity for water.

14.24 The separation of benzene (B) from cyclohexane (C) by distillation at 1 atm is impossible because of a minimum-boiling-point azeotrope at 54.5 mol% benzene. However, extractive distillation with furfural is feasible. For an equimolar feed, cyclohexane and benzene products of 98 and 99 mol%, respectively, can be produced. Alternatively, the use of a three-stage pervaporation process, with selectivity for benzene using a polyethylene membrane, has received attention, as discussed by Rautenbach and Albrecht [47]. Consider the second stage of this process where the feed is 9,905 kg/h of 57.5 wt% B at 75°C. The retentate is 16.4 wt% benzene at 67.5°C and the permeate is 88.2 wt% benzene at 27.5°C. The total permeate mass flux is 1.43 kg/m²-h and the selectivity for benzene is 8. Calculate the flow rates of retentate and permeate in kg/h and the required membrane surface area in m².